PolyPublie
Polytechnique Montréal

POLYTECHNIQUE MONTRÉAL
UNIVERSITÉ D'INGÉNIERIE

Titre: Title:	Robust Predictive Control Model Utilizing Recursive State Estimation for Controlling Indoor Microclimates of Clustered Greenhouses
Auteur: Author:	Ehsan Ghorbani
Date:	2023
Type:	Mémoire ou thèse / Dissertation or Thesis
Référence: Citation:	Ghorbani, E. (2023). Robust Predictive Control Model Utilizing Recursive State Estimation for Controlling Indoor Microclimates of Clustered Greenhouses [Mémoire de maîtrise, Polytechnique Montréal]. PolyPublie. https://publications.polymtl.ca/56734/

Document en libre accès dans PolyPublie
Open Access document in PolyPublie

URL de PolyPublie: PolyPublie URL:	https://publications.polymtl.ca/56734/
Directeurs de recherche: Advisors:	Hanane Dagdougui
Programme: Program:	Maîtrise recherche en mathématiques appliquées

Ce fichier a été téléchargé à partir de PolyPublie, le dépôt institutionnel de Polytechnique Montréal
This file has been downloaded from PolyPublie, the institutional repository of Polytechnique Montréal

https://publications.polymtl.ca

POLYTECHNIQUE MONTRÉAL
affiliée à l'Université de Montréal

Robust Predictive Control Model Utilizing Recursive State Estimation for Controlling Indoor Microclimates of Clustered Greenhouses

EHSAN GHORBANI
Département de mathématiques et de génie industriel

mémoire présenté en vue de l'obtention du diplôme de *Maîtrise ès sciences appliquées*
Mathématiques appliquées

Août 2023

© Ehsan Ghorbani, 2023.

POLYTECHNIQUE MONTRÉAL
affiliée à l'Université de Montréal

Ce mémoire intitulé :

Robust Predictive Control Model Utilizing Recursive State Estimation for Controlling Indoor Microclimates of Clustered Greenhouses

présenté par **Ehsan GHORBANI**
en vue de l'obtention du diplôme de *Maîtrise ès sciences appliquées*
a été dûment accepté par le jury d'examen constitué de :

Issmaïl EL HALLAOUI, président
Hanane DAGDOUGUI, membre et directrice de recherche
Keyhan SHESHYEKANI, membre

DEDICATION

To my parents.

ACKNOWLEDGEMENTS

Special thanks to my great supervisor, full of dignity human-being; Prof. Hanane Dagdougui. Thanks to all who they helped me.

RÉSUMÉ

Face aux grands défis des changements climatiques, de la sécurité alimentaire et la rareté des ressources énergétiques, le développement des méthodes de production alimentaire plus fiables et durables est envisagé comme solution innovante. Au cours des deux dernières décennies, la culture en serres agricoles est devenue un moyen très populaire en raison de nombreux avantages tels que l'augmentation du taux de production et l'amélioration des performances globales. D'abord, l'environnement autonome et bien conditionné des serres agricoles assure une meilleure protection contre les conditions météorologiques et climatiques. Ensuite, la culture en serre intelligente peut assimiler des technologies modernes en matière de mesurage, prédiction et contrôle.

Pour maintenir un climat de croissance optimal à l'intérieur des serres, les perturbations météorologiques rapides nécessitent des méthodes de commande qui réagissent de manière précise et proactive face aux situations indésirables.

L'approche classique se basant sur le contrôle des systèmes multi-entrées et multi-sorties (MIMO) avec une dynamique corrélée ne donne pas une solution optimale, en particulier pour le contrôle d'un environnement de croissance des cultures qui est tellement sensible aux aléas de la météo. Dans le cas du déploiement des serres de petites tailles, l'utilisation de méthodes de contrôle optimisées pourrait constituer un défi gérable. Néanmoins, lors du déploiement de serres agricoles de moyenne à grande tailles, les méthodes de surveillance et de contrôle intelligent sont nécessaires pour maintenir les différents points de consigne souhaités, tout en minimisant les coûts d'exploitation, maximisant le rendement et la qualité des cultures et garantissant l'utilisation la plus efficace des ressources naturelles.

La commande prédictive (MPC) est considérée comme l'une des méthodes qui assurent des meilleurs résultats pour le contrôle des environnements avec des variables et des contraintes MIMO. En général, les serres de grande taille sont vues comme de gros consommateurs d'électricité et utilisateurs de ressources naturelles. Les serres intelligentes sont généralement équipées de ressources distribuées, permettant la satisfaction partielle ou complète des besoins énergétiques. Ces sytèmes peuvent également ajouter de la complexité au contrôle en augmentant l'incertitude et en limitant le contrôleur MPC.

Dans ce cas, le MPC peut être facilement déstabilisé en cas de défaillance dûe à l'incertitude des perturbations. Ce risque potentiel lié à l'utilisation d'un simple MPC est le principal inconvénient de ce contrôleur. De plus, les systèmes réels souffrent de limitations, soit dûes à leur sens physique, soit dans leurs définitions mathématiques. Pour remédier à cette incapac-

ité du MPC, la version robuste a été proposée dans ce mémoire. En bref, dans un problème de commande prédictive robuste (RMPC), l'incertitude est soumise à des contraintes et à des caractéristiques de cartographie des risques dans le problème d'optimisation, sans perturber la faisabilité de la solution. Les études montrent une performance relativement parfaite du RMPC. Dans les applications de serres agricoles, le RMPC couvre les lacunes du MPC classique. Cependant, en raison de la nature lente et conservatrice du RMPC, ce type de robustesse peut entraîner des problèmes de stabilité après avoir été exposé à des perturbations sévères. Lorsque des réseaux de serres sont mis en œuvre, l'inconvénient du RMPC en cas de fortes perturbations sera double. En raison de cette faiblesse du RMPC, la consommation d'énergie augmente, en plus du gaspillage des ressources du fait que les contrôleurs sont déréglés après avoir passé une certaine période de contrôle.

Cette étude vise également à améliorer pour la première fois la méthode RMPC pour le contrôle d'un réseau de serres intelligentes. En pratique, la plupart des contrôleurs réels ne sont pas protégés contre les perturbations de grande ampleur. C'est pourquoi on a abordé le problème de manière plus pratique. Premièrement, un estimateur d'état récursif robuste est implémenté pour filtrer les écarts de grande ampleur. Ensuite, le RMPC utilise un estimateur d'état récursif robuste implémenté pour décomposer le signal, en utilisant la technique d'appartenance à un ensemble et en construisant l'ensemble robuste positivement invariant, puis générer des séquences de contrôle optimales en présence de perturbations et de contraintes.

ABSTRACT

Faced with the major challenges of climate change, food security and the scarcity of energy resources, developing more reliable and sustainable food production methods is considered an innovative solution. Over the past two decades, agricultural greenhouse cultivation has become a very popular way due to many advantages such as increased production rate and improved overall performance. First, autonomous and well-conditioned environment of greenhouses provide better protection against weather and climatic conditions. Then, smart greenhouse cultivation can assimilate modern measurement, prediction and control technologies.

The rapid weather disturbances require control methods that respond precisely and proactively to undesirable situations to maintain an optimal growing climate inside greenhouses.

The traditional approach based on controlling Multi-Input Multi-Output (MIMO) systems with correlated dynamics does not provide an optimal solution, particularly for controlling a crop growth environment that is so sensitive to unforeseen conditions of weather. In the case of small greenhouse deployment, the use of optimized control methods could be a manageable challenge. Nevertheless, when deploying medium to large agricultural greenhouses, intelligent monitoring and control methods are required to maintain various desired set points while minimizing operating costs, maximizing crop yield and quality and ensuring the most efficient use of natural resources.

Model Predictive Control (MPC) is considered one of the methods that ensure the best results for controlling environments with MIMO variables and constraints. In general, large greenhouses are seen as large consumers of electricity and users of natural resources. Smart greenhouses are generally equipped with distributed resources, allowing partial or complete satisfaction of energy needs. These systems can also add complexity to control by increasing uncertainty and limiting the MPC controller.

In this case, the MPC can be easily destabilized in the event of failure due to the uncertainty of the disturbances. This potential risk of using a simple MPC is the main disadvantage of this controller. Furthermore, real systems suffer from limitations, either due to their physical meaning or in their mathematical definitions. To remedy this inability of the MPC, the robust version was proposed in this dissertation. In short, in a Robust Model Predictive Control (RMPC), uncertainty is subject to constraints and risk mapping features in the optimization problem without disturbing the feasibility of the solution. Studies show a relatively perfect performance of RMPC. In agricultural greenhouse applications, RMPC

covers the shortcomings of conventional MPC. However, due to the slow and conservative nature of RMPC, this type of robustness can lead to stability issues after being exposed to severe disturbances. When greenhouse networks are implemented, the disadvantage of RMPC under high disturbances will be twofold. Due to this weakness in RMPC, energy consumption increases, in addition to wasting resources due to controllers being out of adjustment after passing a certain control period.

This study also aims to improve, for the first time, the RMPC method for controlling a network of smart greenhouses. In practice, most real controllers are not protected against large-scale disturbances. This is why we approached the problem in a more practical way. First, a robust recursive state estimator is implemented to filter large deviations. Then, the RMPC uses a robust recursive state estimator implemented to decompose the signal, using the set membership technique and constructing the positively invariant robust set, then generates optimal control sequences in the presence of disturbances and constraints.

TABLE OF CONTENTS

DEDICATION iii

ACKNOWLEDGEMENTS iv

RÉSUMÉ v

ABSTRACT vii

TABLE OF CONTENTS ix

LIST OF TABLES xi

LIST OF FIGURES xii

LIST OF SYMBOLS AND ACRONYMS xv

LIST OF APPENDICES xvii

CHAPTER 1 INTRODUCTION 1
- 1.1 Background & Motivation 1
- 1.2 Problem Statement 2
- 1.3 Research objectives and contributions 4
- 1.4 Outline of Dissertation 4

CHAPTER 2 LITERATURE REVIEW 5
- 2.1 Smart Greenhouse Technology 5
- 2.2 Cluster of GHs 7
- 2.3 Energy consumption in GHs: Impact of uncertainty of disturbances on amount of consumed energy 7
- 2.4 Thermal comfort of GH: Resistance-Capacitance (RC) model 8
- 2.5 Role of Model Predictive Control 9
  - 2.5.1 Model Predictive Controller Performance 10
  - 2.5.2 MPC applied to greenhouse application 11
  - 2.5.3 Common MPC Weaknesses in GH application 12
- 2.6 Robust concept in Model Predictive Control 12
  - 2.6.1 Introducing a RMPC problem 13

2.6.2 Uncertainty representation for RMPC 15
2.6.3 Set-membership utilization in recursive state estimator 16
2.7 Overview of RMPC approaches in literature 18
2.8 Robust Model Predictive Control utilizing recursive state estimation 21

CHAPTER 3 GENERAL ORGANIZATION OF THE DOCUMENT 26

CHAPTER 4 ARTICLE 1: ROBUST MODEL PREDICTIVE CONTROL FOR THE OPTIMAL OPERATION OF A CLUSTER OF SMART GREENHOUSES INDOOR ENVIRONMENT . . . . . 27. . .
4.1 Abstract 27
4.2 Introduction 27
4.3 Literature review 28
4.4 Contributions 29
4.5 Mathematical Modeling of a Cluster of GHs 30
4.5.1 Cluster of Greenhouses 30
4.5.2 GH components modeling 30
4.5.3 Robust Optimal Control Problem for a Cluster of GHs 37
4.6 GH Case Study 41
4.6.1 Data collection & simulation setup 41
4.6.2 Simulation and results 42
4.7 Conclusion 44

CHAPTER 5 GENERAL DISCUSSION 47

CHAPTER 6 CONCLUSIONS AND RECOMMENDATIONS 49
6.1 Summary of Works 49
6.2 Limitations 50
6.3 Future Research 50

REFERENCES 52

APPENDICES 67

LIST OF TABLES

Table 2.1	Different type of constraints in MPC formulation	19
Table 2.2	Control parametrization methods in different resources	19
Table 2.3	Type of uncertainty of disturbances, mentioned in various references .	19
Table 2.4	Deployed feedback policy in RMPC approach across various resources	19
Table 4.1	PV, BESS & Water Pumps Parameters	41
Table 4.2	Comparison the time of computation of two methods over prediction horizon in Fig.4.3: Robust MPC (RMPC) and Robust MPC equipped with proposed algorithm	43
Table A.1	Time of convergence over one window ($t = t_k \rightarrow t = t_{k+1}$)of prediction horizon.	73
Table A.2	comparison of energy level of objective costs in error state estimation between two methods, converging to origin.	74
Table A.3	Cucumber setpoints , GH_1.	76
Table A.4	Tomato setpoints, GH_2.	76
Table A.5	Strawberry setpoints, GH_3.	76
Table A.6	Eggplant setpoints,GH_4.	76

LIST OF FIGURES

Figure 2.1 RC Model of cross section of wall of GH 8
Figure 2.2 Voltage source is modeling temperature 9
Figure 2.3 Current source is modeling HVAC system 9
Figure 2.4 MPC illustration (image obtained from the public domain of Wikipedia article on MPC) 11
Figure 4.1 Cluster of GH 31
Figure 4.2 RC model: Thermal equivalent circuit of GH structure 33
Figure 4.3 Left: Auxiliary input $\mu_{Temp}^{GH_1}$ at step $k = 1$: state feedback (Blue); Proposed method (Red line); feasible set membership for measuring with disturbance (Pink area), Right: closed-loop trajectory of Temperature and ventilation system states in GH_1. 43
Figure 4.4 GHs reference tracking profile of temperature over four days. Other strategy may be faced with problem when constraints are tightened, due to severe fluctuations. 45
Figure 4.5 Top: Power consumption of GH_1 related to temperature control system, Bottom: Price according to D-rate tariff in Quebec. 46
Figure 4.6 Top: BESS action (based on kWh scaling) in GH_1 Bottom: SOC of BESS in GH_1. 46
Figure A.1 Robust Kalman Filter using Huber function on a random signal, Time step in scale of $\times 10$. 68
Figure A.2 Left: Common Kalman Filter (KF); Right:Robust Kalman Filter (RKF) using set-membership concept, deployed on a random signal with noisy measurement. 68
Figure A.3 Improved Robust method Under high noise level, Left to Right: terminal state weight increases, process noise increases, error state set is growing, computational demand rises ($p_w \sim N(0, (0, 4, 8))$, $p_v \sim N(0, 6)$). 69
Figure A.4 Common Robust method under a high level of noise, Left to Right: terminal state weight increases, process noise increases, error state set is growing, but ellipsoid shows reluctant to increase to keep feasibility, resulting in conservatism instead, each step has more residual amount of error state in comparison with improved method ($p_w \sim N(0, (0, 4, 8))$, $p_v \sim N(0, 6)$). 70

Figure A.5 Improved Robust method Under high level of noise, Left to Right: input control weight increases, process noise increases, error state set is growing, computational demand raises.($p_w \sim N(0,(0,5))$, $p_v \sim N(0,(0,4,8))$). 70

Figure A.6 Common Robust method under a high level of noise, Left to Right: input control increases, process noise increases, error state set is growing, ellipsoids also rise in each step to keep feasibility because the state is not tracked very well, resulting conservatism, each step residual amount of error state increases in comparison with improved method ($p_w \sim N(0,(0,5))$, $p_v \sim N(0,(0,4,8))$). 71

Figure A.7 Left-top: Auxiliary input $\mu_{Temp}^{GH_1}$ at step $k=1$: state feedback (Blue); Proposed method (Red line); Left-bottom: real input $u_{Temp}^{GH_1}$ at step $k=1$: state feedback (Blue); Proposed method (Red line); Right-top: closed-loop trajectory of Temperature and ventilation system states in GH_1; Right-bottom: feasible set membership for measuring with disturbance state feedback(Green area), hexagonal-wise area proposed method. 72

Figure A.8 Left-top: Auxiliary input $\mu_{Temp}^{GH_2}$ at step $k=1$: state feedback (Blue); Proposed method (Red line); Left-bottom: real input $u_{Temp}^{GH_2}$ at step $k=1$: state feedback (Blue); Proposed method (Red line); Right-top: closed-loop trajectory of Temperature and ventilation system states in GH_2; Right-bottom: feasible set membership for measuring with disturbance state feedback(Green area), hexagonal-wise area proposed method. 73

Figure A.9 Left-top: Auxiliary input $\mu_{Temp}^{GH_3}$ at step $k=1$: state feedback (Blue); Proposed method (Red line); Left-bottom: real input $u_{Temp}^{GH_3}$ at step $k=1$: state feedback (Blue); Proposed method (Red line); Right-top: closed-loop trajectory of Temperature and ventilation system states in GH_3; Right-bottom: feasible set membership for measuring with disturbance state feedback(Green area), hexagonal-wise area proposed method. 75

Figure A.10 Left-top: Auxiliary input $\mu_{Temp}^{GH_4}$ at step $k = 1$: state feedback (Blue); Proposed method (Red line); Left-bottom: real input $u_{Temp}^{GH_4}$ at step $k = 1$: state feedback (Blue); Proposed method (Red line); Right-top: closed-loop trajectory of Temperature and ventilation system states in GH_4; Right-bottom: feasible set membership for measuring with disturbance state feedback(Green area), hexagonal-wise area proposed method. 77

Figure A.11 GHs reference tracking profile of temperature over four days. Other strategy may be faced with problem when constraints are tightened, due to severe fluctuations. 78

Figure A.12 CO_2 concentration level control inside of GHs over four days under two control strategies. 79

Figure A.13 Humidifier control profile of reference tracking during four days. . . . 80

Figure A.14 Water Pump power control profile in the first day of four days. 80

Figure A.15 Light intensity control profile with on/off reactions during four days. 81

Figure A.16 Top to Bottom: First: Power consumption of GH_1 related to temperature control system; Second: Price according to D-rate bill of Quebec, Third: BESS action in GH_1, Forth: Bottom: SOC of BESS in GH_1. 82

Figure A.17 Top to Bottom: First: Power consumption of GH_2 related to temperature control system, Second: Price according to D-rate bill of Quebec, Third: BESS action in GH_2, Forth: Bottom: SOC of BESS in GH_2. . 83

Figure A.18 Top to Bottom: First: Power consumption of GH_3 related to temperature control system, Second: Price according to D-rate bill of Quebec, Third: BESS action in GH_3, Forth: Bottom: SOC of BESS in GH_3. . 84

Figure A.19 Top to Bottom: First: Power consumption of GH_4 related to temperature control system, Second: Price according to D-rate bill of Quebec, Third: BESS action in GH_4, Forth: Bottom: SOC of BESS in GH_4. . 85

LIST OF SYMBOLS AND ACRONYMS

GH	Greenhouse
MG	Microgrid
RES	Renewable Energy System
WGNC	World Greenhouse Network Community
BESS	Battery Energy Storage System
PCC	Point of Common Coupling
PI	Proportional-Integral
PID	Proportional-Integral-Derivative
MPC	Model Predictive Control
LTI	Linear Time Invariant
RMPC	Robust Model Predictive Control
ML	Machine Learning
MPC	Model Predictive Control
CMPC	Centralized Model Predictive Control
DMPC	Decentralized Model Predictive Control
ISS	Input-to-State Stability
WC	Worst-Case
CLF	Control Lyapunov Functions
PDF	Probability Distribution Function
RPI	Robustly Positive Invariant
RC	Resistance-Capacitance
HVAC	Heating, Ventilation, Air conditioning
GHG	Greenhouse Gas
PV	Photovoltaic
PDE	Partial Differential Equation
ADMM	Alternating Direction Method of Multiplier
LMI	Linear Matrix Inequality
EKF	Extended Kalman Filter
UKF	Unscented Kalman Filter
MIMO	Multi-Input Multi-Output
KF	Kalman Filter
RKF	Robust Kalman Filter
DAE	Differential-Algebraic Equation

LQR	Linear Quadratic Regulator
RKF	Robust Kalman Filter
HVAC	Heating, Ventilation, Air conditioning
SOC	State of charging/discharging
ESS	Energy Storage System
GHs	Greenhouses

LIST OF APPENDICES

Appendix A Supplementary results 67

CHAPTER 1 INTRODUCTION

1.1 Background & Motivation

For three decades, increasing demand for food has been creating daily challenges for industries. Utilizing advanced technologies in industries requires over-exploitation of the environment. This phenomenon brings adverse consequences on plants and crops, like climate change and the unavailability of natural resources in the environment, so that it directly endangers the natural process of horticulture and agriculture production [1]. Over the last decade, greenhouses (GHs) have shown flexible and efficient performance, such technologies have become very popular [2, 3]. In addition, the deployment of modern measuring and controlling systems make GHs more reliable means for sustainable food production industries.

Modern GHs are highly adaptable in installing new technologies like distributed energy resources. The latter has a crucial role in large-scale and clustered GHs, where it helps making constructive interactions with the power grid to minimize energy consumption [4–7]. Not surprisingly, GHs can become a new type of load for smart microgrid (MG). Therefore, the presences of renewable energy sources in MG allows GHs to achieve the best profile of setpoint tracking without compromising on greenhouse (GH)'s life-conditioning situation [8–11].

Smart GHs show also a certain degree of flexibility to adopt Battery Energy Storage System (BESS) for making the best use of Renewable Energy System (RES) [12, 13], deploying controlled & secure connections to balance the local loads with renewable generation.

In the natural way of growing, plants require numerously interdependent states to achieve normal conditions. Considering GH, indoor climate control systems should provide a safe environment to respond to the vital needs of crops, especially in inhospitable regions, to avoid extreme weather conditions like high temperature or humidity levels. Lack of suitable crop conditions causes uncompensated damages, although keeping proper setpoints accelerates crops growing with high quality. In this case, evidently, for preserving healthy conditions, controllers have to function efficiently to maintain the optimal path of tracking the setpoints [14–16]. Hence, implementing a suitable method of controlling brings many advantages, including a high level of efficiency in reducing energy consumption, higher plant fertility, and even obtaining helpful ways to study and recognize various relations of control signals [6, 13, 17–20].

GHs are facing a vast range of unknown & unmodelled uncertainties [21–23]. The existing advanced control methods help to obtain a high rate of productivity in GH, satisfying all

necessary requirements of utilizing renewable energy and controlling indoor' dynamics [13,18].

Despite implementing all advanced control methods on systems like GHs, these facilities are still significantly vulnerable in facing environmental disturbances, so small changes in outside conditions, or even in weather prediction, cause considerable deviation in indoor setpoint tracking, which leads to crop damage, incorrect power demand, and resources dissipation. Nowadays, traditional controllers like Proportional-Integral (PI) or Proportional-Integrator-Derivative (PID) are the dominant type of controllers [24]; however, studies show that complicated relations among GHs' states necessarily need a high level of computational speed in tracking signals and robustness against uncertainties at the same moment [17, 22]. Thus, to enhance the efficiency of the new generation of GHs, implementing more advanced controlling methods is a must, where controllers handle constrained actions autonomously, considering real data and predicting upcoming states to make optimal decisions [18].

1.2 Problem Statement

The MPC method has been introduced to handle numerous states of a process inside GH in parallel with imposing constraints on the uncertainty of disturbances.

Beyond all kinds of controllers and their adjusting criteria, linear MPC has been exposed to various applications to optimize the future control trajectory by utilizing a dynamic model of the system and considering constraints on the system inputs and outputs [6, 13, 20]. The upcoming aspects are a few reasons behind attracting more attention to this advanced controller over two previous decades [25–29]:

- **Prediction horizon:** MPC predicts the system's future behavior over a specified prediction horizon. The prediction horizon defines the length of time over which the future predictions are made. Longer prediction horizons allow for better anticipatory control but increase the computational burden. Advanced MPC methods employ techniques like horizon partitioning to handle long horizons efficiently.

- **Control horizon:** The control horizon determines the length of the future control actions applied to the system. It is typically shorter than the prediction horizon to account for system dynamics and ensure stability. Advanced MPC algorithms can adaptively adjust the control horizon based on the system's response and performance requirements.

- **Optimization:** MPC formulates the control problem as an optimization program that minimizes an objective function subject to system dynamics and constraints. The ob-

jective function can be designed to achieve various control objectives, such as tracking a reference trajectory, regulating a setpoint, minimizing energy consumption, or optimizing economic performance.

- **Constraints handling:** One of the significant advantages of MPC is its ability to handle constraints on the system inputs and outputs. Constraints can be physical limits, safety requirements, or operational limits. Advanced MPC techniques employ approaches like soft constraints, terminal constraints, or constraint tightening to handle constraints robustly and ensure feasibility.

- **State estimation:** MPC requires knowledge of the system states for predictions and control calculations. In practice, states are often not measured directly and must be estimated. Advanced MPC methods incorporate state estimation techniques like Kalman filters, extended Kalman filters, or particle filters to estimate the system states accurately.

These are some advanced aspects of MPC when applied to solve multivariable systems. MPC offers a flexible and powerful control framework capable of handling complex dynamics, constraints, and uncertainties, making it a valuable tool for advanced control applications. However, real-world systems are subject to uncertainties, disturbances, and modelling errors. Advanced MPC approaches address these uncertainties by incorporating robust control techniques, such as robust MPC [11, 17, 30] and stochastic MPC [31].

The main objective of this research is to propose a robust approach to make a resilient structure for GH controllers to perform optimally to boost controller performance in the face of undesirable outside conditions. Implementing robustness in GH, and even industrial GH's on a large scale, not only has beneficial effects on optimal growing conditions for crops, but it also can reduce the power consumption of necessary components inside the GH. Previously, some research works have been conducted on implementing MPC methods in GH applications. However, most of them need to be robustified in facing all possible uncertainties, and in this work, we are focusing on faster RMPC among all kinds of advanced types of MPC. Implementing RMPC in different forms of GH is worth paying attention to, specifically in recognizing and approaching uncertainty, disturbances, and estimation errors. Therefore, this study is trying to develop RMPC method based on a recursive state estimation technique in the cluster of GH applications. Deploying recursive state estimation can help to choose a more enlarged approximation on the uncertainty set, which leads to decreasing computational demand while increasing the feasibility and stability of the whole system with hard constraints.

1.3 Research objectives and contributions

The main objective of this study is to develop and extend RMPC approach, utilizing recursive state estimation and outlier minimization to obtain a more robust and flexible algorithm against uncertainties in controlling a cluster of GHs. The proposed algorithm does not suffer from the high computational time consumption of the exact model of uncertainties because of utilizing the robust state estimation method in the body of RMPC. The main contributions of this work will be:

- Modeling augmented state space dynamics for representing a network of different GHs.
- Adopting robust recursive state estimator based on the M-robust approach to cut high magnitude disturbances, especially in initial states.
- Reducing computation time, accelerating convergence to the controller even in constraint-tightening conditions. Being fast in controlling and handling huge amounts of data will be a noticeable challenge when the number and dimension of GHs are growing.

1.4 Outline of Dissertation

In this dissertation, Chapter 1 describes the background and motivation, problem statement, research objective, and contributions, followed by an outline of the dissertation as the last section. Chapter 2 details the literature review. Firstly, we introduce the concept of smart GH, including its definition and types. We highlight the necessity of robustly controlling the indoor climate control of GH, and then the importance of deploying MPC will be introduced. The literature review chapter presents a deep investigation of RMPC in a deterministic approach. Chapter 3, contains a general explanation of dissertation organization. Chapter 4 consists of the journal paper of this work. A general discussion on methodology and results will be conducted in Chapter 5. Last but not least, Chapter 6 describes the conclusion, overview of work, and prospective point of view on future works.

CHAPTER 2 LITERATURE REVIEW

2.1 Smart Greenhouse Technology

Context

Smart GHs have emerged as advanced agricultural systems that provide optimally controlled plant growth environments. These innovative GHs incorporate various measurement components to monitor and regulate crucial environmental parameters [32, 33]. Sensors, e.g. measure all dynamics, temperature sensors are utilized to track and control the internal temperature and ventilation systems, ensuring plants are kept within the optimal range of growth. Humidity sensors are devised to maintain appropriate moisture levels in the air and soil, optimizing water usage and preventing diseases. Light sensors detect and adjust the intensity and quality of light in the GH, guaranteeing that plants receive the necessary light for photosynthesis. Carbon dioxide (CO_2) detectors also play a vital role in monitoring CO_2 concentrations, leading to improved growth rates and overall productivity [34].

Large-scale and industrial smart GHs interact with the power grid for sustainable operation. In addition, many of these mentioned smart GHs integrate solar power panels [35]. These panels capture renewable energy from the sun to provide power to various GH components, including ventilation systems, lighting, and other controlling mechanisms. Energy storage systems, such as batteries, are deployed to store excess energy generated by renewable sources for nighttime or high energy demand periods. Extra power generated during surplus energy generation by photovoltaic (PV) can be fed back to the grid, reducing greenhouse energy costs and contributing to grid stability. Energy management systems are crucial in optimizing energy consumption patterns within smart greenhouses, reducing reliance on non-renewable sources, and enhancing overall sustainability [36].

Structure of Greenhouse

The physical structure of GHs is designed with specific materials to enhance the efficiency of the growing environment. Commonly, isolated greenhouses use the same materials for walls, roofs, and ceilings [37]. Materials provide insulation and minimize heat transfer. Common materials include double or triple-layered glazing, insulated panels, and Energy-Efficient windows. Using multiple layers of glass or polycarbonate panels with air gaps in between creates insulation that helps retain heat and reduce energy loss. The walls are equipped with insulated windows to maximize light intensity inside of GH. GHs' size varies from small

(domestic) to large (commercial). Usually, in most research [13], [38], [20,39], the commercial size of GHs has been considered. Dimensions of these GHs are 48lengths $\times$ 30width $\times$ 25height foot [40].

Physical type of greenhouses

Generally, GH types are separated into two categories. The following subsections aim to explain these two types of greenhouses.

Isolated Greenhouses

An isolated type of greenhouse, also known as a closed or sealed greenhouse, is a specialized type of greenhouse structure designed to maintain a highly controlled and isolated environment for plant cultivation. Unlike traditional greenhouses that allow air exchange with the outside environment, isolated greenhouses are sealed off from external influences by creating a unique micro-climate. The primary objective of an isolated greenhouse is to maximize control over internal conditions such as temperature, humidity, and CO_2 levels. By isolating the greenhouse, farmers can reduce the risk of pest infestations and diseases that may be entered through external sources. To maintain a suitable growing environment, smart isolated GHs show high flexibility in assimilating precise control systems, comprising a range of sensors and automated equipment to monitor and adjust micro-climate parameters. Isolated GHs often take advantage of energy-efficient technologies and renewable energy sources to reduce reliance on the main grid power network. This may include solar panels for generating electricity and energy storage systems to store excess energy for use during periods of low solar availability [41].

Semi-Closed layout of Greenhouses

Semi-isolated GHs are known as partially sealed or controlled environments. They provide a certain level of isolation and control over the internal environment while still allowing some air exchange with the outside environment [17], [42].

In semi-isolated GHs, the isolation level varies depending on the specific design and requirements. The structure of these types of GHs has sealed walls, floors, and roofs, similar to isolated GHs, to minimize external influences. However, there are usually intentional openings or vents designed to allow controlled air exchange with the outside environment to provide some level of natural ventilation, which can help regulate temperature, humidity, and CO_2 levels. Semi-isolated GHs often incorporate advanced monitoring and control sys-

tems to regulate the internal environment. Energy management in semi-isolated GHs can be similar to isolated GHs, with the integration of energy-efficient technologies and renewable energy sources, including solar panels, energy storage systems, and energy-efficient heating like solar-heating systems or geothermal pipelines, ventilation, and lighting systems.

2.2 Cluster of GHs

In the clustered type of GH entities, every GH keeps one crop species to comply with setpoints well-related to that crop [13, 18]. Many GHs can be connected to a control center, named the centralized controlling method [13], although decentralized/distributed architectures are available in articles [18]. The cluster of GHs, along with PV and BESS facilities, is integrated into a MG. Therefore, deploying a cluster of GHs instead of one GH should necessitate the importance of coordinating advanced control methods [13], [18].

2.3 Energy consumption in GHs: Impact of uncertainty of disturbances on amount of consumed energy

Sensors monitor the state dynamics of the mentioned components; hence, these instruments indispensably need to consume a certain level of accessible and reliable energy to provide the vital needs of crops [26, 43, 44]. It can be concluded that the profile of energy demand in a GH changes according to the size of GH, species of crops inside GH, type of GH, and level of precision of measuring instruments and sensors. Therefore, resilience against disturbances positively impacts GH's energy consumption profile by reducing demanded energy fluctuations and optimizing resource utilization [39, 45, 46]. It makes stable climate control and reduces the need for frequent adjustments, leading to more efficient energy usage. Additionally, resource allocation becomes more efficient, which helps to set predictable environmental conditions, leading to optimized use of resources like energy, water, and lighting systems [18]. Furthermore, mathematically designing control systems with robust features to minor variations focuses on overall stability rather than responding to every small change. Lastly, by being robust against disturbances, GHs can make optimal setpoint adjustments based on long-term trends rather than immediate fluctuations. This allows control systems to optimize energy usage by considering broader patterns of seasonal changes or crop growth stages [13]. To this end, the robust behavior of a cluster of GHs substantiates important maintenance, specifically in large-scale layouts. layouts.

2.4 Thermal comfort of GH: Resistance-Capacitance (RC) model

The Resistance-Capacitance (RC) model is represented mathematically to describe the thermal dynamic behavior of a greenhouse's physical structure. The geometry of a GH can be expressed using an RC model in the form of an electrical circuit [7, 47–49]. This model is adaptable to MPC formulation, such as discrete-time functions and predictive mechanisms [18, 50, 51].

Thermal Characteristics Model of Component

Heat resistance & capacitance are two features of the thermal characteristic description of the material. As it is clear, all materials are intended to be impacted by storing or losing energy in temperature. To deliver a better understanding, a cross-section of the wall of GH is illustrated in Figure. 2.1.

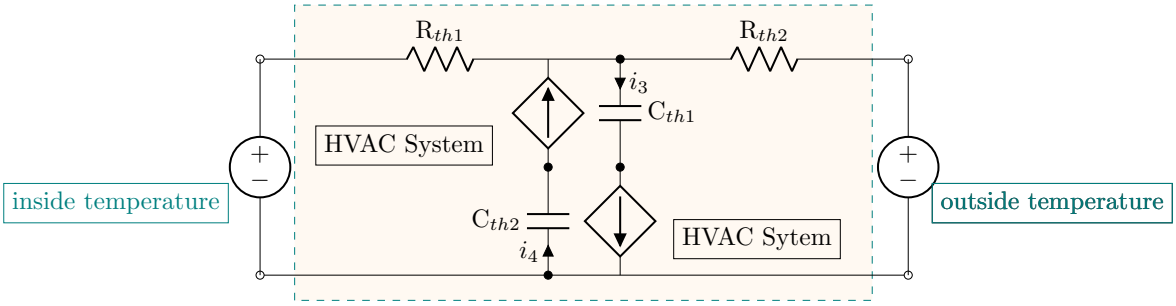

Figure 2.1 RC Model of cross section of wall of GH

a) Resistance: The heat resistance equation shows the dynamic of heating flows, equivalent to the current in an electric circuit:

$$\dot{h} = \frac{1}{R_{th_{eq}}}(Temp_{in} - Temp_{out})$$

is equivalnet to:

$$I_{current} = \frac{1}{R_e}(v_1 - v_2)$$

where, $R_{th_{eq}}$ is equivalent resistance of considered area.

b) Capacitance: Heat capacitance is to express amount of heat, stored in material:

$$\dot{h} \simeq C_{th_{eq}}(\frac{Temp_{in} - Temp_{out}}{dt})$$

is equivalent to:

$$I_{current} = C_e \frac{(v_1 - v_2)}{dt}$$

where, $C_{th_{eq}}$ is equivalent capacitance of related section of area.

c) Voltage sources: are equivalent to temperature sources, emitting heat inside or outside.

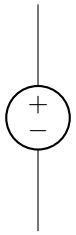

Figure 2.2 Voltage source is modeling temperature

d) Current source: show the functioning of Heating, Ventilation, Air conditioning (HVAC) systems that regulate the temperature inside GHs by air conditioning.

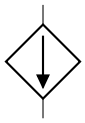

Figure 2.3 Current source is modeling HVAC system

e) Ambient Temperature (Outside): Outside temperature also can be modeled by voltage sources, as like as it is shown in Figure. 2.2.

2.5 Role of Model Predictive Control

Context

Controlling methods of dynamics inside a GH are various. Most famous include PI, PID, and Linear Quadratic Regulator (LQR). Depending on applications in which the classical controllers are deployed, a simple functioning mechanism can show sufficient performance to track ideal setpoints of limited numbers of dynamics in a system. But, in case of dealing with a large number of intertwined dynamics, these controllers cannot outperform. In the real world, dynamics in real situations should be handled with limitations, which require controller designers to put constraints on states. In this regard, modern controllers could propose a solution for covering the shortage of classical approaches. Among all modern controlling methods, MPC has shown a high level of performance in GH applications [6], [38], [20]. In the following subsection, MPC is well-introduced.

MPC technology has evolved as a well-established research field. It focuses on addressing the challenge of achieving optimal control of dynamic systems while considering process constraints and economic incentives. The popularity of MPC can be attributed to two fundamental properties inherent in its algorithms. Firstly, MPC excels in handling constraints explicitly, allowing for effective control actions even in the presence of constraints. Secondly, MPC algorithms offer the capability to achieve efficient operation, striking a balance between optimal and practicality. Thirdly, estimating the state is a substantial part of the mechanism in MPC structure [52–54]. Another notable advantage of MPC algorithms is their flexibility extending to MIMO systems [55]. Various approaches have been developed to tackle MIMO, including Model Algorithmic Control, which utilizes finite impulse response models; Dynamic Matrix Control [56], which employs step response models; and generalized predictive control [57], which utilizes transfer function models. These advancements have allowed for the effective application of MPC in complex systems with multiple inputs and outputs. MPC technique involves obtaining an optimal control sequence by using the current state of the plant as the initial state and applying the first control from this sequence to the plant. Two main objectives in selecting proper optimal control law are necessary: 1) forming the way of forecast to obtain the best performance, and 2) selecting control action to reach that forecast [58, 59]. Output forecasts in MPC are commonly obtained using dynamic models that describe the behavior of the process [60].

2.5.1 Model Predictive Controller Performance

Generally, the MPC algorithm has two main engines: a state estimator and an optimization problem. A MPC problem At each time, step k should meet the below sequences:

- At $k = 1$, initialize the process with actual state.

- Estimate current state of the process.
- Compute an optimal control sequence by solving MPC optimization problem.
- Let $U = \{u^*(k+1), \cdots, u^*(k+N_p)$ be the solution.
- Apply only $u^*(k+1)$ and discard the remaining optimal inputs, then repeat optimization at time $k+1$.

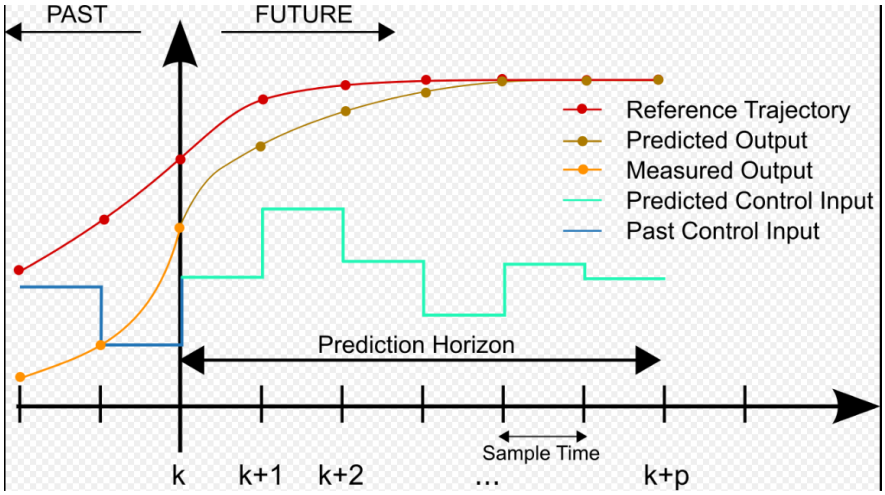

Figure 2.4 MPC illustration (image obtained from the public domain of Wikipedia article on MPC)

2.5.2 MPC applied to greenhouse application

MPC is a highly effective control strategy for smart GHs due to its diverse range of capabilities. It excels in handling the complex dynamics of GHs by utilizing a predictive model, allowing it to anticipate and account for future system behavior [6], [20], [39], [18]. MPC's optimization capability yields optimized control actions based on defined objectives and constraints. By considering inputs such as setpoints, current state, and predictions of future behavior, MPC generates an optimal control sequence for maximizing desired outcomes like plant growth while considering constraints, including energy usage level and resource availability. Furthermore, MPC can handle constraints commonly found in smart GHs, including temperature, humidity, and CO2 levels. MPC is an optimal problem that embodies the constraints of the control optimization process, ensuring that control actions stay within acceptable limits and the system operates within desired boundaries. MPC's adaptability suits

dynamic environments well, as it can quickly adjust control actions based on real-time measurements and predictions. This adaptability allows MPC to effectively respond to changing conditions, such as sudden weather changes or plant growth patterns.

General format of MPC-based Optimization problem formulation applied to GH application

The general mathematical formulation of the optimization problem is expressed as a quadratic cost function to guarantee tracking performance, applied to dynamic states inside of a GH [6, 13].

2.5.3 Common MPC Weaknesses in GH application

Simply saying,MPC needs to be stronger in facing uncertainty. It is natural and rational to incorporate the impact of modelled uncertainty of disturbances, or even unknown-bounded uncertainty, into the prediction model alongside solving optimal control problems. To have relied on nominal forecasts for selecting control actions can lead to an inaccurate operation due to the inevitable deviations from expected values in the controlled variables. Uncertainty significantly influences the optimal control actions in closed-loop predictions, which can lead to a more cautious (pessimistic) or aggressive approach in selecting control actions. So that, the resulting performance levels are also affected by uncertainty [61–63]. Unmodeled dynamics or disturbances cause significant deviation from the nominal model and lead to suboptimal or unstable control behaviour. Robustness analysis in MPC helps to address this weakness. MPC approach deployed on the GH application has been addressed in [13, 18, 20, 38, 39]. All of this research takes advantage of the inherent robustness of closed-loop MPC; however, robustness against uncertainty has remained a challenge that should be considered in the harsh and real-world functioning of GH. The [17] article is just the only work in which the author used model predictive considering real constraints on uncertainty in a semi-closed GH. Thus, it is worth conducting studies on handling constraints in a MPC problem related to GH and the cluster of GH applications.

2.6 Robust concept in Model Predictive Control

Robust control strategies, such as robust control theory, offer effective solutions for achieving robust operation in a contaminated environment with uncertainty. However, a computational price should be paid for robustifying a MPC controller. Many efforts have been made to develop computationally efficient and less pessimistic robust optimization tools within the

framework of MPC, considering feasible and solvable constraints. Ensuring the robustness of an MPC controller is crucial for handling uncertainties, model mismatches, disturbances, constraints, and faults. Robustness enhances the reliability, stability, and performance of the controller, enabling effective control in challenging conditions of operating [64], [65], [66], [47].

2.6.1 Introducing a RMPC problem

A RMPC problem focuses on robust tracking of the desired reference setpoints despite uncertainties and disturbances. Several critical components are considered to formulate a robust tracking mechanism within a predictive model. Primarily, a system dynamics model is established, capturing the relationship between control inputs, system states, and outputs while accounting for uncertainties or disturbances. Next, a desired reference trajectory or setpoint is specified for the system output. An objective function is formulated to minimize the tracking error between the system output and the reference trajectory, considering constraints on uncertainties and disturbances robustly [67], [68].

Constraints on control inputs, system states, or outputs are deployed into the MPC problem formulation, ensuring adherence to rules of physical limits or operational limitations. The MPC problem is then formulated as a constrained optimization problem, where control inputs are computed by minimizing the robust objective function, subject to system dynamics and constraints. The optimized control inputs over the prediction horizon are implemented in a receding horizon manner, where only the first control input is applied at each control interval. By actively adapting to uncertainties and disturbances, the robust tracking MPC controller ensures that the system tracks the reference trajectory within specified limits. Robustness can be achieved by incorporating uncertainty models, worst-case analysis techniques, robust optimization, or disturbance rejection mechanisms within the MPC framework [69], [70], [71].

Among numerous developed versions of MPC, like adaptive, gain-scheduling, data-enabled, data-driven, etc., we select RMPC. As mentioned, studying real constraints in RMPC problems is a new concept in clustered GH applications. In deploying robust ideas on a MPC problem against two types of disturbance on state and measurement noises, discrete-time and linear time-invariant uncertain systems and nominal counterpart of the system are considered [68, 71]:

$$\Delta = \begin{cases} x_{k+1} = \boldsymbol{A}x_k + \boldsymbol{B}u_k + \boldsymbol{H}w_k \\ y_k = \boldsymbol{C}x_k + \boldsymbol{D}u_k + \boldsymbol{I}v_k \end{cases} \tag{2.1}$$

$$\overline{\Delta} = \begin{cases} \overline{x}_{k+1} = \boldsymbol{A}\overline{x}_k + \boldsymbol{B}u_k \\ \overline{y}_k = \boldsymbol{C}\overline{x}_k + \boldsymbol{D}u_k \end{cases} \tag{2.2}$$

where x_k (or $\overline{x}_k$) $\in \mathbb{R}^n$, and $u_k \in \mathbb{R}^{n_u}$, and y_k (or $\overline{y}_k$) $\in \mathbb{R}^{n_y}$ are the state, the control input and output in uncertain (or nominal) representations respectively, while $\forall k \in \mathbb{Z} \geq 0$.

In (2.1) system is exposed to two types of uncertainties that are impacting the state and output measurement. $w_k \in \mathcal{W} \subseteq \mathbb{R}^{n_w}$, and $v_k \in \mathcal{V} \subseteq \mathbb{R}^{n_v}$, are uncertainty of disturbances of process and measurement respectively. In MPC, these uncertainties are represented by determining bounded sets, named set-membership concept (in section 2.6.2 uncertainty bounds are described).

We also assume that the nominal ($\overline{\Delta}$) and real-world (Δ) systems are observable and stabilizable. Uncertain variables are w_k and v_k, that can be defined in vector shape ($\zeta_k^T = [w_k^T, v_k^T]$). The exogenous disturbances with prediction steps in MPC can be expressed as $v_{[0,i-1]|k}$, $w_{[0,i-1]|k}$ [67, 72]. Constraints are considered on states, input, output, and uncertainties and generally are expressed as mixed constraints [17]. The mixed constraint is mapped into the MPC problem so that it is involved in solving the optimization problem in each step. The general format of this constraint is as follows:

$$r_{ij}(x_{j|k}, u_{j|k}, \zeta_{j|k}, y_{j|k}) \leq f, \forall j \in \mathbb{Z}_{[0,N_p-1]}, \forall i \in \mathbb{Z}_{[0,N_c^j]} \tag{2.3}$$

N_p is the MPC problem's prediction horizon, and N_c^j is the number of constraints in step $j, j \leq k$. Each of these aspects significantly affects the closed-loop performance, leading to increasing computational time and complexity in computation. Considering two equations of (2.1), and (2.2), we can launch two MPC problems, which are expressed by $\mathcal{O}(k)$, and $\overline{\mathcal{O}}(k)$ respectively. In below two $\mathcal{O}(k)$, and $\overline{\mathcal{O}}(k)$ can be found:

$$\mathcal{O}(k) = \begin{cases} \min\limits_{u_[0,N_p-1]|k} G(x_k, u_{[0,N_p-1|k]}, \zeta_{[0,N_p-1]|k}) \\ \qquad s.t. \\ x_{j+1|k} = \boldsymbol{A}x_{j|k} + \boldsymbol{B}u_{j|k} + \boldsymbol{H}w_{j|k}, \\ y_{j|k} = \boldsymbol{C}x_{j|k} + \boldsymbol{D}u_{j|k} + \boldsymbol{I}v_{j|k}, \\ r_{ij}(x_{j|k}, u_{j|k}, \zeta_{j|k}, y_{j|k}) \leq f, \\ \forall j \in \mathbb{Z}_{[0,N_p-1]}, \forall i \in \mathbb{Z}_{[0,N_c^j]}, \\ x_{0|k} = x_k, \end{cases} \quad \overline{\mathcal{O}}(k) = \begin{cases} \min\limits_{u_[0,N_p-1]|k} G(\overline{x}_k, u_{[0,N_p-1|k]}, 0) \\ \qquad s.t. \\ \overline{x}_{j+1|k} = \boldsymbol{A}\overline{x}_{j|k} + \boldsymbol{B}u_{j|k}, \\ \overline{y}_{j|k} = \boldsymbol{C}\overline{x}_{j|k} + \boldsymbol{D}u_{j|k}, \\ r_{ij}(\overline{x}_{j|k}, u_{j|k}, \overline{y}_{j|k}) \leq f, \\ \forall j \in \mathbb{Z}_{[0,N_p-1]}, \forall i \in \mathbb{Z}_{[0,N_c^j]}, \\ \overline{x}_{0|k} = \overline{x}_k, \end{cases} \tag{2.4}$$

Where objective function $G(.)$ is generally in the form of a standard quadratic cost function (Or LQR function if prediction and control horizon are equal), which comprises two segments:1) cost on moving horizons and 2) cost on the terminal to perform in maximum minimization on deviated states:

$$\begin{aligned} G(x_k, u_{[0,N_p-1|k]}, \zeta_{[0,N_p-1]|k}) &= \sum_{j=0}^{N_p-1} l_r(x_{j|k}, u_{j|k}) + Q_{tr}(x_{k+N_p}) \\ &= \sum_{j=0}^{N_p-1} x_{j|k}^T \boldsymbol{Q} x_{j|k} + u_{j|k}^T \boldsymbol{R} u_{j|k} + x_{N_p|k}^T \boldsymbol{Q}_{tr} x_{N_p|k} \end{aligned} \tag{2.5}$$

As it was mentioned, in (2.5), l_r segment is *cost to go* function, and l_{tr} is the terminal cost.

Therefore, RMPC problem is an approach that turns the MPC problem into robust. In $\Delta((2.1))$, all constraints ($r_{ij}(.)$) should be considered in solving the optimization problem of $\mathcal{O}(k)$ to generate optimal control sequences. Risk mapping is used to map real systems into nominal systems while considering cost functions on the **terminal** and **cost to go** [67].

2.6.2 Uncertainty representation for RMPC

Context

As we already know, due to a lack of complete knowledge about recognizing and analyzing uncertainty of disturbances in the real world, uncertainty set(s) is (are) typically defined as bounded variations or Worst-Case (WC)-Scenarios in deterministic MPC, so that it affects the system dynamics. Thus, the main objective in handling uncertainty within the deterministic

MPC framework is to design a controller that ensures robust performance under the worst-case conditions. Uncertainty of disturbances, as most portion of the existing uncertainty in the system, cannot be ignored. The uncertainties are described by upper- and lower-bounding the worst-case variations or magnitudes of disturbances [73], [74], [75], [76]. Robust optimization techniques are then deployed to incorporate these uncertainties into the MPC formulation, aiming to produce optimized control actions that minimize worst-case cost or error under the given uncertainty bounds. WC analysis identifies critical scenarios leading to the most considerable system deviations or tracking errors. This analysis allows the controller to design control actions that guarantee robust performance in those scenarios. Due to placing constraints tightening technique as bounds, the deterministic approach introduces conservatism in control design to ensure robustness by keeping proper trade-offs between conservatism and speed of computation [59], [76].

Note: It has been assumed that uncertainty does not affect the system dynamic (internal dynamic). So, only the exogenous type of uncertainty is taken into account.

External uncertainties modeling

The system is impacted by outside (exogenous) uncertainties; v_k in (2.1), represent external uncertainties. Various and well-known ways exist to model external uncertainty effects [64, 65, 73]. Among them, the uncertainties with the finite range of realization are studied. In this case, the uncertainties set is countable (finite), so that these are selected from space, and then they affect the plant endogenously:

$$\Delta = \begin{cases} x_{k+1} = \boldsymbol{A}x_k + \boldsymbol{B}u_k + \boldsymbol{H}w_k \\ y_k = \boldsymbol{C}x_k + \boldsymbol{D}u_k + \boldsymbol{I}v_k \end{cases} \tag{2.6}$$

in which $w_k \in \mathcal{W}$ and $\mathcal{W} := \text{Co}\{w^1, w^2, \ldots, w^{N_n}\}$, and in the same way $v_k \in \mathcal{V}$ and $\mathcal{V} := \text{Co}\{v^1, v^2, \ldots, v^{N_n}\}$, where N_n is the number of vertices, Co is abbreviation of convex hull or compact convex polytope (Briefly, it is called "polytope" for being simple).

2.6.3 Set-membership utilization in recursive state estimator

A technique should be devised to obtain guaranteed bounds on the actual value of a system's state or parameters while using a state estimator in the presence of disturbances of the real. Set membership quantifies the uncertainty or error in the estimated values by defining them as intervals or sets rather than single-point estimates. The mentioned set or interval contains the actual value with a certain level of deviation from a nominal value to achieve acceptable

transient time and proper asymptotic behavior [77]. This approach is advantageous when the system or measurement noise is unknown but bounded [73, 78]. Polytopes, or ellipsoids, construct the set membership. For being simple, literature selects an ellipsoid shape, and then any shape can be obtained out of the ellipsoid [79, 80]. The idea of recursive state estimation under set membership was represented in [79] and then followed in [77]. Much research has been conducted on discrete-time concepts [65] f original work in recent years. The discrete-time state estimator for set membership is an algorithm that operates in discrete time and provides set-based estimates of the system's state.

Set-membership Representation: Representation of set-memberships(bounds) based on dynamics of states and inputs as like as below mathematical expressions:

- **Set-membership on initial state:**

$$\widetilde{\Omega}(x_0) = (x - \overline{x}_0)^T \Omega^{-1} (x - \overline{x}_0) \leq 1, \quad \Omega = \Omega^T \geq 0, \quad \Omega \in \mathbb{R}^{n_x \times n_x}$$

  where $\overline{x}_0$ represent the expected state of x_0, placed in **center** of ellipsoid. Initial state x_0, $k = 1$ is unknown, but inside $\widetilde{\Omega}$, so that $x_0 \in \widetilde{\Omega}(x_0)$.

- **Set-membership on inputs (unknown but bounded):** Inputs have two bounds, so that the first bound is ellipsoid and the second is named energy of inputs.

$$\begin{gathered} E_u = \{u_k^T \mathcal{Q}_u^{-1} u_k \leq 1\}, \quad \mathcal{Q}_u = \mathcal{Q}_u^T \geq 0, \quad \mathcal{Q}_u \in \mathbb{R}^{n_u \times n_u}, \quad k = 1, 2, \ldots, N_p - 1 \\ \int_{t_k}^{t_{k+1}} u_k^T \mathcal{Q}_u^{-1} u_k \leq t_{k+1} - t_k \end{gathered} \tag{2.7}$$

- **Measurement noise (observation error $v_k \in \Pi$, unknown but bounded):**

$$E_v = \{v_k^T \mathcal{R}^{-1} v_k \leq 1\}, \quad \mathcal{R} = \mathcal{R}^T \geq 0, \quad \mathcal{R} \in \mathbb{R}^{n_y \times n_y}, \quad k = 1, 2, \ldots, N_p - 1 \tag{2.8}$$

- **Process noise ($w_k \in \mathcal{W}$, unknown but bounded):**

$$E_w = \{w_k^T \mathcal{Q}^{-1} w_k \leq 1\}, \quad \mathcal{Q} = \mathcal{Q}^T \geq 0, \quad \mathcal{Q} \in \mathbb{R}^{n_w \times n_w}, \quad k = 1, 2, \ldots, N_p - 1 \tag{2.9}$$

We assumed that $w_k \in \mathcal{W}$, $v_k \in \Pi$, there are exists bounded ellipsoid sets (ellipsoid set shape encounters polytope set shape), contained disturbances w_k and v_k, so that we have:

$$w_k \in E_w, \quad v_k \in E_v \quad \forall k \in \mathbb{Z} \geq 0 \tag{2.10}$$

where N_p is prediction horizon.

Note: It should be noted t_k and k have the same meaning in literature, both of them are representing step k, for instance $x(t_k) \equiv x_k$.

2.7 Overview of RMPC approaches in literature

In this section, we will discuss and categorize different literature that contributes to RMPC problem. One particular group of early works, closely associated with the field of WC-MPC is called "pursuit-evasion problems." These works found in [81–84], are closely linked to the advancements in optimal control theory. The pursuit-evasion problems in RMPC deal with situations where one entity (the pursuer) aims to track or control another entity (the evader) while considering uncertainties and disturbances. These problems often involve finding control strategies that minimize the WC-scenario. The other works specifically focused on the receding horizon approach were studied in references [85–88]. Among these works, references [86,88] presented the WC-MPC problem formulation for nonlinear and Differential-Algebraic Equation (DAE) systems, respectively. These contributions elegantly established the foundation for applying WC-MPC in a receding horizon fashion. Additionally, [87] focused on analysing robust performance in the frequency domain.

In [80], the researcher presents a robust stability proof that follows a similar approach to the standard stability arguments used in nominal MPC problems. This demonstrates how robust stability can be ensured in the context of RMPC by employing techniques for analyzing stability in traditional MPC. Another significant contribution to guaranteeing the robust stability property in RMPC is described in [89, 90]. These works utilize Linear Matrix Inequality (LMI)s to address polytopic or parametric internal uncertainties in RMPC problems to achieve robust stability by bounding the cost function and employing positive invariance arguments to enforce constraints on the future trajectory.

Furthermore, the two-level controller achieves robustness against uncertainties and disturbances while optimizing control performance, offering an effective solution for addressing complex control problems. Also, the development of min-max MPC formulations with cost functions expressed as linear norms [91–94]. These works investigate the use of linear norms as cost functions, allowing for the optimization of control actions while considering worst-case scenarios. Moreover, a comprehensive discussion on the application of linear programming techniques in the domain of MPC could be addressed in [95]. The tables below are provided to address conducted research.

Table 2.1 Different type of constraints in MPC formulation

	Constraint Handling Techniques		
	Lipschitz bounding	Tube	RPI set
References	[96], [97], [86], [98], [99], [100], [101], [102]	[67], [103], [104], [105], [106], [53], [107], [108], [109]	[110], [111], [112], [113], [80], [89], [114], [115], [116]

Table 2.2 Control parametrization methods in different resources

	Control Systems Parameterization			
	Feedback stabilizing	Feedback parametrization	control policy	control sequence
References	[117], [111], [118], [119], [103], [120], [113]	[121], [100], [108], [122], [101], [123], [124], [78], [122]	[125], [126], [127], [128], [109], [129]	[109], [114], [130], [131], [132], [133]

Table 2.3 Type of uncertainty of disturbances, mentioned in various references

	Various Type of Uncertainty of Disturbances			
	External	Polytope / ellipsoid	measurement noise	process noise
References	[134], [101], [135], [124], [123], [108]	[98], [86], [89], [94], [75], [110]	[109], [132], [87], [67], [72]	[97], [136], [113], [112], [117], [116]

Table 2.4 Deployed feedback policy in RMPC approach across various resources

	Systems Feedback Model			
	Linear		Nonlinear	
	State Feedback	Output Feedback	State Feedback	Output Feedback
References	[134], [101], [135], [124], [123], [108], and most of references	[72], [110], [111], [137], [67], [87], [136]	, [98], [86], [96], [138], [139], [140], [141]	[130], [109], [142], [131]

Recursive state estimation

context

Recursive state estimation algorithms like the KF combine two main steps. For instance, KF is to find an estimation of the system's state by recursively combining the predictions based on the system model with the measurements obtained from sensors. A high-level overview of how the KF works [143, 144] expresses that four steps should be respected in recursive state estimations. These four are Initialization, Prediction, Update, and Repeat. In the real world, the filter considers the uncertainties associated with the model predictions and the measurement, using statistical properties to weight their contributions appropriately. Uncertainty of disturbances should be bounded; however, it would be unknown. For that reason, the set-membership mechanism deployed is bound to guarantee proper functioning on the state estimator.

In order to describe the dynamic of systems, we consider the representation of a first-order dynamic equation, which is like upcoming Linear Time Invariant (LTI), discrete-time, in the presence of uncertainty [79, 145] :

$$x_{k+1} = \boldsymbol{A}x_k + \boldsymbol{B}u_k + \boldsymbol{H}w_k, \quad x_0 = x(0) \tag{2.11}$$

$$y_k = \boldsymbol{C}x_k + \boldsymbol{I}v_k \tag{2.12}$$

where $x_k \in \mathbb{R}^{n_x \times 1}$ is the state of current time step, likewise $x_{k-1} \in \mathbb{R}^{n_x \times 1}$ is the state of previous time step, $u_k \in \mathbb{R}^{n_u \times 1}$ is a known input and $w_k \in \mathbb{R}^{n_u \times 1}$ is **White Gaussian** noise with zero mean.To obtain a correlation between the *Now*-state and *Previous*-state at each time step, mean of the random variable should be taken. Thus, it is:

$$\overline{x}_{k+1} = E(x_{k+1}) = \boldsymbol{A}\overline{x}_k + \boldsymbol{B}u_k \tag{2.13}$$

where, $\overline{x}_k$ is the expected state or Nominal state.

Robust KF using Huber function: To Minimize estimate deviation from nominal value

Outputs Y_k and states X_k in vector format are expressed as follows: (Note that the vector format is needed in computer implementation for clustered entities in this study.)

$$Y_k = \begin{bmatrix} y_{1k} \\ y_{2k} \\ \vdots \\ y_{ik} \end{bmatrix}_{\mathbb{R}_{n_y \times 1}}, X_k = \begin{bmatrix} x_{1k} \\ x_{2k} \\ \vdots \\ x_{ik} \end{bmatrix}_{\mathbb{R}_{n_x \times 1}}$$

where, y_{ik} is the ith array of vector Y_k, and x_{ik}^T in the ith row of X_k. Relation between Y_k and X_k would be:

$$Y_k = X_k \alpha_k + \beta_k, \tag{2.14}$$

where $\alpha_k = x_k$, and $\beta_k = -Z_k E_k$, while Z_k is obtaining from Cholesky decomposition and E_k is estimation error. Solution of 2.14 would be [146]:

$$\widehat{\alpha}_k = (X_k^T X_k)^{-1} X_k^T Y_k \tag{2.15}$$

$$Ex\{(\alpha_k - \widehat{\alpha}_k)(\alpha_k - \widehat{\alpha}_k)^T\} = (X_k^T X_k)^{-1} \tag{2.16}$$

where $Ex.$ is expectation occurring.

Minimization problem is carried out by M-estimation approach on [147]:

$$\widehat{\alpha}_k = \min_{\alpha} \sum_{i=1}^{n} \sigma(y_{ik} - x_{ik}^T \alpha_k) \tag{2.17}$$

and σ is named Huber score function that has responsibility of filtering out-spikes. Simply put, for representing Huber function, it has been given:

$$\sigma(y(x_k), y(\widehat{x}_k)) = \begin{cases} \frac{1}{2}(y(x_k) - y(\widehat{x}_k))^2, & \text{for } |y(x_k) - y(\widehat{x}_k)| \leq a \\ a(|y(x_k) - y(\widehat{x}_k)| - \frac{1}{2}a), & \text{Otherwise} \end{cases} \tag{2.18}$$

It is worth mentioning that the Huber loss function (Huber function) filters significant deviations. This function has been deployed to set a robust KF.In most cases, ordinary KF has two main problems: 1) losing adjustments in tuned output measurements in continuously facing high magnitude error in estimating mechanism, and 2) wasting time on excessive computation because of high magnitude error of estimation [147], [79]. Hence, minimizing the deviations by utilizing the Huber filter helps cut off extreme errors and reduces the effect of two issues of typical KF deployment.

2.8 Robust Model Predictive Control utilizing recursive state estimation

The last section of this Chapter explains three steps of setting a RMPC problem while considering the robust functioning of the recursive state estimator.

Step 1: System representation

Representation of first order dynamic equation is like linear time invariant (LTI), discrete-time in (2.11), and (2.12), where $x_k \in \mathbb{R}^{n_x}$ is system state vector,$u_k \in \mathbb{R}^{n_u}$ is control input,$y_k \in \mathbb{R}^{n_y}$ is output vector,$w_k \in \mathbb{R}^{n_w}$ is an unknown state disturbance,$v_k \in \mathbb{R}^{n_y}$ is an unknown output disturbance, and ($\boldsymbol{A}$,$\boldsymbol{B}$,$\boldsymbol{H}$,$\boldsymbol{C}$) are determined and known well-defined matrices. System performance is being impacted by measurement noise placed in output and process noise in state dynamic. Considering unknown and bounded noises:

$$w_k \in \mathcal{W}, \quad v_k \in \Pi, \quad \forall k \in \mathbb{Z} \geq 0 \tag{2.19}$$

In which $\mathcal{W}$ and Π are polytope spaces, encompassing $(0, 0)$.

We consider input and state mixed-constraint as like the following inequality in which coefficient matrices have appropriate dimensions [17], [65]:

$$\boldsymbol{F}x_k + \boldsymbol{G}u_k \leq \boldsymbol{f}, \tag{2.20}$$

Step 2: Constrained Optimal Control Problem

To design a robust MPC, estimation of states is obtained through a recursive procedure with devising bounds and regions in space to guarantee proper behavior of steady-state and stability, respectively. The core of the process has two sides:

1. Feedback Policy: To identify and implement a state feedback policy that is suitable for controlling system with an infinite number of dimensions,
2. Set-membership determination: To take into account the impact of the most severe disturbances in the process of calculating the expected uncertainties in the course of attempting to solve the optimal control problem within a limited time frame,

As mentioned earlier, the three objectives are elaborated in the following sections to achieve robustness.

Control policy approximation: Signal Decomposition

We consider the same policies of affine state feedback as articles:

$$u_k(\widehat{x}_k) = \boldsymbol{K}(\widehat{x}_k - s_k) + \mu_k \tag{2.21}$$

In which $K \in \mathbb{R}^{n_u \times n_x}$ is a fixed feedback gain, $(\widehat{x_k})$ is nominal state and μ_k is the nominal state, and μk is the auxiliary control input ("offset"). According to the feedback policy definition, estimation of the state is a nub that can provide the closed-loop system with feedback signals due to the absence of an actual state of the system. It is clear that the parametrization of (2.21), allows the decompose dynamic of states into two categories: 1) nominal state and 2) error state. The error of estimation is defined as:

$$e_k = (\widehat{x}_k) - x_k \tag{2.22}$$

Thus, taking the uncertain state is like $\zeta_k \equiv x_k - s_k$. With considering two equations (2.11), the dynamic of systems can be written in the form of (after decomposing the nominal section and actual state):

$$s_{k+1} = \boldsymbol{A}s_k + \boldsymbol{B}\mu_k, \quad s_0 = \overline{x}_0 \tag{2.23}$$

$$\zeta_{k+1} \ = \boldsymbol{\Psi}\zeta_k + \boldsymbol{H}w_k + \boldsymbol{BK}e_k, \quad \zeta_0 = -e_0 \tag{2.24}$$

where $\Psi := (\boldsymbol{A} + \boldsymbol{BK})$. s_k is the uncertainty-free nominal state, while the uncertain state also consists of process noise and offset. Considering (2.21), and (2.22), mixed-constraint inequality would be transformed into:

$$\boldsymbol{F}s_k + \boldsymbol{G}\mu_k + (\boldsymbol{F} + \boldsymbol{GK})\zeta_k + \boldsymbol{GK}e_k \leq \boldsymbol{f}, \tag{2.25}$$

It should be noted that mixed-constraint inequality(2.25) must be satisfied $\forall w_k \in \mathcal{W}$ and $\forall v_k \in \Pi$. Therefore, (2.25) is substituted instead of all feasible model parameter sets. To this end, the feedback policy (2.21), and decoupled dynamic of the system in (2.23) and (2.24) help us to formulate the optimal problem into the following optimal control:

$$\begin{gathered}
J^*(x(0)) = \min_{v(0),v(1),\ldots} \sum_{k=0}^{\infty} l(s_t, v_t) \\
s.t. \\
\begin{bmatrix} s_{k+1} \\ \zeta_{k+1} \end{bmatrix} = \begin{bmatrix} \boldsymbol{A} & 0 \\ 0 & \boldsymbol{\Psi} \end{bmatrix} \begin{bmatrix} s_k \\ \zeta_k \end{bmatrix} + \begin{bmatrix} \boldsymbol{B} \\ 0 \end{bmatrix} \mu_K + \begin{bmatrix} 0 \\ \boldsymbol{H} \end{bmatrix} w_K + \begin{bmatrix} 0 \\ \boldsymbol{BK} \end{bmatrix} e_k, \\
\boldsymbol{F}s_k + \boldsymbol{G}\mu_k + (\boldsymbol{F}+\boldsymbol{GK})\zeta_k + \boldsymbol{GK}e_k \leq \boldsymbol{f}, \\
\forall w_k \in \mathcal{W}, \forall v_k \in \Pi \\
s_0 = \overline{x_0}, \quad k = 0, 1, 2, \cdots,
\end{gathered} \tag{2.26}$$

in which e_k is error of state estimate at step k.

Set-membership: Bounds on allowable level of deviation in state estimation by error

Recall 2.6.3 section, on error ellipsoid bound can be defined:

$$w_k \in E_w, \quad e_k \in E_e, \quad k = 1, 2, \dots \tag{2.27}$$

where $E_w \equiv \{\gamma | \gamma \boldsymbol{Q}^{-1} \gamma^T \leq 1\}$ and $E_e \equiv \{\varphi | \varphi \boldsymbol{R}^{-1} \varphi^T \leq 1\}$ are including disturbances of $\mathcal{W}$ and Π respectively.

After the first step in the control horizon of state propagating, **measurement update**, obtain measurements from sensors at each time step. It uses these measurements and the measurement equation from the system model to update the set representing the current state estimate. This update is typically performed by incorporating the measurement noise and the uncertainty associated with the measurements. Finally, it **Repeats** the iteration through the measurement update and state propagation steps at each time step to update the set representing the state estimate recursively. The estimation accuracy improves as new measurements are incorporated into the estimation process. A general policy of state estimation in the presence of uncertainty has been provided. This gives the ability to use the set-membership technique in RMPC.

Step 3: Robust Model Predictive Control problem with recursive state estimation method in finite time:

This step implements robust model predictive control regarding the three steps above [148].

$$\begin{gathered}
J^*_{n \to n+N_p}(s^i_n) = \\
\min_{\mu^i_{n|n}, \cdots, \mu^i_{n+N_p-1|n}} \sum_{i=1}^{m} \sum_{k=n}^{n+N_p-1} [l(s^i_{k|n}, \mu^i_{k|n}) + Q(s^i_{n+N_p|n})] \\
s.t. \\
s^i_{k+1|n} = A s^i_{k|n} + B \mu^i_{k|n}, \\
F s^i_{k|n} + G \mu^i_{k|n} \leq f - \Gamma \zeta_n - GK e_k, \\
\forall \zeta_n \in \Theta, \forall e_k \in E_k, \\
s^i_{n|n} = s^i_n, s^i_{n+N_p} \in \mathbf{S} \\
k = n, \cdots, n + N_p - 1
\end{gathered} \tag{2.28}$$

where $l(s_{(.)}, \mu_{(.)})$ is the cost function for selecting proper inputs for attaining the nominal state of dynamic and $Q(s_{(.)})$ is terminal cost; $\Gamma := (F + GK)$; Θ is a set on error dynamics in state estimation , in which $\Gamma\zeta_n = \max_{\zeta_n \in \Theta} \Gamma$ and $GKe_k = \max_{e_k \in E_k} GK$ according to mixed-constraint equation (2.25), and $\mathbf{S}$ is the terminal constraint set, and m is the number of entities in which the objective function is implemented.

CHAPTER 3 GENERAL ORGANIZATION OF THE DOCUMENT

Here, in Chapter 3, the general organization of the study is presented. According to the outline of the research, all objectives have been addressed. An introduction and a literature review have been presented in two previous chapters. Chapter 1 introduces motivation, background, problem statement, research objectives, and dissertation outline. In Chapter 2, a literature review of prior studies has been conducted. In that chapter, smart agricultural GH, the type of GHs, components inside GH, and the theoretical robustness in model predictive control against uncertainty of disturbances have been reviewed.

In Chapter 2, recursive state estimation under uncertainty was also mentioned, and then RMPC-recursive state estimation is equipped with the Huber score function to tackle the high amplitude of disturbances of uncertainty. Then, it is developed into a cluster of GH applications. RMPC in previous research on a GH application was computationally demanding. Thus, firstly, computational demand is compensated using a state estimating engine, and secondly, level uncertainty coming from high-magnitude errors is significantly reduced. In the end, due to having mathematical descriptions of independent GHs in a cluster layout, accessibility to monitoring and measuring signals is showing more practical feedback.

Moreover, RMPC based on recursive state estimation technique regarding harsh uncertainty filtering is an effective way to increase the feasibility of solution in constrained optimization. In practical applications, constrained optimization addresses the inherent uncertainty of disturbances; however, the imposition of constraints concurrently elevates the risk of feasible solution and augments computational time. Therefore, it is essential to attain more effective solutions to alleviate the impact of disturbances. In Chapter 4, an Article on this research is presented, which has been submitted to IEEE Transactions on Control Systems Technology.

In Chapter 4, simulations considering the proposed algorithm and one of the high-performance methods on GH applications are compared. Furthermore, the proposed method is deployed in a cluster of GHs. In addition, the feasibility region and convergence time of the two ways are illustrated. Then, in Chapter 5, controlling performance on results will be discussed. Finally, Chapter 6 proposes conclusions and recommendations for future work.

CHAPTER 4 ARTICLE 1: ROBUST MODEL PREDICTIVE CONTROL FOR THE OPTIMAL OPERATION OF A CLUSTER OF SMART GREENHOUSES

INDOOR ENVIRONMENT

Authors: Ehsan Ghorbani, Hanane Dagdougui, Ahmed Ouammi
Submitted at IEEE Transactions on Control Systems Technology, on July 27, 2023.

4.1 Abstract

Smart greenhouses can be defined as cutting-edge technological systems that efficiently control indoor climate conditions to shield crops from harsh outdoor conditions in order to increase their productivity. In this paper, we develop and implement a robust model pre-dictive control approach that relies on a recursive state estimation method to cope with the impact of measurement and process signal errors. The aim of this approach is to optimally control the internal environment of intelligent greenhouses. A feedback policy problem is decomposing signals for the accessibility of uncertainties. Then, a robust feasibility set can be defined by determining the ellipsoid set on uncertainty to obtain solvable constrained optimization in the CPLEX solver. In the overall formulation, each greenhouse is consid-ered an independent element. This method can improve the quality of set point tracking while reducing the computation time required to arrive at a solution. Extensive numerical simulations involving the application of an innovative and robust algorithm to a cluster of greenhouses were conducted to demonstrate the algorithm's performance and effectiveness.

4.2 Introduction

GHs have received attention as viable and controllable technological systems that are capable of responding to the ever-increasing demand for food while minimizing concerns related to harsh environmental conditions and traditional agriculture methods. The growing human population is putting pressure on resources, especially potable water and cultivable lands. GHs are a reliable, fast, and effective means of coping with food crises by setting indoor crop conditions to maximize productivity [149], [150]. GHs need to operate like controllable facilities to be able to control crop conditions, including the level of CO_2, the amount of irrigation, the indoor temperature, the humidity level, the lighting, the ventilation, and heating and cooling, in real time. Growing demand for food requires using a large cluster of smart GHs. These GHs can be coordinated in a centralized or distributed/decentralized

fashion [13], [18]. Note that GH functionality changes in accordance with the types of crops grown [20]. When the number of GHs increases quickly, their energy consumption will increase considerably [46]. To respond interactively to an ever-growing increase in GH energy demand, RESs and interconnected Energy Storage Systesm (ESS)s [18], [20] are attracting attention as a sustainable means of providing some of the energy needed and reducing the amount of CO_2 emissions produced.

PV power generation's dependency on weather conditions can be compensated for with a battery energy storage system (BESS) to diminish the level of impact the weather has on controlling essential states. Using a BESS also contributes to better energy management modeling for the entire GH [18], [17].

4.3 Literature review

Satisfying a control method criterion for numerous GH states, including temperature, CO_2 concentration, humidity level, and water level, with complicated relationships is the main difficulty hindering the attainment of a desirable control model to simultaneously handle interdependent dynamics. Worst, uncertainty and disturbances related to outside temperature, weather conditions, and errors are very problematic for maintaining proper indoor conditions and reasonable energy consumption levels [13]. Several controlled studies have been conducted, including on the optimal control [6] and nonlinear control [137], [151] of temperature, but uncertainty still needs to be investigated. In [66], [17], and [11], robust optimal controls are proposed to describe complicated relationships between GH parameters.

In [13] and [20], an MPC approach is implemented to model heating and irrigation in several agricultural applications. These works do not consider uncertainty in the controlling approach due to the marginally robust behavior of typical MPC.

The authors of [152] investigated using an MPC framework for MG control, and demonstrated acceptable optimization in a receding horizon to coordinate preplanned demand. However, in the presence of RES uncertainty and changing conditions, their framework performed poorly. In [13], a centralized MPC (CMPC) approach was used to predict RES generation and demand patterns in order to reduce the amount of variation in the predetermined scheduling of energy demand by a cluster of GHs. However, this work also does not consider uncertainty or disturbances.

Mapping uncertainty as constrained inequality in the MPC formulation should lead to feasibility and closed-loop stability in order to incorporate uncertainty in optimal MPC methods [64]. In [38], a group of GHs that rely on an RES were clustered, and then their integrated

MG was controlled by optimal MPC. However, the real uncertainty constraint consideration is ignored in the optimization formulations.

The authors of [18] considered an Alternating Direction Method of Multiplier (ADMM) that proposes to use a decentralized MPC (DMPC) to control a cluster of GHs. They used a typical type of MPC without considering set membership or uncertainty. Their proposed control approach can be fast enough in closed-loop response, but its lack of genuine robust control would compromise overall stability. On one hand, implementing common MPC without tightening the constraints increases the difficulty of problem solving. On the other hand, the constrained optimization problem is time-consuming, so DMPC might lose its core efficiency when it comes to reacting to sudden changes in GH power consumption and load profile. The authors of [17] proposed a data-driven method that is based on control input and output feedback as a worst-case scenario optimization problem to reduce the conservative reaction of the robustness part of MPC. They tried to approach uncertainty without making an approximation. They did this by considering the polytope definition of uncertainty. Then, uncertainty examinations were controlled by an uncertainty generator (WGIK) in MATLAB software. This can raise two issues: 1) the polytope constraint on the optimization model can be computationally demanding, and 2) the uncertainty engine in [17] can frequently create outliers. However, this is a massive hurdle for feasibility and stability because of the increased computational time and control input cost. In this research, the computationally demanding reaction is alleviated by adding slack to the state constraint. Considering the GH structure is semi-closed, the harshness of disturbances cannot be ignored. Again, in this way, the outlier could degrade the overall efficiency of MPC.

In this paper, we investigate a RMPC method and extend recursive state estimation [153], [79] with the robust orientation of the Huber function [146] to dampen the effect of outlier disturbance, which is a novel way of controlling the cluster of GHs application.

4.4 Contributions

In this paper, we develop an RMPC method and extend it with a recursive state estimation approach to consider robustness against outliers and then make adaptive-wise set-membership on uncertainty. The process to render RMPC with recursive state estimation can significantly simplify handling the state dynamics of a cluster of GHs and their related constraints over a rolling time horizon. Hence, the main contributions of this work can be summarized as follows:

- Modeling augmented state space dynamics that consider a network of GHs and then

determining a more exact uncertainty set of GH dynamics by defining proper feasible set approximation (polytope to ellipsoid) with adaptive mixed constraints.

- Proposing a robust estimator that is based on a simple Huber function approach and can be deployed to tame outliers as uncertainty, especially in initial states.
- Making computation ten times faster and, in turn, accelerating controller convergence. Being able to quickly control and handle vast amounts of data will be a noticeable challenge when the number and the dimensions of the GHs increase.

4.5 Mathematical Modeling of a Cluster of GHs

In this section, all dynamics are represented in the linear first-order derivative format of the state space model, besides the constraints and limitations on dynamics and input of GH systems. Then, the actual amount of coefficient of dynamics is substituted for mathematical representations.

4.5.1 Cluster of Greenhouses

Fig. 4.1 shows a cluster of GHs integrated in an MG. The MG has PV panels and a BESS. A centralized controller monitors all the GHs' dynamic states, including temperature, CO_2 level, humidity level, lighting, ventilation, reservoir water level, and heating and cooling. The following subsection sets out a mathematical model of the GH components.

4.5.2 GH components modeling

Photovoltaic Solar Panel Modelling

1) Photovoltaic panel modeling: GHs use PV panels to provide some of the power the GHs need. In the case of existing huge GHs, a considerable number of panels may be used to interact significantly with the main power grid. PV power production is denoted as:

$$\tilde{P}_{pv}[k] = \eta_{pv} p_{pv} S_{pv} G[k] \tag{4.1}$$

The output power of a panel is constrained by the lower and upper bounds as follows:

$$\tilde{P}_{pv,min}[k] \leq \tilde{P}_{pv}[k] \leq \tilde{P}_{pv,max}[k] \tag{4.2}$$

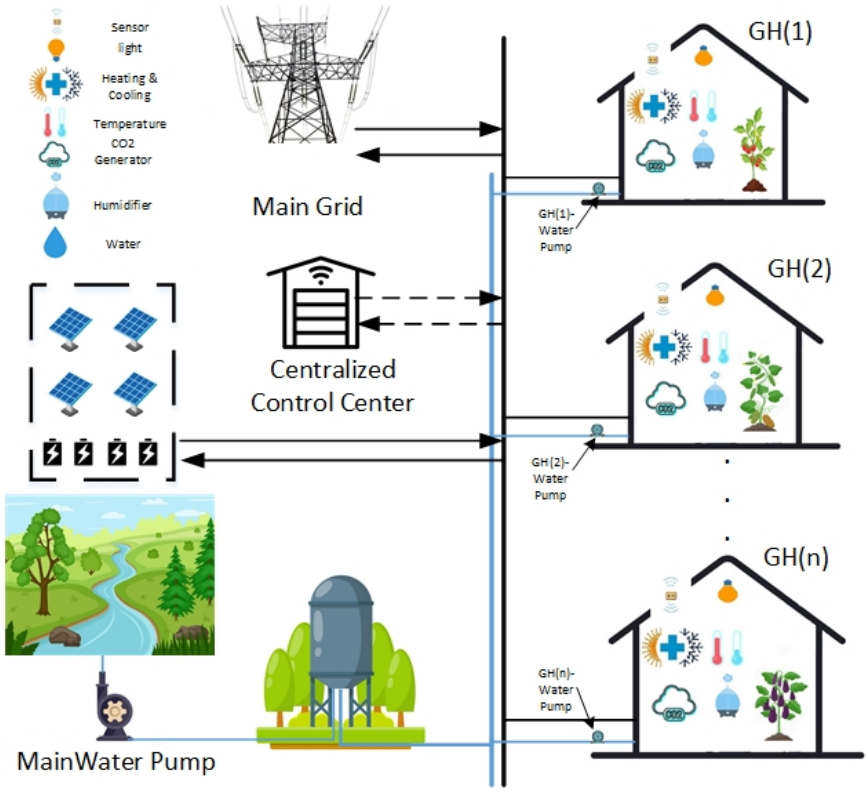

Figure 4.1 Cluster of GH

Where, p_{pv} is Packing factor, S_{pv} is surface of PV panels of i's greenhouse[m^2], η_{pv} is efficiency greenhouse i's PV panels, and G is solar radiation[W/m^2].

PV panel characteristics and specifications

Technical specification of solar PV panels has been selected according to the datasheet in reference [154]. In this application, a maximum of 90 PV panels have been deployed.

Battery Energy Storage System(BESS)

2) Energy storage system: The ESS fulfills several essential roles, including compensating for the intermittency of PV power generation, powering the GHs' components, and decreasing the GHs' dependence on the main grid. The ESS can be dynamically represented in the form of state space as [155]:

$$x_{b,soc}[k+1] = x_{b,soc}[k] + (\eta_{cha} P_{b,cha}[k\Delta t - \frac{1}{\eta_{dis}} P_{b,dis}[\Delta t]) - (x_b^{loss}[k] + x_b^{degr}[k]) \qquad (4.3)$$

Where, η_{cha} is charging efficiency , η_{dis} is charging efficiency of BESS, $x_{b,soc}$ is state dynamic, x^{loss} is loss dynamic, x^{degr} is degradation dynamic of BESS; $P_{b,cha}$ is charging power and $P_{b,dis}$ is charging power of BESS[kW].

By considering a binary parameter $\delta^b[k] \in \{0, 1\}$, the relationship between power and state of charging (SOC) can be expressed as:

$$\begin{cases} 0 \leq P_{b,cha} \leq \delta^b[k] P^{max}_{b,cha}, \\ 0 \leq P_{b,dis} \leq (1 - \delta^b[k]) P^{max}_{b,dis}, \end{cases} \tag{4.4}$$

The SOC's constraints mean that the dynamic SOC must be between its upper and lower bounds in the presence of disturbances, so it is noted that:

$$\begin{cases} x^{min}_{b,soc}[k] \leq x_{b,soc}[k] \leq x^{max}_{b,soc}[k] & \\ 0 \leq P_{b,cha}[k] \leq \ P^{max}_{b,cha}, & \text{(charging mode)} \\ 0 \leq P_{b,dis}[k] \leq \ P^{max}_{b,dis}, & \text{(discharging mode)} \end{cases} \tag{4.5}$$

Considering the general power balance equation in the presence of PV panels, a BESS, and a main grid can be written as:

$$P_{grid}[k] + P_b[k] + \tilde{P}_{pv}[k] = (P^{demand}[k] + P^{loss}[k]) \tag{4.6}$$

where, P_{grid} is GH power interaction with grid[kW], P^{demand,GH_i} is i's GH power demand[kW] and (P^{loss,GH_i} is i's GH power loss[kW].

$$P^{demand}[k] = \sum_{i=1}^{n_{GH}} (P^{GH_i}[k]) \tag{4.7}$$

where $P^{GH_i}[k]$ is the power consumption of GH i's components. Note, however, that this assumes an ideal storage system model, but the state of charging and of discharging do not behave linearly in an ESS.

Battery characteristics and specifications

Also, the technical specification of BESS can be found [156]. In this design, 2 BESS have been deployed.

3) GH resistance-capacitance(RC) modeling: The equivalent thermal capacitance and resistance models for the GH's structure, which comprises the walls, the ceiling, and the floor,

are combined to form the RC model as an electrical circuit (see Fig. 4.2). Based on [18], the GH's thermal dynamic can be expressed as:

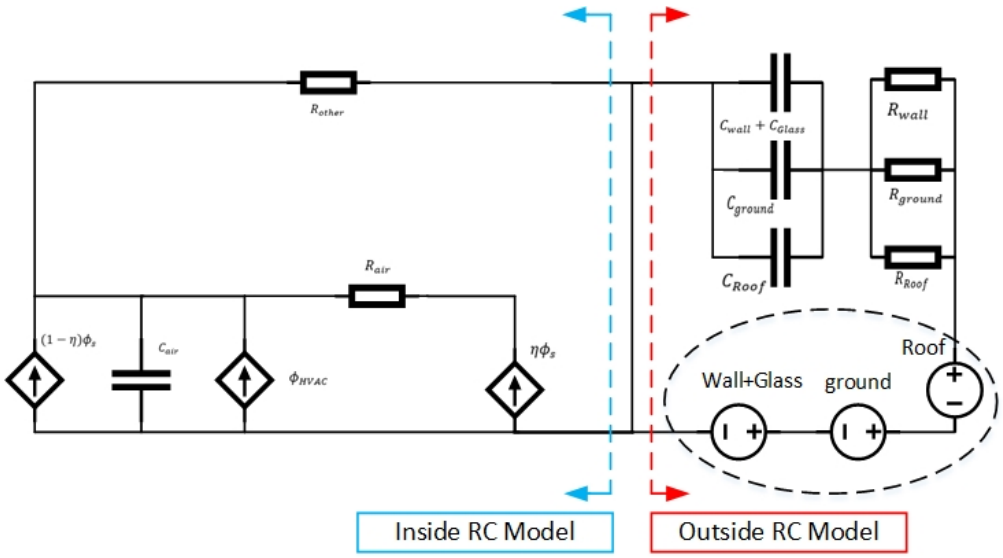

Figure 4.2 RC model: Thermal equivalent circuit of GH structure

$$\boldsymbol{x}^{GH_i}_{Temp}[k+1] = \begin{bmatrix} 0 & r_i & -r_i \\ 0 & r_i & r_i \\ \frac{r^i_{eq}+r^i_{other}}{-a_i} & 0 & \frac{r^i_{eq}}{a_i} \end{bmatrix} \boldsymbol{x}^{GH_i}_{Temp}[k] + \begin{bmatrix} 0 \\ \frac{1}{C^i_{air}} \\ 0 \end{bmatrix} u^{GH_i}_{Temp}[k] + \begin{bmatrix} \frac{r^i_{other}}{a_i} & 0 \\ 0 & \frac{1}{C^i_{air}}\eta_i \\ 1 & \frac{1}{C^i_{air}}(1-\eta_i) \end{bmatrix} \begin{bmatrix} T_{out}[k] \\ \phi_{solar}[k] \end{bmatrix} \tag{4.8}$$

$$y^{GH_i}_{Temp}[k] = \begin{bmatrix} 0 & 1 & 0 \end{bmatrix} \begin{bmatrix} \tilde{x}^{GH_i}_{Temp_3}[k] \\ \tilde{x}^{GH_i}_{Temp_2}[k] \\ \tilde{x}^{GH_i}_{Temp_1}[k] \end{bmatrix} \tag{4.9}$$

$$\begin{cases} r_i = \frac{1}{C^i_{air}R^i_{air}} \\ a_i = c^i_{eq}r^i_{eq}r^i_{other} \\ \frac{1}{r^i_{eq}} = \frac{1}{R^i_{roof}} + \frac{1}{R^i_{ground}} + \frac{1}{R^i_{wall}+R^i_{glass}} \\ c^i_{eq} = C^i_{roof} + C^i_{ground} + (C^i_{wall} + C^i_{glass}) \end{cases}$$

Due to the large scale of the GHs, nonlinearity can be omitted (refer to [18] for more information). The temperature states are comprised of: 1) $\tilde{x}^{GH_i}_{Temp_1}$, which is the temperature of the GH's physical structure (ceiling, walls, floor), 2) $\tilde{x}^{GH_i}_{Temp_2}$, which is the air temperature (note

that it cannot change quickly due to the large amount of space inside a GH and is therefore almost the same in each place), and 3) $\tilde{x}^{GH_i}_{Temp_3}$, which is the temperature, keeping by corps. In light of the state and input constraints, we have:

$$\begin{cases} 0 \leq u^{GH_i}_{Temp_{heating}}[k] \leq u^{GH_i}_{max}[k] \\ 0 \leq u^{GH_i}_{Temp_{cooling}}[k] \leq u^{GH_i}_{max}[k] \end{cases} \tag{4.10}$$

$$\begin{cases} \tilde{x}^{GH_i}_{Temp_{min}}[k] \leq \tilde{x}^{GH_i}_{Temp_2}[k] \leq \tilde{x}^{GH_i}_{Temp_{max}}[k] \\ \tilde{x}^{GH_i}_{Temp_{min}}[k] \leq y^{GH_i}_{Temp}[k] \leq \tilde{x}^{GH_i}_{Temp_{max}}[k] \end{cases} \tag{4.11}$$

Where, $x^{GH_i}_{TH}$ is GH i's temperature dynamic, and $u^{GH_i}_{TH_heating}$ is GH i's heating system control input[kW], C^i is GH i's thermal capacitance in structure (wall, roof, ground), ϕ_{solar} is surface temperature of solar light, and T_{out} is outside temperature, η_i is absorbing surface temperature of solar light coefficient. Also, $R^i_{(.)}$ is related to temperature resistance.

4) Relative humidity control: Relative humidity levels should be measured to maximize plant growth. Relative humidity can be mathematically expressed as [20]:

$$RH_{out}[k] = \frac{P_{par}[k]}{P_{sat}[k]} \times 100 \tag{4.12}$$

A humidifier can act as a fogger (release humidity) or a dehumidifier (absorb it), and this dynamic is represented as:

$$\begin{gathered} h^{GH_i}[k+1] = h^{GH_i}[k] + \\ \frac{k}{\rho_a V}[h_{evp}A + \rho_a A u_{vent}[k](h_{out}[k] - h^{GH_i}[k]) + \\ [u^{GH_i,setpoint}_{fog} h^{GH_i,max}_{fog} A - u^{GH_i,setpoint}_{deh} h^{GH_i,max}_{deh} A] + \\ \gamma^{Hum}_{disturbance}[k] \end{gathered} \tag{4.13}$$

where outdoor humidity, $h_{out}[k]$, is determined from the following empirical formula:

$$h_{out}[k] = \frac{RH_{out}[k](-K_1 + K_2 e^{C\phi_{out}[k]})}{P_{atm}} \tag{4.14}$$

$$u^{GH_i}_{fog}[k] = u^{GH_i,setpoint}_{fog}[k] \times P^{GH_i}_{fog} \tag{4.15}$$

$$u_{deh}^{GH_i}[k] = u_{deh}^{GH_i,setpoint}[k] \times P_{deh}^{GH_i} \tag{4.16}$$

$$u_{fog}^{GH_i}[k] \times u_{deh}^{GH_i}[k] = 0 \tag{4.17}$$

The upper and lower bounds of relative humidity are denoted as:

$$h^{GH_i}[k] \leq RH_{in,max} \frac{P_{sat}[k]}{P_{atm}[k]} \tag{4.18}$$

$$h^{GH_i}[k] \geq RH_{in,min} \frac{P_{sat}[k]}{P_{atm}[k]} \tag{4.19}$$

$u_{deh}^{GH_i,setpoint}$ is the setpoint of dehumidifying of GH i, and $u_{fog}^{GH_i,setpoint}$ is the setpoint of humidifying system control input[kW] of GH i . $P_{fog}^{GH_i}$ is GH i's fogging, $P_{deh}^{GH_i}$ is GH i's dehumidifying system power[kW]. ϕ_{out} is outside temperature, P_{atm} is atmospheric pressure [101, 325Pa] and P_{sat} is atmospheric saturation pressure [$1.1 \times P_{atm}$], K_1 is Humidity Constant[%], K_2 is Temperature-Humidity Constant[%], A is inside total surface, ρ_a is air density[1.1226kg/m^3].

5) CO_2 level dynamic: CO_2 generator systems are responsible for regulating the CO_2 concentration level inside the GH in accordance with other indoor GH elements, such as air circulation, temperature, and lighting. The dynamic model representation of the CO_2 level can be derived as follows [13], [6]:

$$\begin{gathered} CO_2^{in,GH_i}[k+1] = CO_2^{in,GH_i}[k] + \\ \frac{k}{\rho_a V}[K_{inj}^{max} u_{CO2}^{GH_i,setpoint} A + \\ \rho_a A u_{vent}^{GH_i}[k](CO_2^{outside}[k] - CO_2^{GH_i,in}[k+1]) + \\ K_{res}^{GH_i} A(K_6 + K_7 \phi_{in}^{GH_i}[k]) - \frac{K_{photo} I_{in}^{GH_i}[k] A}{R_{th}}] + \\ \gamma_{disturbance}^{CO_2}[k] \end{gathered} \tag{4.20}$$

We need to consider the CO_2 generators' power as an input:

$$u_{CO_2}^{GH_i}[k] = u_{CO_2}^{GH_i,setpoint}[k] \times P_{CO_2}^{GH_i} \tag{4.21}$$

and take into account the constraints that apply to CO_2 concentration inside a GH:

$$CO_{2,in}^{GH_i,min}[k] \leq CO_{2,in}^{GH_i}[k] \leq CO_{2,in}^{GH_i,max}[k] \tag{4.22}$$

Where, $CO_{2,in}^{GH_i,max}$ is maximum indoor CO_2, and $CO_{2,in}^{GH_i,min}$ is minimum indoor CO_2 level[ppm], $u_{vent}^{GH_i}$ is GH i's ventilation control input[kW], K_6 is related to CO_2 Constant[%], and K_7 is Temperature-CO_2 Constant[%], I^{GH_i} is GH i's light intensity[W/m^2], and A is effective surface of GH [m^2]

6) Reservoir water level control: Each GH has a water reservoir to meet water demands inside the GH. The reservoir's water level should be controlled so that the dynamic of the water level is evaluated at each time step and then an action command is sent to the water pump. The dynamic of the reservoir's water level is expressed as [20]:

$$l[k+1] = l[k] + [M_s[k] - M_{gh}^{GH_i}[k]] + \gamma_{disturbance}^{water}[k] \tag{4.23}$$

In (4.23), water inflows and outflows are related to the electrical power of the pump:

$$M_s[k] = \frac{u_s[k]}{3600\rho g d_s}\eta_s \tag{4.24}$$

$$M_{gh}^{GH_i}[k] = \frac{u_{gh}^{GH_i}[k]}{3600\rho g d_{gh}^{i}}\eta_{gh}^{GH_i} \tag{4.25}$$

Where, M_s is water flow in main reservoir,$M_{gh}^{GH_i}$is GH i's inward water flow, d_s is main pump head[m], g is gravitational constant[$\frac{\mathrm{m}}{\mathrm{s}^2}$], ρ is water density [1000kg/m^3], η_s is main water pump, $\eta_{gh}^{GH_i}$ is GH i's water pump efficiency.

Water level control dynamic is also coming along with constraints:

$$l_{min} < l[k] < l_{max} \tag{4.26}$$

$$\alpha_{sp}[k+1]M_{s,min} \leq M_s[k+1] \leq \alpha_{sp}[k+1]M_{s,max} \tag{4.27}$$

$$\alpha_{pgh}[k+1]M_{gh,min}^{GH_i} \leq M_{gh}^{GH_i}[k+1] \leq \alpha_{pgh}[k+1]M_{gh,max}^{GH_i} \tag{4.28}$$

where

$$\alpha_{sp}[k+1] = \begin{cases} 0, & \text{if } M_s[k+1] \leq M_{s,min} \\ 1, & \text{if } M_s[k+1] \geq M_{s,min} \end{cases} \tag{4.29}$$

$$\alpha_{pgh}[k+1] = \begin{cases} 0, & \text{if } M_{gh}^{GH_i}[k+1] \leq M_{gh,min}^{GH_i} \\ 1, & \text{if } M_{gh}^{GH_i}[k+1] \geq M_{gh,min}^{GH_i} \end{cases} \tag{4.30}$$

7) Artificial lighting: GH lighting systems can be turned on or off. Thus, the lighting system's power consumption in time step k is represented as a coefficient of illumination I as follows [18]:

$$P_{light}^{GH_i}[k] = \alpha_{light}^{GH_i} \times I^{GH_i}[k] \tag{4.31}$$

where the constraint on illumination for the outside radiation level is:

$$u_{light}^{GH_i}[k] = \begin{cases} P_{light}^{GH_i}[k], & \text{if } I_{outside} \leq I^{GH_i}[k] \\ 0, & \text{if } I_{outside} \geq I^{GH_i}[k] \end{cases} \tag{4.32}$$

$P_{light}^{GH_i}$ is GH i's indoor light power[kW], and I^{GH_i} is GH i's light intensity[W/m^2].

8) Ventilation system dynamic and control: The dynamic of the ventilation system in a closed GH environment is expressed as [13]:

$$u_{vent}^{GH_i}[k] = 3600 \frac{A_v C_d}{A} [2g(\frac{\phi_{out}[k] - \phi_{in}^{GH_i}[k]}{\phi_{out}[k]})(\frac{L_v}{4})]^{(\frac{1}{2})} \tag{4.33}$$

Where, L_v is Ventilation volume dimension[m], and A_d is surface of ventilation [m^2]

4.5.3 Robust Optimal Control Problem for a Cluster of GHs

First, this section describes how to decompose the fundamental dynamics of a GH to obtain a robust model predictive control mechanism. Second, it explains that robustness is necessary to keep the system functioning optimally in terms of tracking the GH's dynamics and interacting with power sources.

Robust positively invariant (RPI) set

We consider the representation of a discrete-time first-order linear time-invariant (LTI) equation that is adapted to the GH's dynamics in the presence of uncertainty:

$$\begin{gathered} \boldsymbol{x}_{k+1}^{GH_i} = \boldsymbol{A}^{GH_i} \boldsymbol{x}_k^{GH_i} + \boldsymbol{B}^{GH_i} \tilde{\boldsymbol{u}}_k^{GH_i} + \boldsymbol{H}^{GH_i} \boldsymbol{w}_k^{GH_i}, \\ \boldsymbol{x}_0^{GH_i} = \boldsymbol{x}^{GH_i}(0) \end{gathered} \tag{4.34}$$

$$\boldsymbol{y}_k^{GH_i} = \boldsymbol{C}^{GH_i}\boldsymbol{x}_k^{GH_i} + \boldsymbol{v}_k^{GH_i} \tag{4.35}$$

$$\boldsymbol{x}_k^{GH_i} = \begin{bmatrix} x^i_{Temp}[k] \\ x^i_{CO2}[k] \\ x^i_{water}[k] \\ x^i_{light}[k] \\ x^i_{Hum}[k] \\ x^{b,i}_{soc}[k] \\ x^{grid,i}[k] \end{bmatrix}_{\in \mathbb{R}^{n_x \times 1}} \qquad \tilde{\boldsymbol{u}}_k^{GH_i} = \begin{bmatrix} \tilde{u}^i_{Temp}[k] \\ \tilde{u}^i_{CO2}[k] \\ \tilde{u}^i_{water}[k] \\ \tilde{u}^i_{light}[k] \\ \tilde{u}^i_{Hum}[k] \\ \tilde{u}^{b,i}_{soc}[k] \\ \tilde{u}^{grid}[k] \end{bmatrix}_{\in \mathbb{R}^{n_{\tilde{u}} \times 1}} \tag{4.36}$$

$$\boldsymbol{w}_k^{GH_i} = \begin{bmatrix} w^i_{Temp}[k] \\ w^i_{CO2}[k] \\ w^i_{water}[k] \\ w^i_{light}[k] \\ w^i_{Hum}[k] \\ w^{b,i}_{soc}[k] \\ w^{grid}[k] \end{bmatrix}_{\in \mathbb{R}^{n_w \times 1}} \qquad \boldsymbol{e}_k^{GH_i} = \begin{bmatrix} e^i_{Temp}[k] \\ e^i_{CO2}[k] \\ e^i_{water}[k] \\ e^i_{light}[k] \\ e^i_{Hum}[k] \\ e^{b,i}_{soc}[k] \\ e^{grid}[k] \end{bmatrix}_{\in \mathbb{R}^{n_e \times 1}} \tag{4.37}$$

where $\boldsymbol{x}_k^{GH_i}$ is the system state vector, $\tilde{\boldsymbol{u}}_k^{GH_i}$ is the control input, $\boldsymbol{y}_k^{GH_i}$ is the output vector, $\boldsymbol{w}_k^{GH_i} \in \mathbb{R}^{n_w \times 1}$ is a vector of unknown state disturbance, $\boldsymbol{v}_k^{GH_i} \in \mathbb{R}^{n_e \times 1}$ is a vector of unknown output disturbance, and ($\boldsymbol{A}$, $\boldsymbol{B}$, $\boldsymbol{H}$, $\boldsymbol{C}$) are predetermined and known well-defined matrices. The output measurement noise and the state dynamic process noise are considered unknown bounded noises:

$$\boldsymbol{w}_k^{GH_i} \in \mathcal{W}, \quad \boldsymbol{v}_k^{GH_i} \in \Pi, \quad \forall k \in \mathbb{Z} \geq 0 \tag{4.38}$$

where $\mathcal{W}$ and Π are ellipsoidal spaces encompassing $(0, 0)$. First, we apply a feedback policy such as those used in [79], [64], and [148]:

$$\tilde{\boldsymbol{u}}_k^{GH_i}(\widehat{\boldsymbol{x}}_k^{GH_i}) = \boldsymbol{K}(\widehat{\boldsymbol{x}}_k^{GH_i} - \boldsymbol{s}_k^{GH_i}) + \boldsymbol{\mu}_k^{GH_i} \tag{4.39}$$

where $\boldsymbol{K} \in \mathbb{R}^{n_{u^{GH_i}} \times n_{x^{GH_i}}}$ is the feedback gain, $\widehat{\boldsymbol{x}}_k^{GH_i}$ is the nominal state, $\boldsymbol{\mu}_k^{GH_i}$ is the auxiliary control input (offset), and $\boldsymbol{s}_k^{GH_i}$ is the uncertainty-free state. According to the definition of feedback policy, state estimation is a tool that can provide a closed-loop system with feedback signals due to the absence of an actual system state. Utilizing (4.39) makes it possible to decompose the dynamic of a state into two categories: 1) nominal state and 2) error state.

Estimation error is defined as:

$$\boldsymbol{e}_k^{GH_i} = (\widehat{\boldsymbol{x}}_k^{GH_i}) - \boldsymbol{x}_k^{GH_i} \tag{4.40}$$

A robust positive invariant set is considered to deal with mapped uncertainty into objective function as mixed and hard constraints for input and system states:

$$\boldsymbol{F}\boldsymbol{x}_k^{GH_i} + \boldsymbol{G}\tilde{\boldsymbol{u}}_k^{GH_i} \leq \boldsymbol{f}, \tag{4.41}$$

system dynamic is decoupled by considering $\boldsymbol{\zeta}_k^{GH_i} \equiv \boldsymbol{x}_k^{GH_i} - \boldsymbol{s}_k^{GH_i}$ so that error can be written as:

$$\boldsymbol{\zeta}_{k+1}^{GH_i} = \boldsymbol{\Psi}^{GH_i}\boldsymbol{\zeta}_k^{GH_i} + (\boldsymbol{H}^{GH_i}\boldsymbol{w}_k^{GH_i}) + \boldsymbol{B}^{GH_i}\boldsymbol{K}\,\boldsymbol{e}_k^{GH_i}, \quad \boldsymbol{\zeta}_0^{GH_i} = -\boldsymbol{e}_0^{GH_i} \tag{4.42}$$

where all state estimation errors are $\boldsymbol{e}_k^{GH_i} \in \mathcal{E}_k^{GH_i}$, an ellipsoid in the $\mathbb{R}^{n_x}$ space. We consider an approximation of ellipsoid sets so that $\boldsymbol{e}_k^{GH_i} \in \mathcal{E}_k^{GH_i} \subset E$, where E is a set comprising all $\mathcal{E}_k^{GH_i}$. Therefore, equation (4.42) can be expressed as:

$$\boldsymbol{\zeta}_{k+1}^{GH_i} = \boldsymbol{\Psi}^{GH_i}\boldsymbol{\zeta}_k^{GH_i} + \boldsymbol{d}_k^{GH_i}, \quad \boldsymbol{\zeta}_0^{GH_i} = -\boldsymbol{e}_0^{GH_i} \tag{4.43}$$

comparing with state estimate error dynamics:

$$\boldsymbol{d}_k^{GH_i} = \boldsymbol{H}^{GH_i}\boldsymbol{w}^{GH_i} + \boldsymbol{B}^{GH_i}\boldsymbol{K}\,\boldsymbol{e}_k^{GH_i}, \forall \boldsymbol{w}_k^{GH_i} \in \mathcal{W}, \quad \forall \boldsymbol{e}_k^{GH_i} \in \mathcal{E}_k^{GH_i}$$

and then a simple manipulation yields:

$$\boldsymbol{F}\boldsymbol{s}_k^{GH_i} + \boldsymbol{G}\boldsymbol{\mu}_k^{GH_i} + (\boldsymbol{F}+\boldsymbol{G}\boldsymbol{K})\boldsymbol{\zeta}_k^{GH_i} + \boldsymbol{G}\boldsymbol{K}\,\boldsymbol{e}_k^{GH_i} \leq \boldsymbol{f}, \forall \boldsymbol{d}_k^{GH_i} \in \boldsymbol{H}^{GH_i}\mathcal{W} \oplus \boldsymbol{B}^{GH_i}\boldsymbol{K}E, \quad \forall \boldsymbol{e}_k^{GH_i} \in E \tag{4.44}$$

where $\oplus$ represents Minkowski's sum to come up with a lump sum of uncertainty. Thus, taking an RPI set in each step (we name it $\Theta_n^{GH_i}$) is the subset in space $\mathbb{R}^{n_x}$ with rank n_x.

GH states Dynamic Decomposition

If we consider an uncertain state to be $\boldsymbol{\zeta}_k^{GH_i} \equiv \boldsymbol{x}_k^{GH_i} - \boldsymbol{s}_k^{GH_i}$, the general form of the state space representation of the GH's dynamics is:

$$\begin{cases} \boldsymbol{s}_{k+1}^{GH_i} = \boldsymbol{A}^{GH_i}\boldsymbol{s}_k^{GH_i} + \boldsymbol{B}^{GH_i}\boldsymbol{\mu}_k^{GH_i}, \\ \boldsymbol{\zeta}_{k+1}^{GH_i} = \boldsymbol{\Psi}^{GH_i}\boldsymbol{\zeta}_k^{GH_i} + \boldsymbol{H}^{GH_i}\boldsymbol{w}_k^{GH_i} + \\ \qquad\qquad (\boldsymbol{B}^{GH_i}\boldsymbol{K})\boldsymbol{e}_k^{GH_i}, \end{cases} \tag{4.45}$$

where $\boldsymbol{s}_k^{GH_i}$ and $\boldsymbol{\mu}_k^{GH_i}$ are vectors in $\in \mathbb{R}^{n_x \times 1}$ and $\in \mathbb{R}^{n_\mu \times 1}$, respectively, and

$$\boldsymbol{A}_{Aug} = diag(\boldsymbol{A}^{GH_1}, \boldsymbol{A}^{GH_2}, \cdots, \boldsymbol{A}^{GH_i})$$

where $\boldsymbol{s}_k^{GH_i}$ is the uncertainty-free part of state, $\boldsymbol{\mu}_k^{GH_i}$ of GH i in time step k, and $\boldsymbol{A}_{Aug} \in \mathbb{R}^{(n_x \times n_{GH}) \times n_{GH}}$ is the state matrix. $\mu_{(.)}^i[k]$ are the control input sequences for each of GH i's states at time step k. Recall that we consider an uncertain state element $\boldsymbol{\zeta}^{GH_i} \equiv \boldsymbol{x}^{GH_i} - \boldsymbol{s}^{GH_i}$ so we can deduce $\boldsymbol{\zeta}_k^{GH_i}$ is a vector $\in \mathbb{R}^{n_x \times 1}$. Also, $\boldsymbol{B}_{Aug}, \boldsymbol{\Psi}_{Aug}$ and $\boldsymbol{H}_{Aug}$ can easily be deduced the same way as $\boldsymbol{A}_{Aug}$.

Recursive state estimation

Back to 2.6.3 the process of state propagation in a reliable bounding set addresses that All computations on constructing proper bounds are like 2.6.3, and subsection 2.8.

Improved Robust MPC with Recursive State Estimation on cluster of GHs

Highly intense deviation from the nominal state increases the risk of being unsafe against disturbances. In this section, first, the actual signal is filtered using a Huber function-based robust recursive state estimator to remove high-magnitude deviations [146]. Then, a finite robust optimal problem with predetermined constraints in finite time is deployed with functional error state estimation as follows [157], [158], [79], [159]:

Step 1: State deviation minimization

$$J_{\zeta_{k|n}^{GH_i}} = arg \min_{k=n,\ldots,n+N_p} \sum_{GH=1}^{i} \sum_{k=n}^{n+N_p} \sigma[\boldsymbol{s}_k^{GH_i{}^T}\boldsymbol{s}_k^{GH_i} - \boldsymbol{x}_k^{GH_i{}^T}\boldsymbol{x}_k^{GH_i}] \tag{4.46}$$

where σ is the Huber scoring function used to reduce the effect of deviations (outliers) based on the intensity of the signal at that step.

Step 2: Error state dynamic minimization

$$
\begin{aligned}
&J^{*}_{n\to n+N_p}(\boldsymbol{s}_n^{GH_i}) = \\
&\min_{\boldsymbol{\mu}_{k|n}^{GH_i},\cdots,\boldsymbol{\mu}_{n+N_p-1|n}^{GH_i}} \sum_{GH=1}^{i} \sum_{k=n}^{n+N_p-1} [\boldsymbol{l}(\boldsymbol{s}_{k|n}^{GH_i}, \boldsymbol{\mu}_{k|n}^{GH_i}) + \boldsymbol{Q}(\boldsymbol{s}_{n+N_p|n}^{GH_i})] \\
&s.t. \\
&\boldsymbol{s}_{k+1|n}^{GH_i} = \boldsymbol{A}\boldsymbol{s}_{k|n}^{GH_i} + \boldsymbol{B}\boldsymbol{\mu}_{k|n}^{GH_i}, \\
&\boldsymbol{F}\boldsymbol{s}_{k|n}^{GH_i} + \boldsymbol{G}\boldsymbol{\mu}_{k|n}^{GH_i} \leq \boldsymbol{f} - \boldsymbol{\Gamma}\boldsymbol{\zeta}_{k|n}^{GH_i} - \boldsymbol{G}\boldsymbol{K}\boldsymbol{e}_{k|n}^{GH_i}, \\
&\forall \boldsymbol{\zeta}_k \in \Theta_n^{GH_i}, \forall \boldsymbol{e}_k \in E_k, \\
&\boldsymbol{s}_{n|n}^{GH_i} = \boldsymbol{s}_n^{GH_i}, \boldsymbol{s}_{k|n}^{GH_i} \in \boldsymbol{S}, k = n, \cdots, n+N_p-1
\end{aligned}
\tag{4.47}
$$

where $\boldsymbol{\Gamma} := (\boldsymbol{F} + \boldsymbol{G}\boldsymbol{K})$, in which $\boldsymbol{\Gamma}\boldsymbol{\zeta}_k^{GH_i} = \max_{\zeta_k \in \Theta_n^{GH_i}} \boldsymbol{\Gamma}$ and $\boldsymbol{G}\boldsymbol{K}\boldsymbol{e}_k^{GH_i} = \max_{\boldsymbol{e}_k \in E_k} \boldsymbol{G}\boldsymbol{K}$, and $\boldsymbol{S}$ is a terminal constraint. The feedback gain $\boldsymbol{K}$ is obtained using the LQR method. RMPC is considered with constraint configuration on all states and control inputs, consisting cost stage, which is $\boldsymbol{l}(\boldsymbol{s}^{GH_i}, \boldsymbol{\mu}^{GH_i}) = \boldsymbol{s}^{GH_i{}^T}\boldsymbol{P}_{lqr}\boldsymbol{s}^{GH_i} + \boldsymbol{\mu}^{GH_i{}^T}\boldsymbol{R}_{lqr}\boldsymbol{\mu}^{GH_i}$, terminal cost, which is $\boldsymbol{Q}(\boldsymbol{s}^{GH_i}) = \boldsymbol{s}^{GH_i{}^T}\boldsymbol{P}_{N_p}\boldsymbol{s}^{GH_i}$, and $\boldsymbol{P}_{N_p}$ in positive definite.

4.6 GH Case Study

4.6.1 Data collection & simulation setup

In the case study section, we consider data in real-world conditions where crops grow and PV panels generate. Disturbances and errors of estimation are not the same for different GHs, resulting in different ellipsoidal shapes in the initial state at each step. Four GHs have been considered as case study plants. Each of them is preserving one species. Table 4.1 expresses information given by the manufacturer on PV and BESS. Data on solar radiation, temperature data, humidity, and outside CO_2 concentration have been collected from June 2019 to June 2020, and the Price of buying and selling energy can be found in [160].

Table 4.1 PV, BESS & Water Pumps Parameters

Solar Panel(Nominal Power)	15 kW
Battery(Li-ion) Capacity	10 kWh
Power of GH Water Pump	0.5 kW
Power of Main Water Pump	5.5 kW

Crops show different biological reactions in each period of growth. To extend more, during

the beginning stage of the plantation, keeping set points at the proper level is crucial; for instance, temperature and watering levels should be maintained within each period. This fact can affect objective function, set membership on uncertainties, and control input and state constraints. Empirically, the life period of each crop is divided into four sections from planting to maturity. Thus, it is clear that a GH with the mature plant should be treated by different reactions of the robust controller against disturbances and level of robustness compared with that GH with crops in the early growth stage. Linear feedback decomposition is a mean that determines which decision should be taken at each time, and then the uncertainty set is chosen according to each period of crop life.

The robust method of model predictive simulation has been run for four days, each day 24 hours of prediction horizon, 96 hours of control horizon, and 15 minutes as control interval bracket of time. To track a better state of State of charging/discharging (SOC) in BESS, the proposed RMPC was deployed to improve battery action. GHs' indoor temperature varies according to the type of crops and outdoor conditions during the day- and nighttime. In [161], set points for considered crops can be found. CO_2 Concentration levels differ over 24 hours, such that during the day, between 7:00 A.M. and 4 P.M., crops need a high-level concentration of CO_2 to do photosynthesis. Following CO_2 level concentration adjustment via the CO_2 generator system, light intensity is necessary for crops to complete daily biological cycles. Light intensity(lux) usually varies between 4500-5500 lux for different crops.

4.6.2 Simulation and results

Graphical illustrations show the ability to tackle harsh cases of disturbances. Signals tracking the performance of the proposed method have been compared simultaneously with the penalty on constraints violation approach. Constraints are tightened to overcome uncertainties and impacts while the solution is happening. Estimating the state is an effective remedy to decrease the downside of placing constraints. This feature is a tradeoff between conservatism behavior, faster convergence, and preserving constraints tightening aspects in a robust optimal control problem. Having been carried out simulations, it can express constraint violations hardly ever occurred. Due to having the most influential effect of temperature control on other state dynamics, the closed-loop trajectory of the proposed controlling approach has been compared with the ventilation system state in 4.3, then, we don't depict different trajectories of other states. In Fig.4.4., it can be seen that applying the robust control method inside GHs' dynamic states harnesses the effect of disturbances on temperature. Set-point tracking is guaranteed by keeping the signal in upper- and lower bounds. Furthermore, considering legroom and headroom on estimation error shows adaptive-like behavior

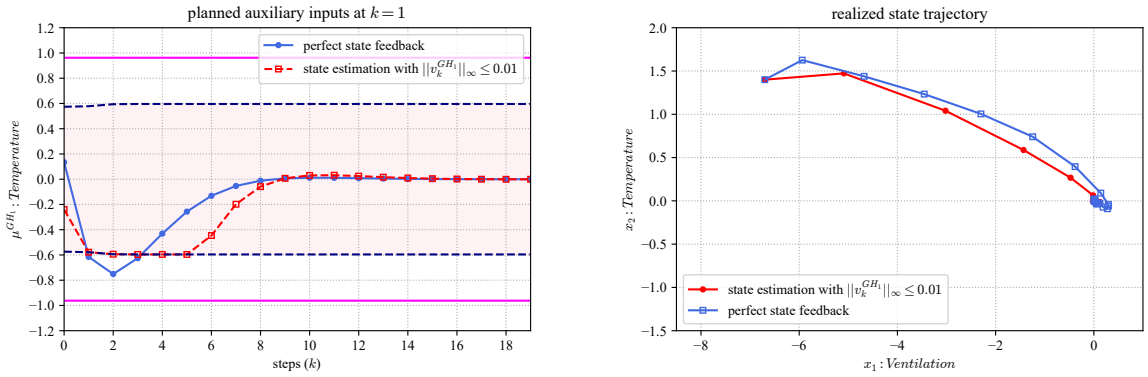

Figure 4.3 Left: Auxiliary input $\mu_{Temp}^{GH_1}$ at step $k = 1$: state feedback (Blue); Proposed method (Red line); feasible set membership for measuring with disturbance (Pink area), Right: closed-loop trajectory of Temperature and ventilation system states in GH_1.

set-membership related to the estimation error. It means when time passes, an uncertainty set can be obtained with considerably less effort(This notion clearly expresses the coincidence of reducing conservatism originated by constraints). Moreover, in Table. 4.2 we can see the convergence time of the robust model predictive control and the other robust controller using the proposed algorithm with attenuating outlier effects. The simulation has been embedded on Intel(R) Core(TM) i7-8750H CPU @ 2.20GHz 2.21 GHz, using the CPLEX Optimization Studio library in Python.

Table 4.2 Comparison the time of computation of two methods over prediction horizon in Fig.4.3: Robust MPC (RMPC) and Robust MPC equipped with proposed algorithm

RMPC	0.11945s
Improved RMPC	0.01373s

By GHs' component representation in section 4.5, in practice, state dynamics of inside GH climate conditions have correlations, so this fact about dynamics would be a part of typical deviations from measurements.

We assumed that Water flows in the pipeline without any effects of cavitation. Thus, Water can be continuously and immediately available Water. In Fig. 4.4., we figure that uncertainty in measuring temperature is the main source of the lack of proper set-point tracking of water level in the reservoir and relative humidity control. Relative humidity has been impacted by uncertainties in temperature, moisturized soil, and respiration activity of crops. Plants show different actions and reactions during nighttime and daytime. To cope with an unhealthy environment (in terms of causing fungal and parasitic disease) for crops with a

three-folded humidity source, relative humidity dynamics should be deliberately dealt with over-conservative reaction by considering constraints of two other sources of humidity in the whole controlling horizon.

CO_2 concentration levels varied day and night, as shown in Fig.4.4. Illustrates, during daytime, photosynthesis is accelerated, so then demand for CO_2 is growing by crops. As we already know, in large-scale GHs, relative humidity and CO_2 concentration level are the most challenging dynamics to be controlled because of 2 explicit reasons: 1) humidity and CO_2 are in gas phases entity, thus controlling the level of these two states shows some extend of latency in feedback response, and 2) these two dynamics are most sensitive towards interrelation effect of dynamics due to impacting by almost all other dynamics directly. These physical dynamics allow us to recognize better the approximation of Robustly Positive Invariant (RPI) sets on Humidity and CO_2 concentration level control.

Controlling robustly of inside dynamic profiles implies that ignoring uncertainties not only can gravely impact the controller's performance but also can change GH's energy consumption profile, especially when dealing with a cluster of GH (see Fig.4.5). Without explaining more details, choosing the proper RPI set on error state estimation ameliorates the performance of energy storage actions dealing with grid and PV panels. In Fig.4.6., considering the marginal band in closed-loop steady-state response, charging and discharging procedures show controlled behavior over the controlling horizon.

4.7 Conclusion

In this paper, we developed a robust model predictive control approach that relies on a recursive state estimation method and implemented it by applying it to a cluster of insulated GHs housing different crops in various conditions. Splitting the optimization problem into two steps made it possible to improve the proposed method's performance in the presence of uncertainty and have the computation time compensated for by a robust state estimation mechanism. Set points were tracked without violating constraints. Moreover, in-layer actions of taking augmented systems and then separating algorithms for set membership formation and optimization as considering all-in-one help to scope every single dynamic within GHs and all interactions between dynamic states as modular systems when implemented in the real world.

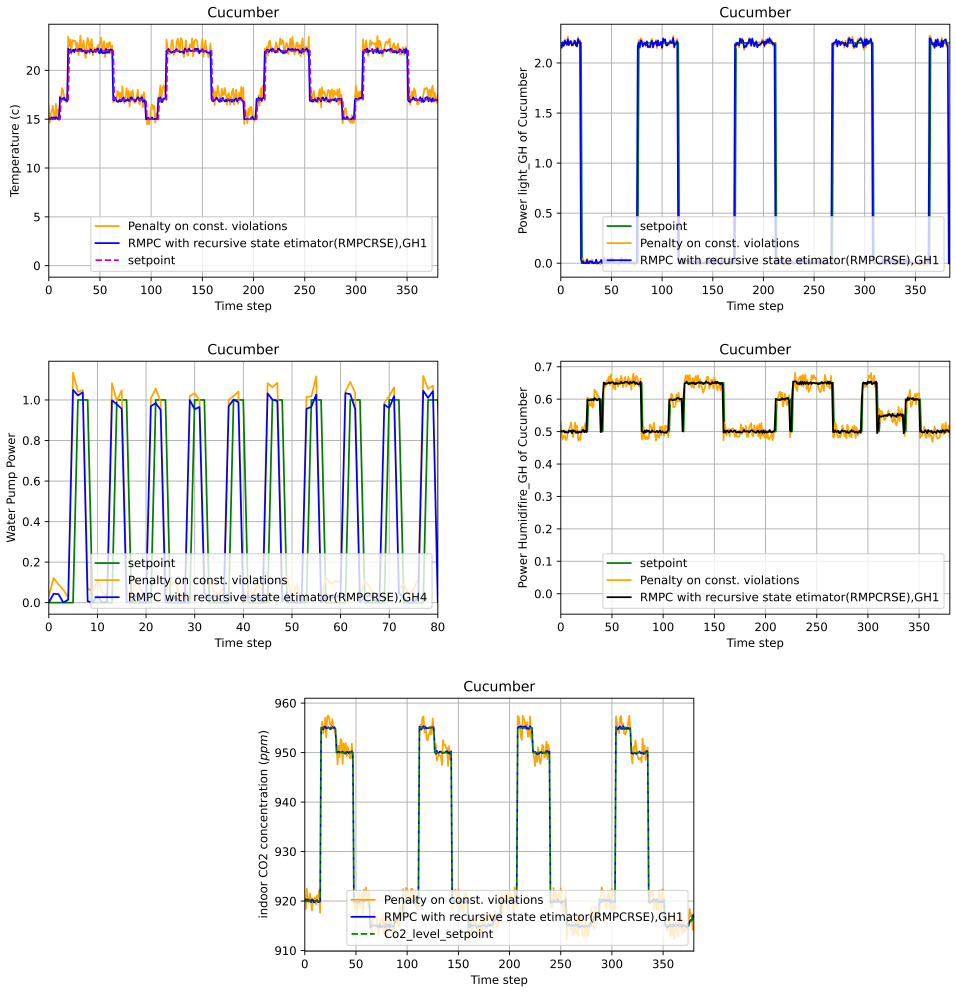

Figure 4.4 GHs reference tracking profile of temperature over four days. Other strategy may be faced with problem when constraints are tightened, due to severe fluctuations.

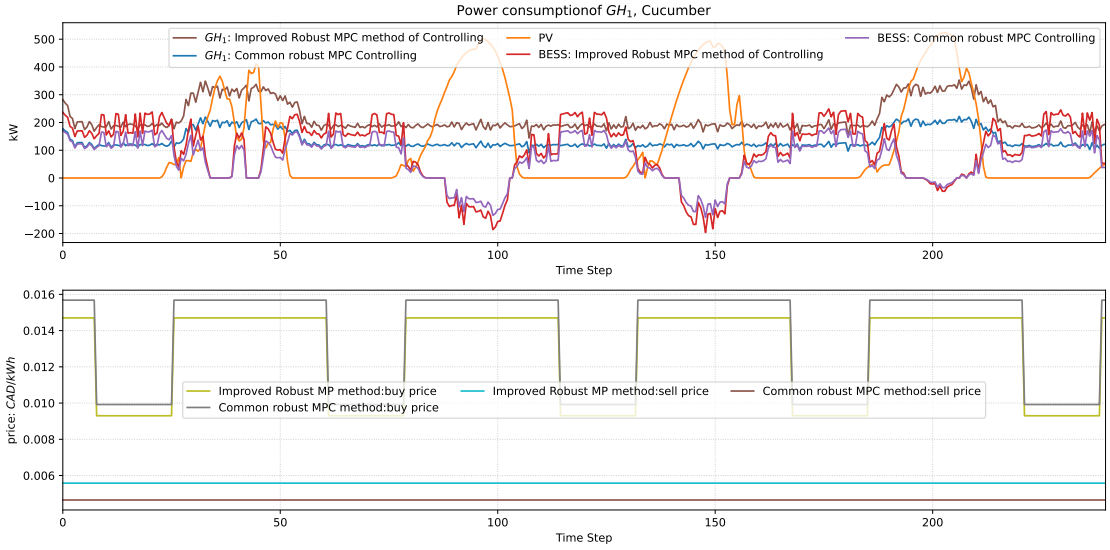

Figure 4.5 Top: Power consumption of GH_1 related to temperature control system, Bottom: Price according to D-rate tariff in Quebec.

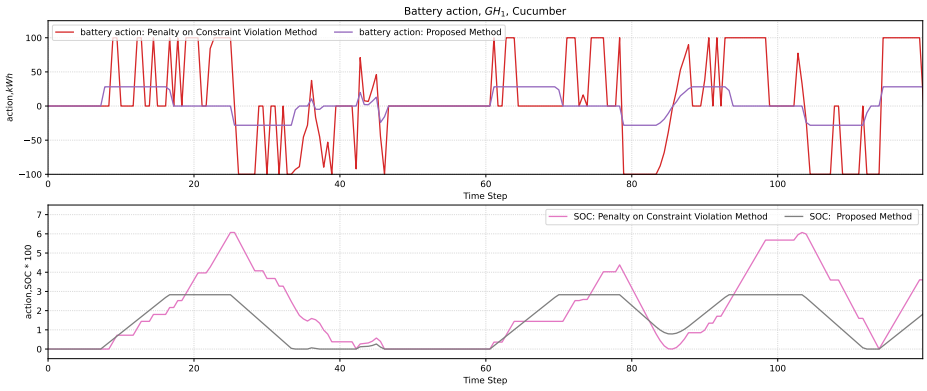

Figure 4.6 Top: BESS action (based on kWh scaling) in GH_1 Bottom: SOC of BESS in GH_1.

CHAPTER 5 GENERAL DISCUSSION

It has been explained that the MPC-based optimization method effectively controls GH and clusters of GH applications. However, relying on the internal robustness of MPC, functioning in a closed-loop, is not enough to tackle the impact of contaminated state dynamics by the uncertainty of disturbances, including process and measurement noises. Thus, the substantial objective of this research is to develop and implement an Improved RMPC to cover the weakness of MPC in facing high-magnitude disturbances. In addition to disturbing the proper transient and asymptotic behaviour, the uncertainty of disturbances leads to the gradual degradation of controller adjustment.

The RMPC method proposes a solution for functioning in real-world conditions that are affected by disturbances and noises. RMPC based on the Machine Learning data-driven method has already been presented in a semi-closed GH application on controlling three-state dynamics. This study can be the first research on robustfying MPC utilizing a resilient recursive state estimator applied to indoor dynamics of GH and cluster of GHs. The proposed method shows less effort in computation.

Due to the robustness section in RMPC, this method needs to exploit computational resources. Again, this research is more concentrated on controlling state signals in the presence of real-world anomalies. To improve the previous Robust MPC, it has been tried to increase the calculation speed by reducing the conservative behavior of a common RMPC. One effective way to address computationally demanding issues is using a recursive state estimator.

In a simple RMPC problem, tracking the references can be challenging in high-magnitude disturbances. In that case, even if RMPC could track the references in significantly life-risking conditions inside of a GH, this RMPC cannot outperform, especially in controlling many interconnected dynamics (more than five states). Therefore, RMPC utilizing RKF as a robust recursive estimator using set membership shows adequate ability to handle state dynamics in real-world conditions.

Another challenge in using the RMPC problem is recursive feasibility. This kind of feasibility is vital to ensure the existence of the optimal solution. The state of art in RMPC is generally using the RPIs concept. So that, as far as the initialized states are selected from the RPI set, stability and tracking of the references in the presence of disturbances are guaranteed. On the one hand, deploying set-membership helps controllers to work under impacting disturbances. On the other hand, a robust Positively invariant set determines a specific region is a state

space in which the system is stable so that as long as the process is initialized from this region, it cannot be unstable.

RMPC utilizing a robust recursive state estimator using set membership bolsters computation speed by bounding actual signals in facing disturbances. In addition to deploying set-membership, RPIs are addressed to ensure whole stability. RMPC utilizing a robust recursive state estimator can cover downsides of disturbances effects, including conservative behavior and aggressive closed-loop response. In Chapter 3, RMPC using a recursive state estimator has been reviewed. Then, the robust model of a linear KF has been suggested to strengthen set-membership functioning encountering high magnitude disturbance and reduce the burden of computational time issues in explicit mean. Then, it helps find a feasible region of solution implicitly.

Based on the results shown in Chapter 4, the proposed algorithm in 4.5.3 can outperform in harsh environments.

CHAPTER 6 CONCLUSIONS AND RECOMMENDATIONS

This chapter contains a summary of work limitations, along with recommendations on the future path of this line of research.

6.1 Summary of Works

In this research, a literature review has been conducted to investigate potential gaps for improving the controlling methods on indoor GHs' state dynamics. In isolated types of GHs, controllers should have fast action in real-world applications. It is vital to keep proper setpoints of crops to maximize productivity in highly sensitive conditions inside GHs. In most recent works, MPC has been selected to deal with numerous states. On the one hand, it was clear that PI and PID controllers cannot cope with complicated and multiple inter-dependant dynamics. On the other hand, deploying MPC and even RMPC had specific problems with feasibility and computational time issues, usually over considering the vast number of dynamics in GH. Thus, it was necessary to address the deficiency of the previous RMPC method to devise an improved approach for maintaining indoor dynamics. This challenge is crucially important when cluster of GHs or/and large scale of GHs are working.

In a simple problem, the authors attempted to define an MPC-based optimization problem with quadratic modeling to reduce the deviation of states from setpoints in a single GH or cluster of GH entities. Sometimes, this model of approaching the problem did not yield an efficient response because of the vulnerability of MPC controllers in facing uncertainties. The authors could solve this downside by considering the constraints on an ordinary MPC to define a RMPC problem on such complicated dynamics inside an isolated microclimate. However, RMPC guarantees the existence of a solution under uncertainty. RMPC can show tracking performance of the references in environments with harsh disturbances, although it needs to be improved. Moreover, the computational time issue is directly impacting stability due to following the state tracking in a common RMPC. This kind of RMPC should guarantee robust tracking and stability in each controlling horizon. In some cases, when the size of the prediction horizon is more significant than the controlling horizon, due to computational burden, stability would not be guaranteed. Determining set membership and RPIs could propose effective solutions to attain a possible set of states and then generate optimal control input sequences, especially with high-magnitude disturbances.

In most recent works, one author used a method that proposed a penalty of a constraint

violation; the other one utilized Alternating Direction Method of Multiplier (ADMM). The latter is not taking advantage of RMPC when considering set-membership techniques, and the former is not deploying the method on a cluster of isolated GH.

In this work, the RMPC problem equipped by recursive state estimator has been considered, with the goal to improve the overall RMPC controller performance by deploying Robust KF(RKF) in cluster layout of GHs. This RKF using set-membership and Huber function compensates computational time issues and prevents enormous deviations from the nominal state caused by harsh disturbances. As we already know, deviations from reference points have direct relations with wasting resources in computing or materials. The recursion relieves challenging & risky calculations on finding a solution to the energy function after each step of time, and the Huber function helps to guarantee time reduction of finding a solution. This combination could implicitly give a degree of freedom to cover more contaminated dynamic states with disturbances.

6.2 Limitations

Improved RMPC presents acceptable performance in handling large amounts of dynamic states in clustered GHs compared to RMPC. In practice, GH dynamics show nonlinear behavior. In real-world cases, these nonlinear dynamics are accompanied by errors, occasionally creating immense hardships in finding optimal solutions. The dynamics equation should be inevitably linearized to be compatible with digital controllers. Moreover, to address the limitations, it is better to point out the mathematical opportunities that can make improvements at the end. Thus, for limitations, it can be mentioned:

- Linearizing non-linearity adds uncertainty to inevitable real-world [69], [99].
- Finding the energy function to transit set membership to the next step over the controlling horizon is sometimes impossible when the prediction horizon is much bigger than the controlling horizon [68].
- Deployment of numerous state dynamics leads to a growing number of constraints. This phenomenon has two main issues: 1) over-exploitation of the computational resources and 2) finding feasible and optimal solutions.

6.3 Future Research

As mentioned, there are a few research on RMPC in GH applications to investigate a cluster of GHs using the following research avenues:

- Reducing the massive number of constraints on the rolling horizon in implementing decentralized RMPC.
- Using reinforcement learning to approach the uncertainty of disturbances so that when uncertainty appears, constraints are tightened. Conversely, when uncertainty is not causing an out-spike, the constraints are removed.
- Deploying combinatorial optimization of constraints and then using vectorization method (in Julia environment) to reduce computational time.
- Generalizing this method regarding cyber-security attack detection and voltage stability in large-scale GHs.
- Developing this method with energy management orientation in large-scale GHs integrated to the grid.
- Adding learning optimizer instead of common optimization methods. By utilizing a learning optimizer, energy and time of computation could be saved.

REFERENCES

[1] G. van Straten *et al.*, *The Optimal Control of Greenhouse Cultivation (1st ed.)*. CRC Press. https://doi.org/10.1201/b10321, 2010.

[2] G. van Straten and E. J. van Henten, "Optimal greenhouse cultivation control: Survey and perspectives," *IFAC Proceedings Volumes*, vol. 43, no. 26, pp. 18–33, 2010, 3rd IFAC Conference in Modelling and Control in Agriculture, Horticulture and Post-Harvest Processing - Agricontrol. [Online]. Available: https://www.sciencedirect.com/science/article/pii/S1474667015310326

[3] S. Blackmore, K. Apostolidi, and S. Fountas, "Futurefarm: Addressing the needs of the european farm of the future: Findings of the first two years," *IFAC Proceedings Volumes*, vol. 43, no. 26, pp. 1–17, 2010, 3rd IFAC Conference in Modelling and Control in Agriculture, Horticulture and Post-Harvest Processing - Agricontrol. [Online]. Available: https://www.sciencedirect.com/science/article/pii/S1474667015310314

[4] Y. Achour *et al.*, "Supervisory model predictive control for optimal operation of a greenhouse indoor environment coping with food-energy-water nexus," *IEEE Access*, vol. 8, pp. 211 562–211 575, 2020.

[5] A. Ouammi *et al.*, "Supervisory model predictive control for optimal energy management of networked smart greenhouses integrated microgrid," *IEEE Transactions on Automation Science and Engineering*, vol. 17, no. 1, pp. 117–128, 2020.

[6] ——, "Optimal operation scheduling for a smart greenhouse integrated microgrid," *Energy for Sustainable Development*, vol. 58, pp. 129–137, 2020.

[7] S. Chatzivasileiadis *et al.*, "Cyber–physical modeling of distributed resources for distribution system operations," *Proceedings of the IEEE*, vol. 104, no. 4, pp. 789–806, 2016.

[8] B. Paris *et al.*, "Energy use in greenhouses in the eu: A review recommending energy efficiency measures and renewable energy sources adoption," *Applied Sciences*, vol. 12, no. 10, p. 5150, 2022.

[9] J. Riahi *et al.*, "Smart and renewable energy system to power a temperature-controlled greenhouse," *Energies*, vol. 14, no. 17, p. 5499, 2021.

[10] O. Abedrabboh, M. Koç, and Y. Biçer, "Modelling and analysis of a renewable energy-driven climate-controlled sustainable greenhouse for hot and arid climates," *Energy Conversion and Management*, vol. 273, p. 116412, 2022.

[11] G. Hu and F. You, "Renewable energy-powered semi-closed greenhouse for sustainable crop production using model predictive control and machine learning for energy management," *Renewable and Sustainable Energy Reviews*, vol. 168, p. 112790, 2022.

[12] A. Desai, I. Mukhopadhyay, and A. Ray, "Techno-economic-environment analysis of solar pv smart microgrid for sustainable rural electrification in agriculture community," in *2021 IEEE 48th Photovoltaic Specialists Conference (PVSC)*. IEEE, 2021, pp. 2281–2285.

[13] A. Ouammi *et al.*, "Supervisory model predictive control for optimal energy management of networked smart greenhouses integrated microgrid," *IEEE transactions on automation science and engineering*, vol. 17, no. 1, pp. 117–128, 2019.

[14] S. Hemming *et al.*, "Cherry tomato production in intelligent greenhouses—sensors and ai for control of climate, irrigation, crop yield, and quality," *Sensors*, vol. 20, no. 22, p. 6430, 2020.

[15] P. Jones, J. Jones, and Y. Hwang, "Simulation for determining greenhouse temperature setpoints," *Transactions of the ASAE*, vol. 33, no. 5, pp. 1–1728, 1990.

[16] O. Körner, *Crop based climate regimes for energy saving in greenhouse cultivation*. Wageningen University and Research, 2003.

[17] W.-H. Chen and F. You, "Semiclosed greenhouse climate control under uncertainty via machine learning and data-driven robust model predictive control," *IEEE Transactions on Control Systems Technology*, vol. 30, no. 3, pp. 1186–1197, 2021.

[18] E. Rezaei, H. Dagdougui, and K. Ojand, "Hierarchical distributed energy management framework for multiple greenhouses considering demand response," *IEEE Transactions on Sustainable Energy*, vol. 14, no. 1, pp. 453–464, 2022.

[19] Y. Su and L. Xu, "Greenhouse climate setpoint optimization: An online decision strategy," *IEEE Access*, vol. 9, pp. 140 298–140 314, 2021.

[20] Y. Achour *et al.*, "Supervisory model predictive control for optimal operation of a greenhouse indoor environment coping with food-energy-water nexus," *IEEE Access*, vol. 8, pp. 211 562–211 575, 2020.

[21] N. Bennis *et al.*, "Greenhouse climate modelling and robust control," *Computers and electronics in agriculture*, vol. 61, no. 2, pp. 96–107, 2008.

[22] W.-H. Chen and F. You, "Efficient greenhouse temperature control with data-driven robust model predictive," in *2020 American Control Conference (ACC)*. IEEE, 2020, pp. 1986–1991.

[23] J. Moreno *et al.*, "Robust control of greenhouse climate exploiting measurable disturbances," *IFAC Proceedings Volumes*, vol. 35, no. 1, pp. 271–276, 2002.

[24] M. Zhang *et al.*, "Energy-saving design and control strategy towards modern sustainable greenhouse: A review," *Renewable and Sustainable Energy Reviews*, vol. 164, p. 112602, 2022.

[25] D. Q. Mayne, "Model predictive control: Recent developments and future promise," *Automatica*, vol. 50, no. 12, pp. 2967–2986, 2014.

[26] C. Bersani *et al.*, "Model predictive control of smart greenhouses as the path towards near zero energy consumption," *Energies*, vol. 13, no. 14, p. 3647, 2020.

[27] Y. Ding *et al.*, "Model predictive control and its application in agriculture: A review," *Computers and Electronics in Agriculture*, vol. 151, pp. 104–117, 2018.

[28] S. Piñón *et al.*, "Constrained predictive control of a greenhouse," *Computers and Electronics in Agriculture*, vol. 49, no. 3, pp. 317–329, 2005.

[29] A. Ramírez-Arias *et al.*, "Improving efficiency of greenhouse heating systems using model predictive control," *IFAC Proceedings Volumes*, vol. 38, no. 1, pp. 40–45, 2005.

[30] F. Mahmood *et al.*, "Data-driven robust model predictive control for greenhouse temperature control and energy utilisation assessment," *Applied Energy*, vol. 343, p. 121190, 2023.

[31] F. García-Mañas *et al.*, "Multi-scenario model predictive control for greenhouse crop production considering market price uncertainty," *IEEE Transactions on Automation Science and Engineering*, 2023.

[32] E. Sanyé-Mengual *et al.*, "An environmental and economic life cycle assessment of rooftop greenhouse (rtg) implementation in barcelona, spain. assessing new forms of urban agriculture from the greenhouse structure to the final product level," *The International journal of life cycle assessment*, vol. 20, no. 3, pp. 350–366, 2015.

[33] M. Taki *et al.*, "Modeling and experimental validation of heat transfer and energy consumption in an innovative greenhouse structure," *Information Processing in Agriculture*, vol. 3, no. 3, pp. 157–174, 2016.

[34] N. Choab *et al.*, "Review on greenhouse microclimate and application: Design parameters, thermal modeling and simulation, climate controlling technologies," *Solar Energy*, vol. 191, pp. 109–137, 2019.

[35] S. Gorjian *et al.*, "A review on opportunities for implementation of solar energy technologies in agricultural greenhouses," *Journal of Cleaner Production*, vol. 285, p. 124807, 2021.

[36] G. Srinivasan and P. Muthukumar, "A review on solar greenhouse dryer: Design, thermal modelling, energy, economic and environmental aspects," *Solar Energy*, vol. 229, pp. 3–21, 2021.

[37] N. Bibi-Triki *et al.*, "Modeling, characterization and analysis of the dynamic behavior of heat transfers through polyethylene and glass walls of greenhouses," *Physics Procedia*, vol. 21, pp. 67–74, 2011.

[38] A. Ouammi, "Model predictive control for optimal energy management of connected cluster of microgrids with net zero energy multi-greenhouses," *Energy*, vol. 234, p. 121274, 2021.

[39] Y. Achour, A. Ouammi, and D. Zejli, "Technological progresses in modern sustainable greenhouses cultivation as the path towards precision agriculture," *Renewable and Sustainable Energy Reviews*, vol. 147, p. 111251, 2021.

[40] I. Gothic Arc Greenhouses, "Different commercial greenhosues dimension," 2023, https://www.gothicarchgreenhouses.com/plastic-planting-pots.htm [Accessed: (Use the date of access)].

[41] A. Vadiee and V. Martin, "Energy management strategies for commercial greenhouses," *Applied Energy*, vol. 114, pp. 880–888, 2014.

[42] T. Qian *et al.*, "Comparison of climate and production in closed, semi-closed and open greenhouses," in *International Symposium on High Technology for Greenhouse Systems: GreenSys2009 893*, 2009, pp. 807–814.

[43] S. Zhang *et al.*, "Methodologies of control strategies for improving energy efficiency in agricultural greenhouses," *Journal of Cleaner Production*, vol. 274, p. 122695, 2020.

[44] M. A. Khan *et al.*, "Global estimates of energy consumption and greenhouse gas emissions," *Renewable and Sustainable Energy Reviews*, vol. 29, pp. 336–344, 2014.

[45] E. Iddio *et al.*, "Energy efficient operation and modeling for greenhouses: A literature review," *Renewable and Sustainable Energy Reviews*, vol. 117, p. 109480, 2020.

[46] M. Djevic and A. Dimitrijevic, "Energy consumption for different greenhouse constructions," *Energy*, vol. 34, no. 9, pp. 1325–1331, 2009.

[47] M. Tanaskovic *et al.*, "Robust adaptive model predictive building climate control," *Ifac-Papersonline*, vol. 50, no. 1, pp. 1871–1876, 2017.

[48] D. Sturzenegger *et al.*, "Model predictive climate control of a swiss office building: Implementation, results, and cost–benefit analysis," *IEEE Transactions on Control Systems Technology*, vol. 24, no. 1, pp. 1–12, 2015.

[49] A. Thavlov and H. W. Bindner, "Thermal models for intelligent heating of buildings," in *Proceedings of the International Conference on Applied Energy, Suzhou, China*, 2012, pp. 5–8.

[50] X. Zhang *et al.*, "Scenario-based mpc for energy-efficient building climate control under weather and occupancy uncertainty," in *2013 european control conference (ECC)*. IEEE, 2013, pp. 1029–1034.

[51] F. Amara *et al.*, "Comparison and simulation of building thermal models for effective energy management," *Smart Grid and renewable energy*, vol. 6, no. 04, p. 95, 2015.

[52] W. Langson *et al.*, "Robust model predictive control using tubes," *Automatica*, vol. 40, no. 1, pp. 125–133, 2004. [Online]. Available: https://www.sciencedirect.com/science/article/pii/S0005109803002838

[53] D. Q. Mayne and E. C. Kerrigan, "Tube-based robust nonlinear model predictive control1," *IFAC Proceedings Volumes*, vol. 40, no. 12, pp. 36–41, 2007, 7th IFAC Symposium on Nonlinear Control Systems. [Online]. Available: https://www.sciencedirect.com/science/article/pii/S1474667016354994

[54] D. Mayne *et al.*, "Robust output feedback model predictive control of constrained linear systems," *Automatica*, vol. 42, no. 7, pp. 1217–1222, 2006. [Online]. Available: https://www.sciencedirect.com/science/article/pii/S0005109806001221

[55] J. Richalet *et al.*, "Model predictive heuristic control: Applications to industrial processes," *Automatica*, vol. 14, no. 5, pp. 413–428, 1978. [Online]. Available: https://www.sciencedirect.com/science/article/pii/0005109878900018

[56] C. R. Cutler and B. L. Ramaker, "Dynamic matrix control?? a computer control algorithm," in *joint automatic control conference*, no. 17, 1980, p. 72.

[57] D. Clarke, C. Mohtadi, and P. Tuffs, "Generalized predictive control—part i. the basic algorithm," *Automatica*, vol. 23, no. 2, pp. 137–148, 1987. [Online]. Available: https://www.sciencedirect.com/science/article/pii/0005109887900872

[58] D. Mayne *et al.*, "Constrained model predictive control: Stability and optimality," *Automatica*, vol. 36, no. 6, pp. 789–814, 2000. [Online]. Available: https://www.sciencedirect.com/science/article/pii/S0005109899002149

[59] M. Morari and J. H. Lee, "Model predictive control: past, present and future," *Computers Chemical Engineering*, vol. 23, no. 4, pp. 667–682, 1999. [Online]. Available: https://www.sciencedirect.com/science/article/pii/S0098135498003019

[60] M. Annergren *et al.*, "On the way to autonomous model predictive control: A distillation column simulation study1," *IFAC Proceedings Volumes*, vol. 46, no. 32, pp. 713–720, 2013, 10th IFAC International Symposium on Dynamics and Control of Process Systems. [Online]. Available: https://www.sciencedirect.com/science/article/pii/S1474667015383427

[61] R. D'Andrea, F. Paganini, and J. C. Doyle, "Uncertain behavior," 1993.

[62] R. D'Andrea and F. Paganini, "Interconnection of uncertain behavioral systems for robust control," in *Proceedings of 32nd IEEE Conference on Decision and Control*. IEEE, 1993, pp. 3642–3647.

[63] A. Ben-Tal, L. El Ghaoui, and A. Nemirovski, *Robust optimization*. Princeton university press, 2009, vol. 28.

[64] M. B. Saltık *et al.*, "An outlook on robust model predictive control algorithms: Reflections on performance and computational aspects," *Journal of Process Control*, vol. 61, pp. 77–102, 2018.

[65] T. Ji, J. Geng, and K. Driggs-Campbell, "Robust model predictive control with state estimation under set-membership uncertainty," *arXiv preprint arXiv:2008.04980*, 2020.

[66] L. Chen *et al.*, "Robust model predictive control for greenhouse temperature based on particle swarm optimization," *Information processing in agriculture*, vol. 5, no. 3, pp. 329–338, 2018.

[67] D. Q. Mayne *et al.*, "Robust output feedback model predictive control of constrained linear systems: Time varying case," *Automatica*, vol. 45, no. 9, pp. 2082–2087, 2009.

[68] G. Goodwin, D. Carrasco, and M. Seron, "Predictive control: a historical perspective," *International Journal of Robust and Nonlinear Control*, vol. 22, no. 12, pp. 1296–1313, 2012.

[69] D. M. Raimondo *et al.*, "Min-max model predictive control of nonlinear systems: A unifying overview on stability," *European Journal of Control*, vol. 15, no. 1, pp. 5–21, 2009.

[70] J. P. Hespanha, *Linear systems theory*. Princeton university press, 2018.

[71] G. C. Goodwin *et al.*, "Robust model predictive control: reflections and opportunities," *Journal of Control and Decision*, vol. 1, no. 2, pp. 115–148, 2014.

[72] D. Q. Mayne *et al.*, "Robust output feedback model predictive control of constrained linear systems," *Automatica*, vol. 42, no. 7, pp. 1217–1222, 2006.

[73] B. Kouvaritakis and M. Cannon, "Model predictive control," *Switzerland: Springer International Publishing*, vol. 38, 2016.

[74] D. P. Bertsekas, "Control of uncertain systems with a set-membership description of the uncertainty." Ph.D. dissertation, Massachusetts Institute of Technology, 1971.

[75] J. B. Rawlings, "Tutorial overview of model predictive control," *IEEE control systems magazine*, vol. 20, no. 3, pp. 38–52, 2000.

[76] D. Q. Mayne *et al.*, "Constrained model predictive control: Stability and optimality," *Automatica*, vol. 36, no. 6, pp. 789–814, 2000.

[77] D. Bertsekas and I. Rhodes, "Recursive state estimation for a set-membership description of uncertainty," *IEEE Transactions on Automatic Control*, vol. 16, no. 2, pp. 117–128, 1971.

[78] B. Kouvaritakis, M. Cannon, and R. Yadlin, "On the centres and scalings of robust and stochastic tubes," 2010.

[79] F. Schweppe, "Recursive state estimation: Unknown but bounded errors and system inputs," *IEEE Transactions on Automatic Control*, vol. 13, no. 1, pp. 22–28, 1968.

[80] P. O. Scokaert and D. Q. Mayne, "Min-max feedback model predictive control for constrained linear systems," *IEEE Transactions on Automatic control*, vol. 43, no. 8, pp. 1136–1142, 1998.

[81] D. P. Bertsekas and I. B. Rhodes, "On the minimax reachability of target sets and target tubes," *Automatica*, vol. 7, no. 2, pp. 233–247, 1971.

[82] H. Witsenhausen, "A minimax control problem for sampled linear systems," *IEEE Transactions on Automatic Control*, vol. 13, no. 1, pp. 5–21, 1968.

[83] J. Glover and F. Schweppe, "Control of linear dynamic systems with set constrained disturbances," *IEEE Transactions on Automatic Control*, vol. 16, no. 5, pp. 411–423, 1971.

[84] L. S. Pontryagin, "Linear differential games," *SIAM Journal on Control*, vol. 12, no. 2, pp. 262–267, 1974.

[85] E. Zafiriou, "Robust model predictive control of processes with hard constraints," *Computers & Chemical Engineering*, vol. 14, no. 4-5, pp. 359–371, 1990.

[86] H. Michalska and D. Q. Mayne, "Robust receding horizon control of constrained nonlinear systems," *IEEE transactions on automatic control*, vol. 38, no. 11, pp. 1623–1633, 1993.

[87] J. Lee and Z. Yu, "Tuning of model predictive controllers for robust performance," *Computers & chemical engineering*, vol. 18, no. 1, pp. 15–37, 1994.

[88] D. Bertsimas and A. Thiele, "Robust and data-driven optimization: modern decision making under uncertainty," in *Models, methods, and applications for innovative decision making*. INFORMS, 2006, pp. 95–122.

[89] M. V. Kothare, V. Balakrishnan, and M. Morari, "Robust constrained model predictive control using linear matrix inequalities," *Automatica*, vol. 32, no. 10, pp. 1361–1379, 1996.

[90] D. Peaucelle and D. Arzelier, "Robust performance analysis with lmi-based methods for real parametric uncertainty via parameter-dependent lyapunov functions," *IEEE Transactions on Automatic Control*, vol. 46, no. 4, pp. 624–630, 2001.

[91] P. J. Campo and M. Morari, "Model predictive optimal averaging level control," *AIChE Journal*, vol. 35, no. 4, pp. 579–591, 1989.

[92] P. Campo and M. Morari, "Robust control of processes subject to saturation nonlinearities," *Computers & Chemical Engineering*, vol. 14, no. 4-5, pp. 343–358, 1990.

[93] J. Allwright and G. Papavasiliou, "On linear programming and robust model-predictive control using impulse-responses," *Systems & Control Letters*, vol. 18, no. 2, pp. 159–164, 1992.

[94] A. Bemporad, F. Borrelli, and M. Morari, "Min-max control of constrained uncertain discrete-time linear systems," *IEEE Transactions on automatic control*, vol. 48, no. 9, pp. 1600–1606, 2003.

[95] D. R. Saffer II and F. J. Doyle III, "Analysis of linear programming in model predictive control," *Computers & chemical engineering*, vol. 28, no. 12, pp. 2749–2763, 2004.

[96] D. L. Marruedo, T. Alamo, and E. F. Camacho, "Input-to-state stable mpc for constrained discrete-time nonlinear systems with bounded additive uncertainties," in *Proceedings of the 41st IEEE Conference on Decision and Control, 2002.*, vol. 4. IEEE, 2002, pp. 4619–4624.

[97] H. Chen, C. W. Scherer, and F. Allgower, "A game theoretic approach to nonlinear robust receding horizon control of constrained systems," in *Proceedings of the 1997 American Control Conference (Cat. No. 97CH36041)*, vol. 5. IEEE, 1997, pp. 3073–3077.

[98] M. Bell, D. Limebeer, and R. Sargent, "Robust receding horizon optimal control," *Computers & chemical engineering*, vol. 20, pp. S781–S786, 1996.

[99] E. C. Kerrigan and J. M. Maciejowski, "Robustly stable feedback min-max model predictive control," in *Proceedings of the 2003 American Control Conference, 2003.*, vol. 4. IEEE, 2003, pp. 3490–3495.

[100] V. Adetola and M. Guay, "Robust adaptive mpc for constrained uncertain nonlinear systems," *International Journal of Adaptive Control and Signal Processing*, vol. 25, no. 2, pp. 155–167, 2011.

[101] S. V. Rakovic *et al.*, "Parameterized tube model predictive control," *IEEE Transactions on Automatic Control*, vol. 57, no. 11, pp. 2746–2761, 2012.

[102] K. I. Kouramas *et al.*, "An algorithm for robust explicit/multi-parametric model predictive control," *Automatica*, vol. 49, no. 2, pp. 381–389, 2013.

[103] A. Voelker, K. Kouramas, and E. N. Pistikopoulos, "Simultaneous design of explicit/multi-parametric constrained moving horizon estimation and robust model predictive control," *Computers & chemical engineering*, vol. 54, pp. 24–33, 2013.

[104] S. V. Rakovic, "Minkowski algebra and banach contraction principle in set invariance for linear discrete time systems," in *2007 46th IEEE Conference on Decision and Control*. IEEE, 2007, pp. 2169–2174.

[105] M. Cannon *et al.*, "Robust tubes in nonlinear model predictive control," *IEEE Transactions on Automatic Control*, vol. 56, no. 8, pp. 1942–1947, 2011.

[106] D. Q. Mayne, E. C. Kerrigan, and P. Falugi, "Robust model predictive control: advantages and disadvantages of tube-based methods," *IFAC Proceedings Volumes*, vol. 44, no. 1, pp. 191–196, 2011.

[107] S. Raković and D. Mayne, "A simple tube controller for efficient robust model predictive control of constrained linear discrete time systems subject to bounded disturbances," *IFAC Proceedings Volumes*, vol. 38, no. 1, pp. 241–246, 2005.

[108] S. V. Raković *et al.*, "Fully parameterized tube model predictive control," *International Journal of Robust and Nonlinear Control*, vol. 22, no. 12, pp. 1330–1361, 2012.

[109] D. Sui, L. Feng, and M. Hovd, "Robust explicit moving horizon control and estimation: a batch polymerization case study," 2009.

[110] Y. J. Wang and J. B. Rawlings, "A new robust model predictive control method i: theory and computation," *Journal of Process Control*, vol. 14, no. 3, pp. 231–247, 2004.

[111] Z. Wan and M. V. Kothare, "Robust output feedback model predictive control using off-line linear matrix inequalities," *Journal of Process Control*, vol. 12, no. 7, pp. 763–774, 2002.

[112] C. Løvaas, M. M. Seron, and G. C. Goodwin, "Robust output-feedback mpc with integral action," *IEEE Transactions on Automatic Control*, vol. 55, no. 7, pp. 1531–1543, 2010.

[113] ——, "Robust output-feedback model predictive control for systems with unstructured uncertainty," *Automatica*, vol. 44, no. 8, pp. 1933–1943, 2008.

[114] C. Lovaas, M. M. Seron, and G. C. Goodwin, "A dissipativity approach to robustness in constrained model predictive control," in *2007 46th IEEE Conference on Decision and Control*. IEEE, 2007, pp. 1180–1185.

[115] T. Tran, K. V. Ling, and J. M. Maciejowski, "Model predictive control via quadratic dissipativity constraint," in *53rd IEEE Conference on Decision and Control*. IEEE, 2014, pp. 6689–6694.

[116] S. Kanev and M. Verhaegen, "Robustly asymptotically stable finite-horizon mpc," *Automatica*, vol. 42, no. 12, pp. 2189–2194, 2006.

[117] A. Casavola, D. Famularo, and G. Franzé, "Robust constrained predictive control of uncertain norm-bounded linear systems," *Automatica*, vol. 40, no. 11, pp. 1865–1876, 2004.

[118] Z. Wan and M. V. Kothare, "Efficient robust constrained model predictive control with a time varying terminal constraint set," *Systems & control letters*, vol. 48, no. 5, pp. 375–383, 2003.

[119] L. Özkan, M. V. Kothare, and C. Georgakis, "Control of a solution copolymerization reactor using multi-model predictive control," *Chemical engineering science*, vol. 58, no. 7, pp. 1207–1221, 2003.

[120] M. Rodrigues and D. Odloak, "Output feedback mpc with guaranteed robust stability," *Journal of Process Control*, vol. 10, no. 6, pp. 557–572, 2000.

[121] P. J. Goulart, E. C. Kerrigan, and D. Ralph, "Efficient robust optimization for robust control with constraints," *Mathematical Programming*, vol. 114, no. 1, pp. 115–147, 2008.

[122] P. J. Goulart and E. C. Kerrigan, "Input-to-state stability of robust receding horizon control with an expected value cost," *Automatica*, vol. 44, no. 4, pp. 1171–1174, 2008.

[123] D. H. van Hessem and O. H. Bosgra, "A conic reformulation of model predictive control including bounded and stochastic disturbances under state and input constraints," in *Proceedings of the 41st IEEE Conference on Decision and Control, 2002.*, vol. 4. IEEE, 2002, pp. 4643–4648.

[124] P. J. Goulart and E. C. Kerrigan, "Relationships between affine feedback policies for robust control with constraints," *IFAC Proceedings Volumes*, vol. 38, no. 1, pp. 608–613, 2005.

[125] P. J. Goulart, E. C. Kerrigan, and J. M. Maciejowski, "Optimization over state feedback policies for robust control with constraints," *Automatica*, vol. 42, no. 4, pp. 523–533, 2006.

[126] M. Lazar *et al.*, "Min-max nonlinear model predictive control with guaranteed input-tostate stability," in *17th Symposium on Mathematical Theory for Networks and Systems. Kyoto, Japan.* Citeseer, 2006.

[127] ——, "On input-to-state stability of min–max nonlinear model predictive control," *Systems & Control Letters*, vol. 57, no. 1, pp. 39–48, 2008.

[128] D. Raimondo *et al.*, "Regional input-to-state stability of min-max model predictive control," *IFAC Proceedings Volumes*, vol. 40, no. 12, pp. 42–47, 2007.

[129] M. Diehl and J. Bjornberg, "Robust dynamic programming for min-max model predictive control of constrained uncertain systems," *IEEE Transactions on Automatic Control*, vol. 49, no. 12, pp. 2253–2257, 2004.

[130] X. Yang, D. W. Griffith, and L. T. Biegler, "Nonlinear programming properties for stable and robust nmpc," *IFAC-PapersOnLine*, vol. 48, no. 23, pp. 388–397, 2015.

[131] D. Q. Mayne *et al.*, "Tube-based robust nonlinear model predictive control," *International journal of robust and nonlinear control*, vol. 21, no. 11, pp. 1341–1353, 2011.

[132] P. Mhaskar, N. H. El-Farra, and P. D. Christofides, "Stabilization of nonlinear systems with state and control constraints using lyapunov-based predictive control," *Systems & Control Letters*, vol. 55, no. 8, pp. 650–659, 2006.

[133] A. Bemporad, F. Borrelli, and M. Morari, "Robust model predictive control: Piecewise linear explicit solution," in *2001 European Control Conference (ECC).* IEEE, 2001, pp. 939–944.

[134] S. V. Rakovic *et al.*, "Invariant approximations of the minimal robust positively invariant set," *IEEE Transactions on automatic control*, vol. 50, no. 3, pp. 406–410, 2005.

[135] M. Cannon *et al.*, "Stochastic tubes in model predictive control with probabilistic constraints," *IEEE Transactions on Automatic Control*, vol. 56, no. 1, pp. 194–200, 2010.

[136] C. Løvaas, M. M. Seron, and G. C. Goodwin, "Robust model predictive control of input-constrained stable systems with unstructured uncertainty," in *2007 European Control Conference (ECC).* IEEE, 2007, pp. 3303–3310.

[137] F. Rodríguez, M. Berenguel, and M. R. Arahal, "Feedforward controllers for greenhouse climate control based on physical models," in *2001 European control conference (ECC)*. IEEE, 2001, pp. 2158–2163.

[138] D. Limon *et al.*, "Input-to-state stability: a unifying framework for robust model predictive control," *Nonlinear Model Predictive Control: Towards New Challenging Applications*, pp. 1–26, 2009.

[139] W.-K. Chen, Ed., *Analog and VLSI Circuits: The Circuits and Filters Handbook*, 3rd ed. Boca Raton, FL: CRC Press, 2009. [Online]. Available: http://www.crcnetbase.com/doi/book/10.1201/9781420058925

[140] M. Lazar *et al.*, "On the stability and robustness of non-smooth nonlinear model predictive control," in *Workshop on Assessment and Future Directions of NMPC*. Citeseer, 2005, pp. 327–334.

[141] G. Pin *et al.*, "Robust receding-horizon control of nonlinear systems with state dependent uncertainties: an input-to-state stability approach," in *2008 American Control Conference*. IEEE, 2008, pp. 1667–1672.

[142] A. L. Cervantes, O. E. Agamennoni, and J. L. Figueroa, "A nonlinear model predictive control system based on wiener piecewise linear models," *Journal of process control*, vol. 13, no. 7, pp. 655–666, 2003.

[143] S. Särkkä and L. Svensson, *Bayesian filtering and smoothing*. Cambridge university press, 2023, vol. 17.

[144] R. E. Kalman, "A new approach to linear filtering and prediction problems," 1960.

[145] D. Simon, *Optimal state estimation: Kalman, H infinity, and nonlinear approaches*. John Wiley & Sons, 2006.

[146] Z. M. Durovic and B. D. Kovacevic, "Robust estimation with unknown noise statistics," *IEEE Transactions on Automatic Control*, vol. 44, no. 6, pp. 1292–1296, 1999.

[147] P. J. Huber, "Robust statistics," in *International encyclopedia of statistical science*. Springer, 2011, pp. 1248–1251.

[148] M. Bujarbaruah *et al.*, "Adaptive mpc for iterative tasks," in *2018 IEEE Conference on Decision and Control (CDC)*. IEEE, 2018, pp. 6322–6327.

[149] A. Y. Prosekov and S. A. Ivanova, "Food security: The challenge of the present," *Geoforum*, vol. 91, pp. 73–77, 2018. [Online]. Available: https://www.sciencedirect.com/science/article/pii/S0016718518300666

[150] P. A. Loring and S. C. Gerlach, "Searching for progress on food security in the north american north: A research synthesis and meta-analysis of the peer-reviewed literature," *Arctic*, vol. 68, no. 3, pp. 380–392, 2015. [Online]. Available: http://www.jstor.org/stable/43872256

[151] G. Pasgianos *et al.*, "A nonlinear feedback technique for greenhouse environmental control," *Computers and electronics in agriculture*, vol. 40, no. 1-3, pp. 153–177, 2003.

[152] Q. Zou *et al.*, "Model predictive control based on particle swarm optimization of greenhouse climate for saving energy consumption," in *2010 World Automation Congress*. IEEE, 2010, pp. 123–128.

[153] C. Mark and S. Liu, "Recursively feasible data-driven distributionally robust model predictive control with additive disturbances," *IEEE Control Systems Letters*, vol. 7, pp. 526–531, 2022.

[154] I. Mitsubishi, "Pv panel made by mitsubishi company," 2023, https://studylib.net/doc/18057350/mlu-specification-sheet-250-255w [Accessed: (Use the date of access)].

[155] A. Parisio, E. Rikos, and L. Glielmo, "A model predictive control approach to microgrid operation optimization," *IEEE Transactions on Control Systems Technology*, vol. 22, no. 5, pp. 1813–1827, 2014.

[156] I. Honewell, "Battery energy storage system, made by honeywell company," 2021, https://process.honeywell.com/content/dam/process/en/documents/gated/hps_flr_bess.pdf [Accessed: (Use the date of access)].

[157] A. Bemporad and M. Morari, "Robust model predictive control: A survey," in *Robustness in identification and control*. Springer, 2007, pp. 207–226.

[158] A. Bemporad and A. Garulli, "Predictive control via set-membership state estimation for constrained linear systems with disturbances," in *1997 European Control Conference (ECC)*. IEEE, 1997, pp. 1738–1743.

[159] F. Schlaepfer and F. Schweppe, "Continuous-time state estimation under disturbances bounded by convex sets," *IEEE Transactions on Automatic Control*, vol. 17, no. 2, pp. 197–205, 1972.

[160] HydroQuebec. Flat d rate price, april 2023. https://www.hydroquebec.com/residential/customer-space/rates/rate-flex-d-billing.html.

[161] L. T. Evans, *Environmental control of plant growth*. Elsevier, 2012.

APPENDIX A SUPPLEMENTARY RESULTS

In Appendix A, supplementary results are shown. In the first step, the performance of KF and RKF will be illustrated in the presence of considerable uncertainty of disturbances. Then, graphics evaluate the improved RMPC method utilizing RKF as a robust recursive state estimator by comparing it with an adopted method from RMPC based on the penalized constraint violation approach in [17] in a similar plant of GH. Next, control input actions and constraints will be shown graphically. Then, it can be seen how constraint tightening and losing are functioning. Based on the constraint violation method, we compare the closed-loop trajectory of improved RMPC by RKF and RMPC. Finally, improved RMPC efficiency is shown on cluster entities of GHs preserving various plants.

Robust Kalman Filter: Huber function

As shown in Fig. A.1, studying an utterly random signal contaminated by uncertainty of disturbances shows out-spikes in measurement. This phenomenon causes computational burdens on the controller, creating inaccuracy in closed-loop feedback. However, deploying the RKF dynamic of states can control the level of disturbances.

Note: robustness in KF helps to determine more accurate set membership by selecting smaller ellipsoid bounds on estimate states so that it helps to reduce computational time.

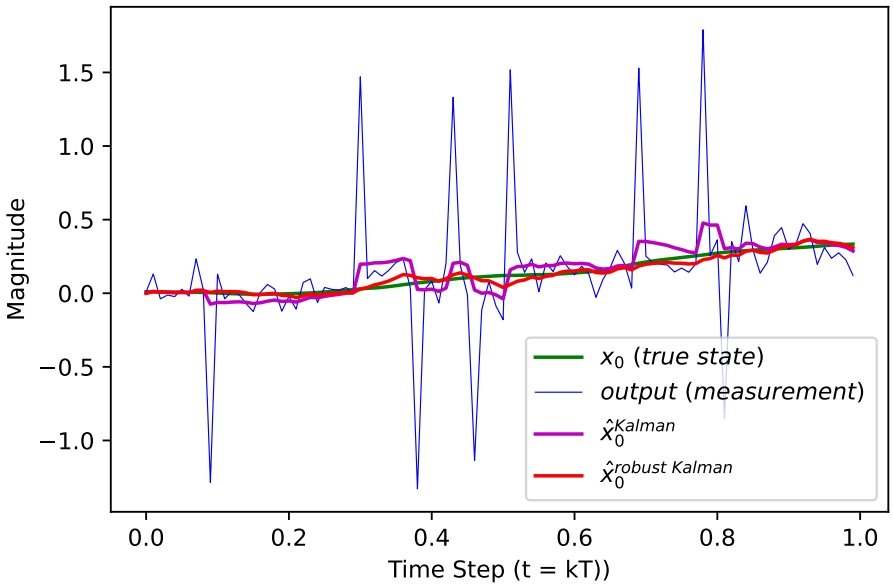

Figure A.1 Robust Kalman Filter using Huber function on a random signal, Time step in scale of $\times 10$.

Kalman Filter and Robust Kalman Filter

Fig.A.2 shows the tracking ability of KF (left-hand side) and RKF (right-hand side) using the set-membership concept, facing noise in the measurement process. The maximum deviation caused by noisy measurement is around 12.5% from the nominal value. RKF using set-membership to bounding the disturbances on state estimation is functioning well.

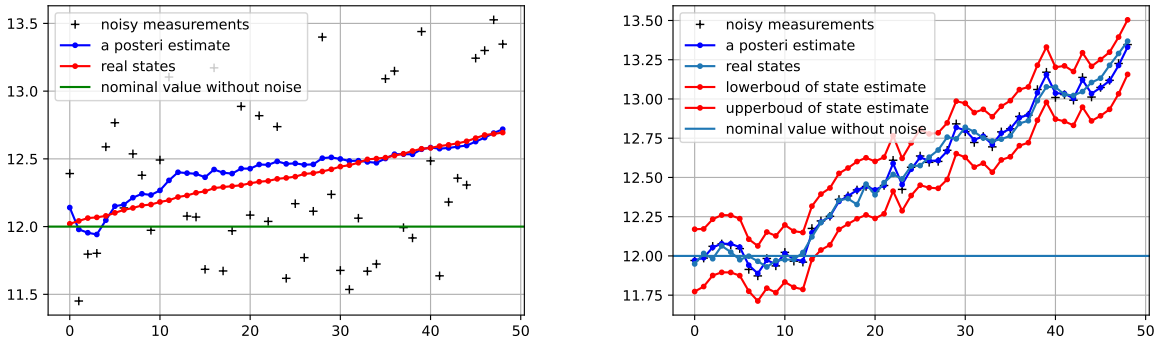

Figure A.2 Left: Common KF; Right:RKF using set-membership concept, deployed on a random signal with noisy measurement.

Improved KF evaluation under uncertainty of disturbances:

This section notes how the uncertainty of disturbances and state estimation error affects the ellipsoid surface dimension of set membership. Various noise incidence probabilities on process and measurement are considered to show how disturbances impact the state estimation process.

In Fig. A.3, considering constant disturbance on measurement, the different incidences of uncertainties on the state are placed. It is tried to increase the probability of the disturbances happening from left to right. Due to deploying RKF using the set-membership technique, the ellipsoid's surface has increased a diminutive amount in its initial state. In the second step of state estimation, exposed to the high probability of happening of disturbance ($p_w \sim N(0, 8)$), RKF harnesses the ellipsoid dimension. It is worth mentioning that when the likelihood of incidence of disturbances increases, the ellipsoid's surface should be expanded to guarantee acceptable state estimation under the harsh incidence of disturbances. This reaction causes conservative behavior of RMPC so that it raises computational time. Second, with increasing the ellipsoid surface, the expectation of the constraint violation also increases, and instability and inadequate steady-state behavior might occur. The advantage of utilizing RKF using set membership appears during computation. This filtering can relieve the burden of set-membership approximation and reduce computation time.

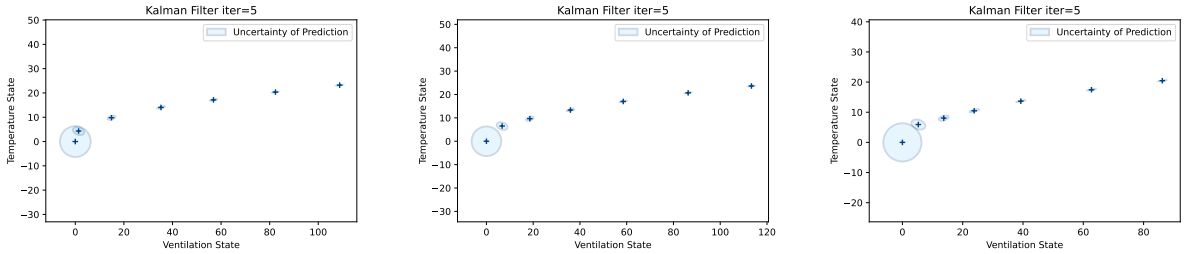

Figure A.3 Improved Robust method Under high noise level, Left to Right: terminal state weight increases, process noise increases, error state set is growing, computational demand rises ($p_w \sim N(0, (0, 4, 8))$, $p_v \sim N(0, 6)$).

In Fig. A.4 a common RMPC progress has been depicted. The set membership is selected according to the RPI set, which can make a long-lasting time burden until the final iteration (even in case of not having harsh disturbances.). Ellipsoid shapes have been stretched to increase the surface for 1) preserving the feasibility of solution optimal problem and 2) keeping acceptable transient and asymptotic behavior of closed-loop time response. The remaining error in each step of state estimation, which appears as an ellipsoid around the state, is because of the inadequacy of RMPC in removing the residual error of the previous step.

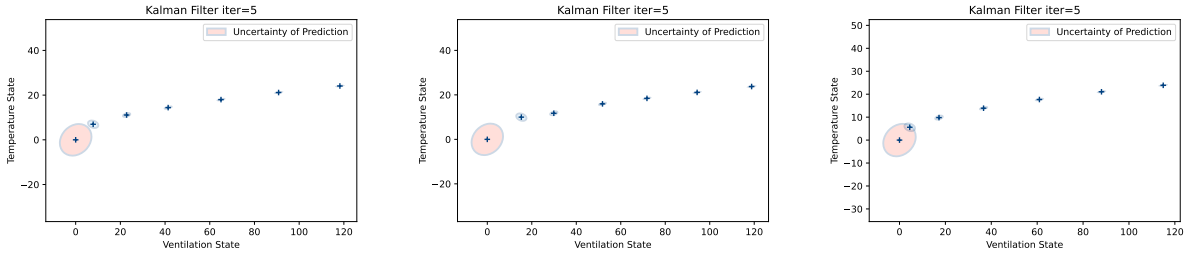

Figure A.4 Common Robust method under a high level of noise, Left to Right: terminal state weight increases, process noise increases, error state set is growing, but ellipsoid shows reluctant to increase to keep feasibility, resulting in conservatism instead, each step has more residual amount of error state in comparison with improved method ($p_w \sim N(0,(0,4,8))$, $p_v \sim N(0,6)$).

Once again, with almost the same considerations as previously, in Fig. A.5, and Fig. A.6, Improved robust and ordinary robust methods have been studied, respectively. The challenge with an ordinary RMPC is keeping feasibility at the cost of consuming resources by tightening the constraints on states and output. Deploying simple filtering and feeding data to approximate the proper set of possible states can be a sufficient remedy.

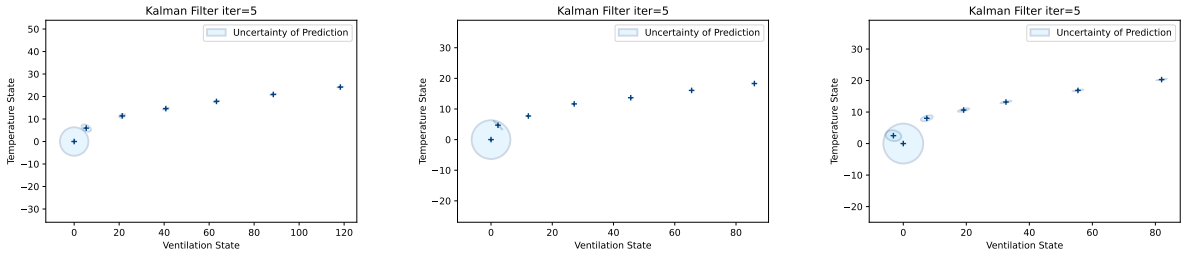

Figure A.5 Improved Robust method Under high level of noise, Left to Right: input control weight increases, process noise increases, error state set is growing, computational demand raises.($p_w \sim N(0,(0,5))$, $p_v \sim N(0,(0,4,8))$).

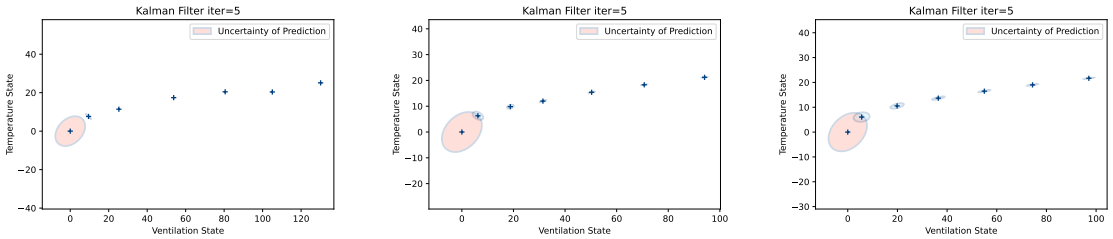

Figure A.6 Common Robust method under a high level of noise, Left to Right: input control increases, process noise increases, error state set is growing, ellipsoids also rise in each step to keep feasibility because the state is not tracked very well, resulting conservatism, each step residual amount of error state increases in comparison with improved method ($p_w \sim N(0,(0,5))$, $p_v \sim N(0,(0,4,8))$.

Closed-loop signal tracking performance, corresponding feasible set

RMPC using recursive estimation introduced in section **??** has been implemented on actual data related to different GH's. The temperature signal has been considered to avoid showing closed-loop control input among all dynamics. Also, for realized closed-loop trajectory, temperature versus ventilation controlling state dynamic state of systems has been illustrated due to having: 1) significant impact on other states, 2) Slow dynamics in comparison with other states.

In Left-top section of Fig. A.7, the auxiliary input of temperature of GH_1 ($\mu_{Temp}^{GH_1}$) is illustrated. The effect of disturbances of measurement on auxiliary control input is investigated. Constraints are met on the realization of the contaminated measurement, and then constraints are tightened on auxiliary input to respect the robustness rules. It should be mentioned that the constraints will be loosened after passing steps due to shrinkage of error dynamics (refer to explanations of RPIs section). In the Left-bottom control, inputs of two methods have been depicted. Systems with RMPC show more conservative behavior than the Improved RMPC method.

The proposed method is compared with a common RMPC in Right-top for illustrating the closed-loop trajectory. The improved approach of RMPC is showing less aggressive, taking a few steps less than the common RMPC method to converge to the origin. In the bottom right, the determined area inside the green strip shows the feasible temperature and ventilation parameters set. It can be concluded that RMPC utilizing a recursive state estimator is working with a smaller feasible region of RPI, which is related to the shaded area in the Left-top under tightened constraints.

Back to section 4.5.3, cutting harsh disturbances is working with a high level of performance

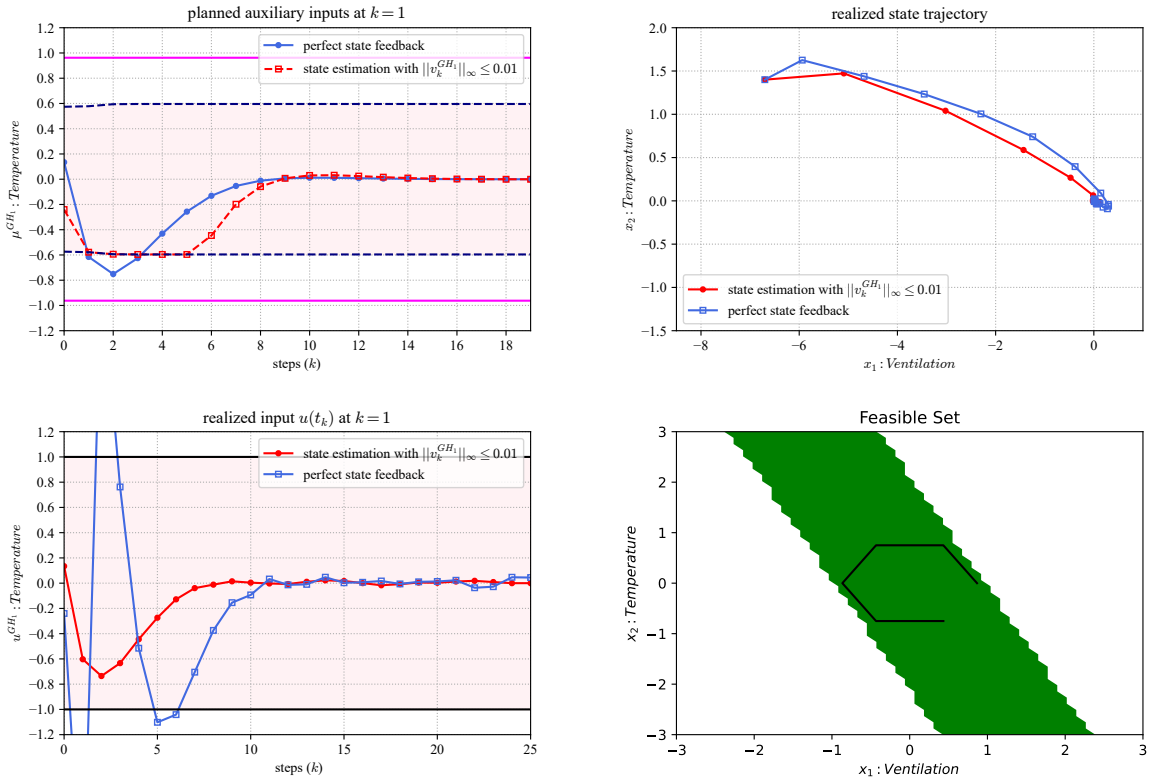

Figure A.7 Left-top: Auxiliary input $\mu_{Temp}^{GH_1}$ at step $k = 1$: state feedback (Blue); Proposed method (Red line); Left-bottom: real input $u_{Temp}^{GH_1}$ at step $k = 1$: state feedback (Blue); Proposed method (Red line); Right-top: closed-loop trajectory of Temperature and ventilation system states in GH_1; Right-bottom: feasible set membership for measuring with disturbance state feedback(Green area), hexagonal-wise area proposed method.

so that stability and steady-state response have been preserved, convergence speed has been grown, and then feasibility set is respected in the course of shrinkage of states. Input constraints have also been kept, as shown in the margins (pink area) in Figures A.7, A.8, A.9 and A.10 which could keep constraints on input under harsh disturbances; however, the constraint violation penalty approach could not handle severe disturbances and reduced computational time at the same moment. The main reason is the definition of uncertainty set based on a machine algorithm.

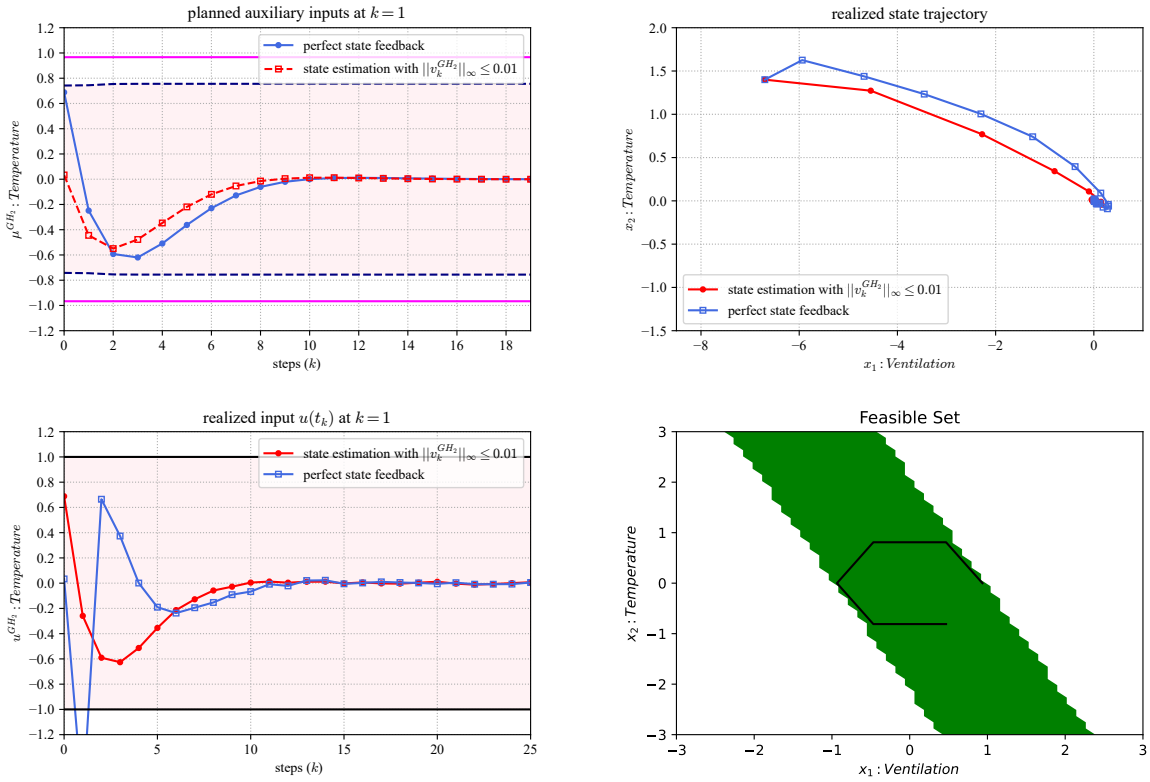

Figure A.8 Left-top: Auxiliary input $\mu_{Temp}^{GH_2}$ at step $k = 1$: state feedback (Blue); Proposed method (Red line); Left-bottom: real input $u_{Temp}^{GH_2}$ at step $k = 1$: state feedback (Blue); Proposed method (Red line); Right-top: closed-loop trajectory of Temperature and ventilation system states in GH_2; Right-bottom: feasible set membership for measuring with disturbance state feedback(Green area), hexagonal-wise area proposed method.

Objective function cost on error state estimation and speed of convergence

To obtain proper scale in terms of superiority of proposed method in cluster of GH application, two indices of performance in the presence of harsh disturbances are being compared.

Table A.1 Time of convergence over one window $(t = t_k \rightarrow t = t_{k+1})$of prediction horizon.

RMPC	Improved RMPC
$0.14062(s)$	$0.010950(s)$

Table A.2 comparison of energy level of objective costs in error state estimation between two methods, converging to origin.

RMPC	Improved RMPC
45.2589	19.03
17.5018	8.19101
7.65857	3.66628
3.42498	1.61211
1.49536	0.684183
0.629374	0.279721
0.255291	0.110494
0.100136	0.0423365
0.0381311	0.0157923
0.0141461	0.00575266
0.00512801	0.00205153
0.00182077	0.000717702
0.000634431	0.000246692
0.000217264	8.34153e-005
7.32103e-005	2.77734e-005
2.42954e-005	9.11194e-006
7.94566e-006	2.94716e-006
2.56202e-006	9.40024e-007
8.14695e-007	2.95713e-007
2.55509e-007	9.17446e-008
7.90281e-008	2.80655e-008
2.40995e-008	8.46203e-009
7.24261e-009	

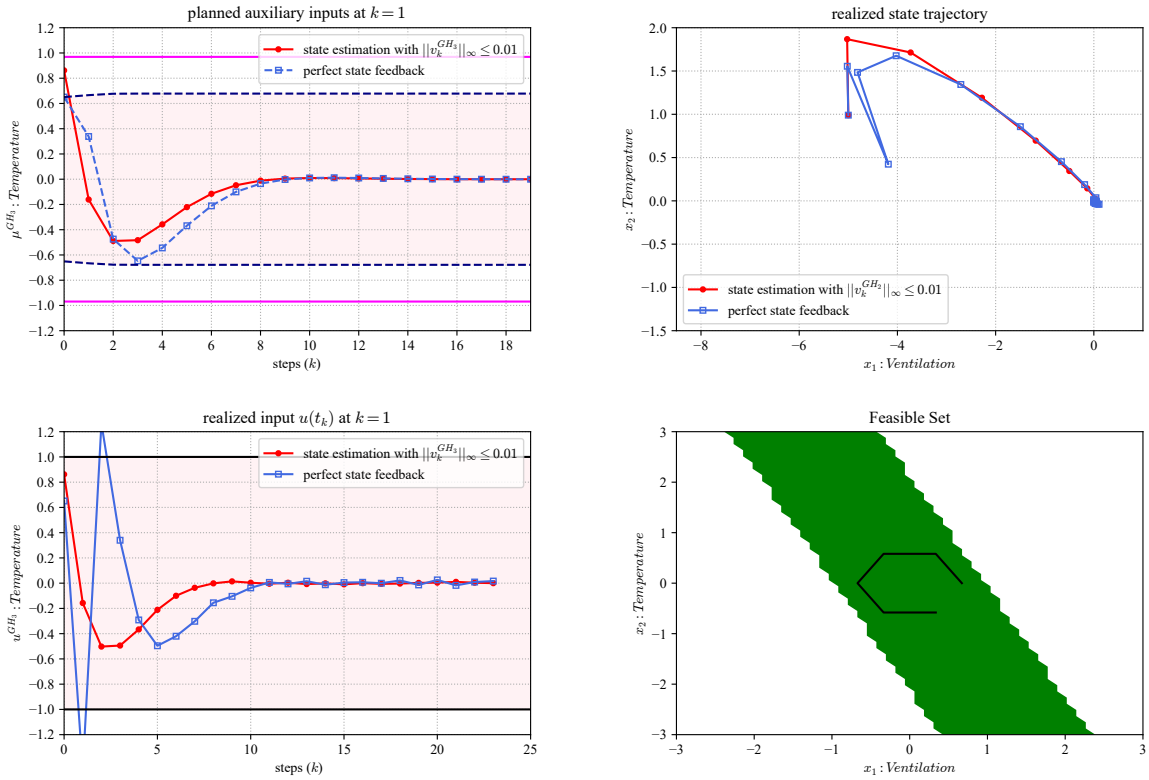

Figure A.9 Left-top: Auxiliary input $\mu_{Temp}^{GH_3}$ at step $k = 1$: state feedback (Blue); Proposed method (Red line); Left-bottom: real input $u_{Temp}^{GH_3}$ at step $k = 1$: state feedback (Blue); Proposed method (Red line); Right-top: closed-loop trajectory of Temperature and ventilation system states in GH_3; Right-bottom: feasible set membership for measuring with disturbance state feedback(Green area), hexagonal-wise area proposed method.

Performance of proposed algorithm on real application Every single GH keeps one type of crop. Horticultural parameters for preserving life conditions inside GHs are shown in tablesA.3 to A.6.

Temperature, humidity, and CO_2 concentration have the most vulnerable and complicated dynamics in terms of tracking. Physically, the mentioned states have a gas shape that is affected easily by disturbances, making it difficult to control. Studying these three dynamics with a high degree of difficulty in control makes clear the necessity of utilizing a robust recursive state estimator and set-membership concept in the process of the estimating step. It was already mentioned that the temperature state is the most important one among all necessary states to keep flawless growth inside the isolated GHs. This state has a thermodynamic correlation with other states. Firstly, utilizing a robust state estimator to dampen the effect of error allows the controllers to predict the next steps. This boosts tracking signal perfor-

Table A.3 Cucumber setpoints , GH_1.

Physical Parameters of Cucumber	Range
CO_2 level	920-1000 ppm
Temperature	$16°C(\text{night}), 24°C(\text{day})$
Artificial light	$\leq 2.1kW$
Humidity	50 % -70%
Water	1.1kW

Table A.4 Tomato setpoints, GH_2.

Physical Parameters of Tomato	Range
CO_2 level	810-990 ppm
Temperature	$17.5°C(\text{night}), 22°C(\text{day})$
Artificial light	$\leq 2.2kW$
Humidity	30 % -70%
Water	1.22kW

Table A.5 Strawberry setpoints, GH_3.

Physical Parameters of Strawberry	Range
CO_2 level	760-950 ppm
Temperature	$19°C(\text{night}), 23°C(\text{day})$
Artificial light	$\leq 2.12kW$
Humidity	47% - 65%
Water	0.9-1.1kW

Table A.6 Eggplant setpoints,GH_4.

Physical Parameters of Eggplant	Range
CO_2 level	900-925 ppm
Temperature	$18°C(\text{night}), 25°C(\text{day})$
Artificial light	$\leq 2.3kW$
Humidity	50 %-60%
Water	0.95-1.05kW

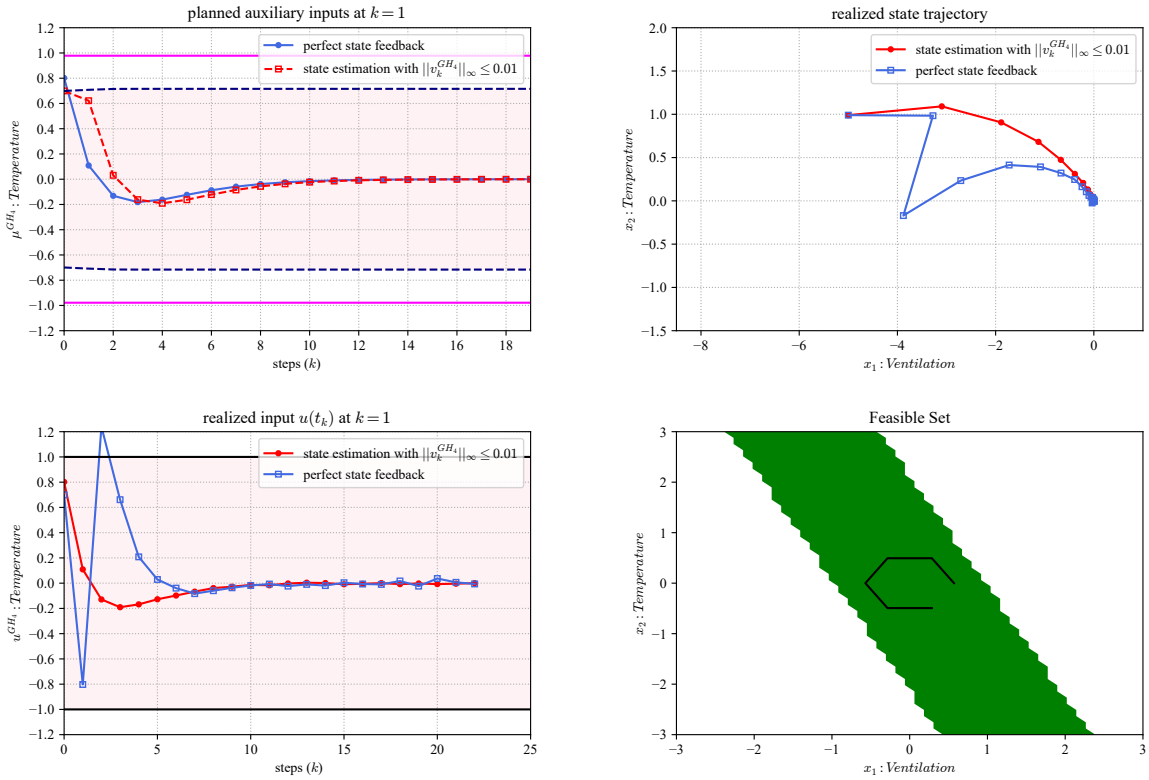

Figure A.10 Left-top: Auxiliary input $\mu_{Temp}^{GH_4}$ at step $k = 1$: state feedback (Blue); Proposed method (Red line); Left-bottom: real input $u_{Temp}^{GH_4}$ at step $k = 1$: state feedback (Blue); Proposed method (Red line); Right-top: closed-loop trajectory of Temperature and ventilation system states in GH_4; Right-bottom: feasible set membership for measuring with disturbance state feedback(Green area), hexagonal-wise area proposed method.

mance with minimum deviation from the reference in highly sensitive environments inside GH. In addition to deploying a set-membership technique to bind the steady state behavior, the trajectory of the improved method leaves a certain level of margin from constraints of the three gases dynamic to prevent any constraint violation. Implicitly, this margin is reinforced controller to tolerate more disturbances without disrupting the performance due to the conservative behaviour of the RMPC engine.

Moreover, in the real case of studies (or even in the worst-case scenario), it is expected that harsh conditions outdoors, like errors in weather prediction or fast climate change, are making a high magnitude of error in indoor temperature measurement.

Fig. A.11 shows the temperature reference tracking profile inside of all considered GHs.

In Fig. A.11 the main reason for the poor performance of the penalty on constraint violation method is the functionality of RMPC. In that approach, RMPC leaves a wider margin,

especially from 6 A.M. to around 5:30 P.M., then 7 P.M. to 6 A.M. This originated from the conservative behavior of RMPC facing disturbances. Sometimes, harsh disturbances severely impact reference tracking, so RMPC could not be practically handled as well as the way improved RMPC has done. When the outside temperature is lower or higher than the predicted temperature state, the inside temperature of GHs cannot stay above or under the minimum and maximum desirable temperatures; this is the reason for the violation of constraints.

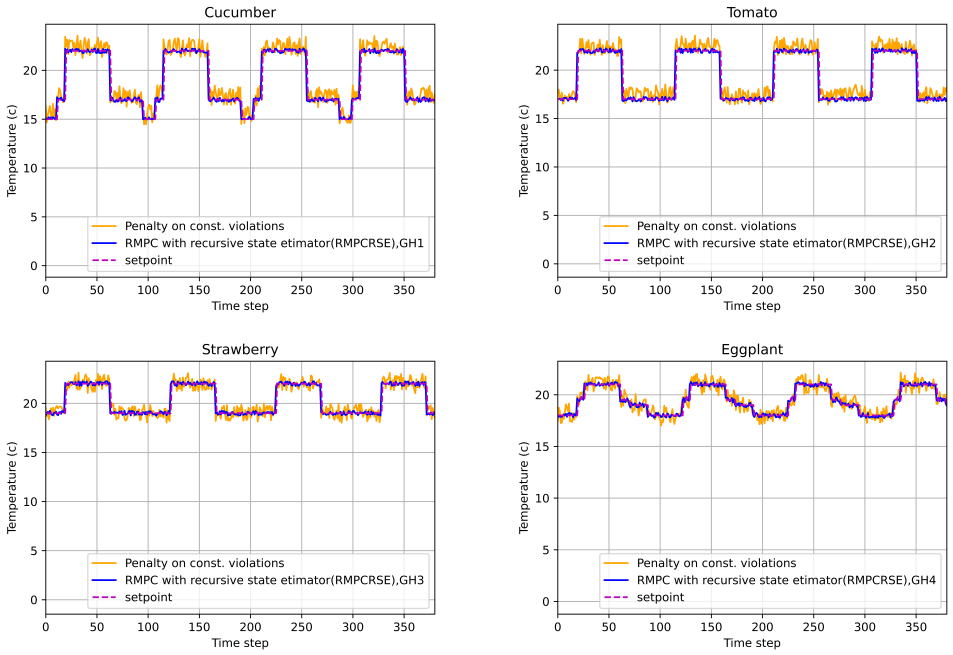

Figure A.11 GHs reference tracking profile of temperature over four days. Other strategy may be faced with problem when constraints are tightened, due to severe fluctuations.

As we know, the photosynthesis of crops starts with daylight. During the daytime CO_2 level should be regulated; however, over nighttime CO_2 generator is not working frequently due to CO_2 production by crops. Fig. A.12, shows CO_2 concentration has been regulated over daytime and nighttime without significant deviation from setpoints. The main reason for deviating from references in other methods is the error leakage of weather prediction and temperature fluctuation inside the GH. This change is affected by the implemented state estimator mechanism in RMPC. This error controller suffers from computational burden, causing conservative behavior for the sake of this error controller. For instance, when the temperature fluctuates during the day, CO_2 level changes. In Cucumber GH when the temperature declines under the minimum threshold, CO_2 levels face high-magnitude disturbances. To address this downside, in Fig. A.12 the ability of improved RMPC outperforms

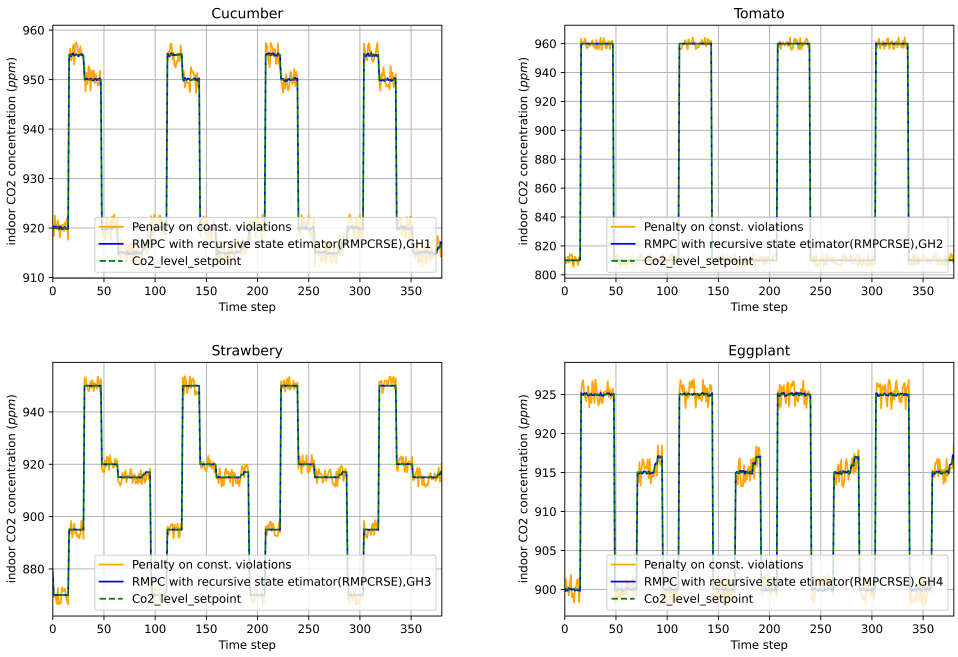

Figure A.12 CO_2 concentration level control inside of GHs over four days under two control strategies.

in comparison with RMPC. Because of utilizing the robust recursive state estimator, margin violation barely happens during the daytime.

in Fig. A.13, Humidifier systems control performance has been compared under the two most efficient strategies in four GHs. As we mentioned earlier, the humidity level is changing over 24 hours. Relative humidity fluctuates depending on the crop type and air temperature, but it is important to look into temperature and humidity reference tracking graphics simultaneously.

Due to the functioning of the controller in closed and sealed GHs, during daytime and nighttime, air temperature is raised, and more humidity is needed for transpiration. However, humidity evaporation of soil is also increased. Thus, the constraint violation probability is relatively high compared to two other gas phase dynamics. To cover this weakness, RMPC is considering a wider margin to ensure the constraint limits to keep plants environment away from fungus disease. These efforts increase the computational time and then conservative behavior. However, improved RMPC shows more robust performance in tracking references (setpoints) than the penalty on constraint violation method.

In Fig.A.14 Water pump tracking performance is compared under two methods of controlling based on RMPC. Watering or irrigation controllers should keep interacting with relative

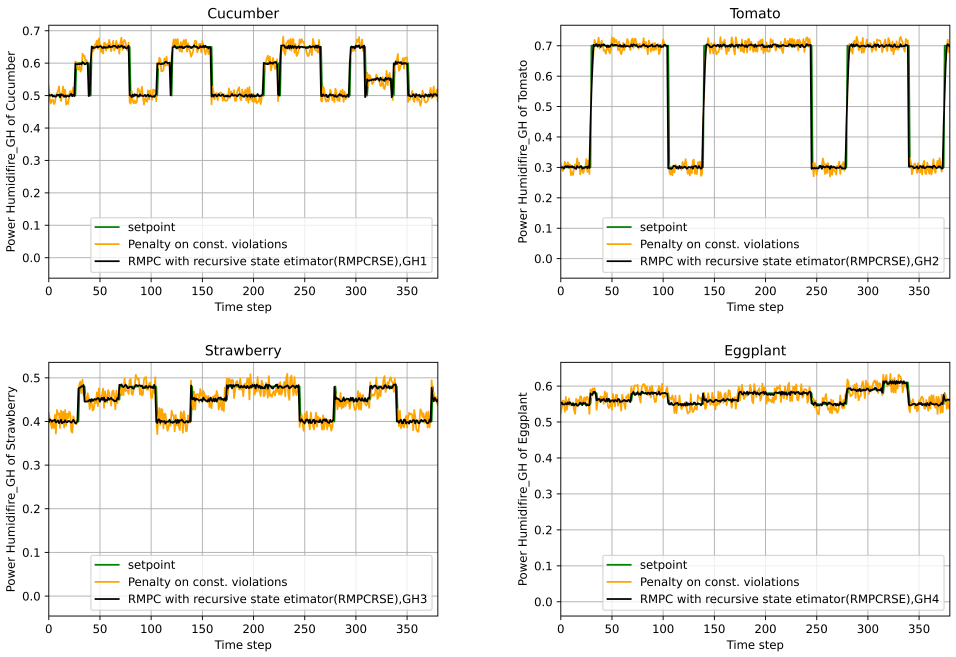

Figure A.13 Humidifier control profile of reference tracking during four days.

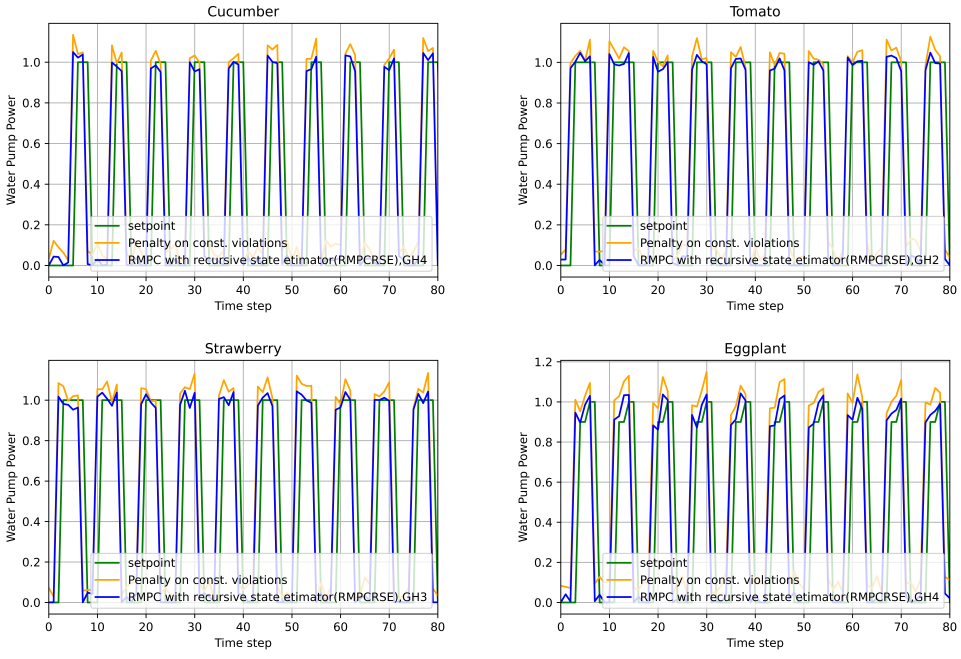

Figure A.14 Water Pump power control profile in the first day of four days.

humidity levels and temperature. To satisfy the performance of dynamic tracking without reducing the whole feasibility of solving optimal problems, RMPC considers a broader margin

to maintain the constraints. That is why the method of placing a penalty on constraint violation has yet to outperform, like improved RMPC. Intertwined relations among irrigation systems, relative humidity level control, temperature control, and ventilation systems cause delays in tracking references. In Fig.A.15 the lighting intensity control system has the most

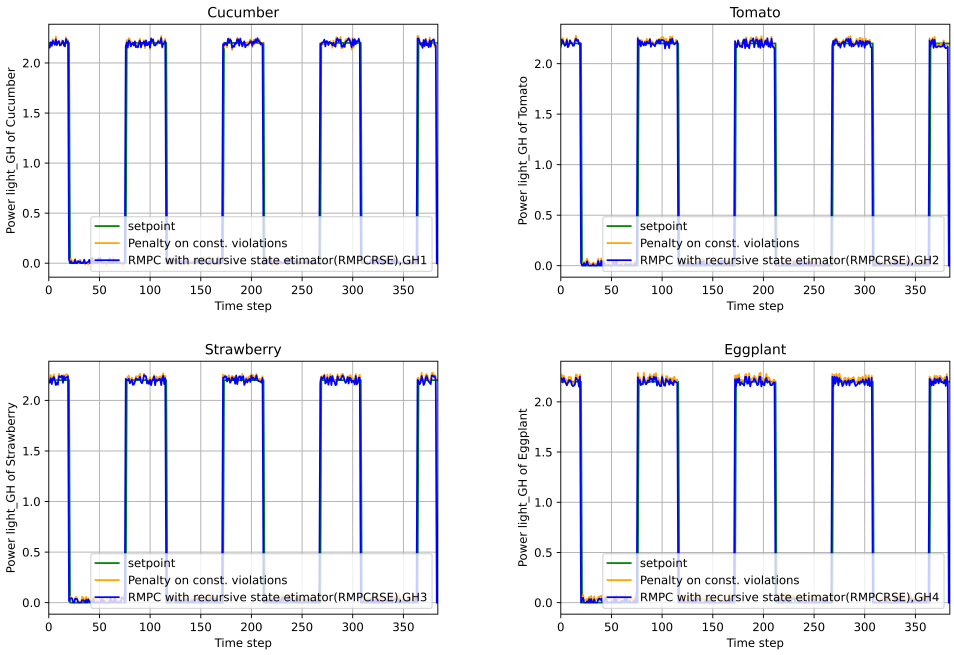

Figure A.15 Light intensity control profile with on/off reactions during four days.

rapid response in the control loop due to the nature of the on/off light. In this case, the uncertainty set is less impacted by the uncertainty of disturbances outside; however, in facing high-magnitude disturbances in lighting, improved RMPC outperforms slightly better than RMPC, shown in Fig. A.15.

Profile of power consumption, PV power generation, BESS functioning, the interaction of each GH with the power grid, batter actions in BESS, and SOC based on power consumption are shown in Fig. A.16 to A.19.

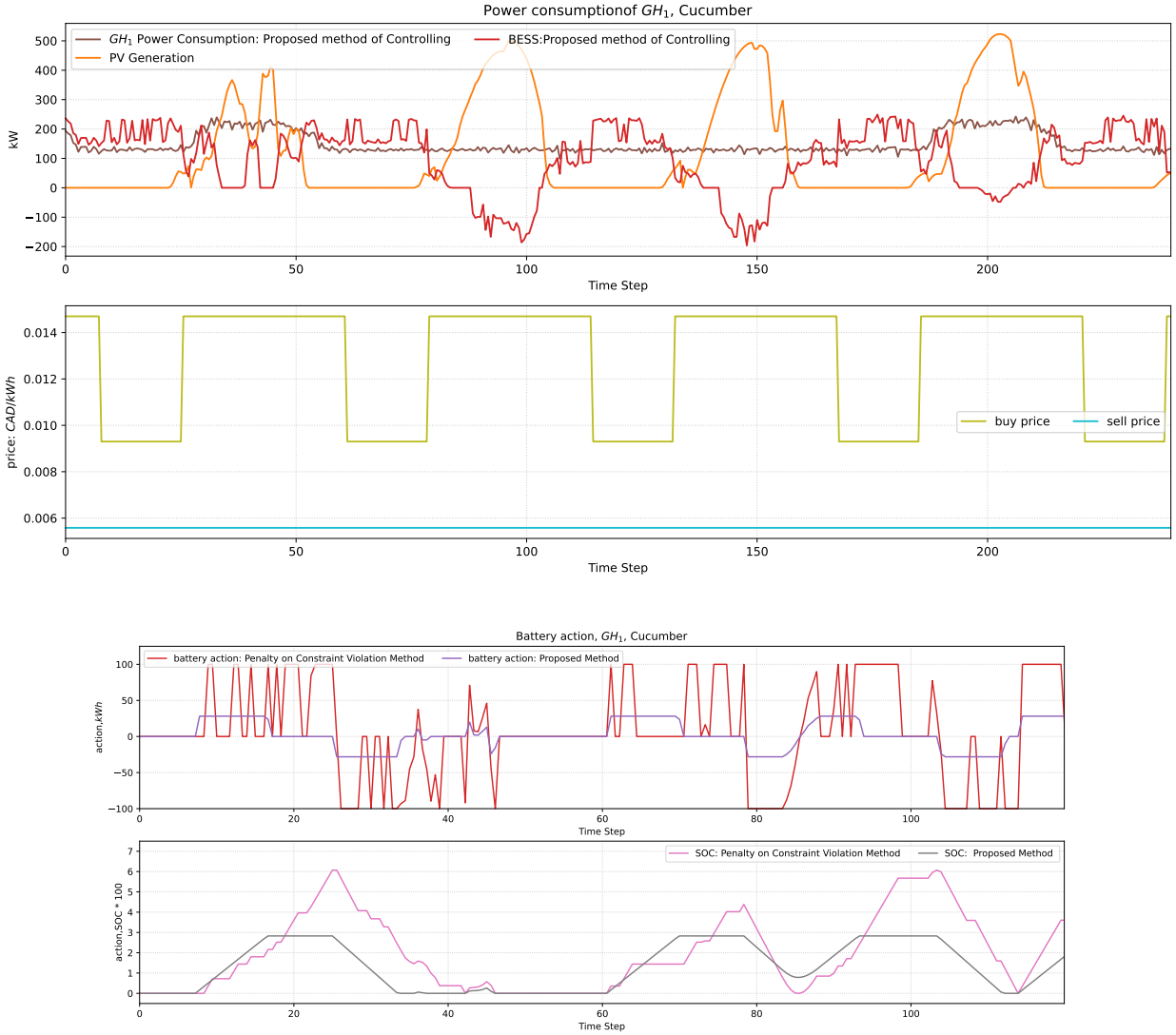

Figure A.16 Top to Bottom: First: Power consumption of GH_1 related to temperature control system; Second: Price according to D-rate bill of Quebec, Third: BESS action in GH_1, Forth: Bottom: SOC of BESS in GH_1.

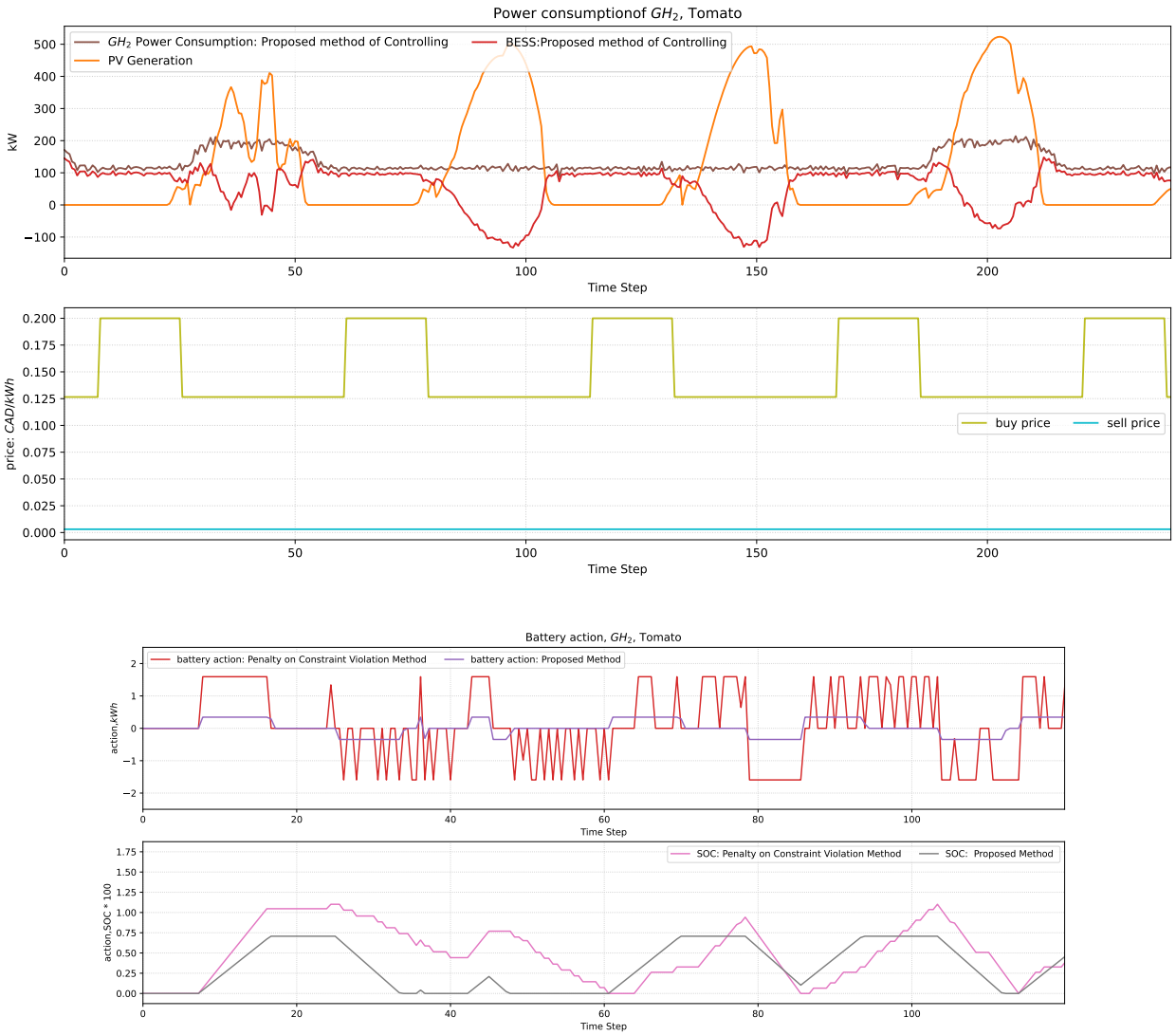

Figure A.17 Top to Bottom: First: Power consumption of GH_2 related to temperature control system, Second: Price according to D-rate bill of Quebec, Third: BESS action in GH_2, Forth: Bottom: SOC of BESS in GH_2.

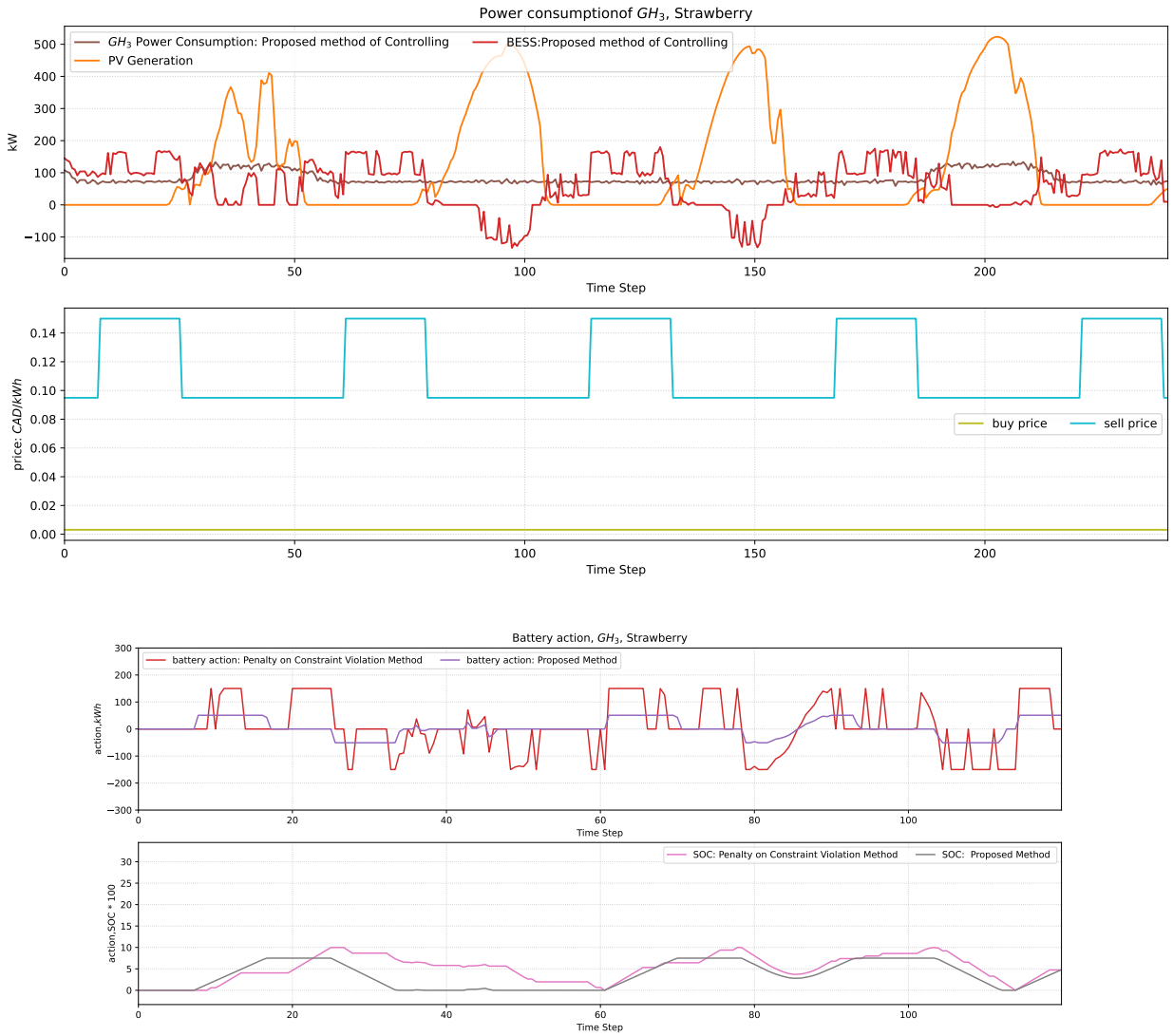

Figure A.18 Top to Bottom: First: Power consumption of GH_3 related to temperature control system, Second: Price according to D-rate bill of Quebec, Third: BESS action in GH_3, Forth: Bottom: SOC of BESS in GH_3.

Figure A.19 Top to Bottom: First: Power consumption of GH_4 related to temperature control system, Second: Price according to D-rate bill of Quebec, Third: BESS action in GH_4, Forth: Bottom: SOC of BESS in GH_4.